The application of non-dispersive X-Ray fluorescence spectroscopy to the analysis of single elements and simple mixtures

Chan, Ching Chee

"THE APPLICATION OF NON-DISPERSIVE X-RAY FLUORESCENCE SPECTROSCOPY TO THE ANALYSIS OF SINGLE ELEMENTS AND SIMPLE MIXTURES"

- o - o - o - o -

T H E S I S

presented in candidature for the degree of

MASTER OF SCIENCE

of the

UNIVERSITY OF DURHAM

by

Ching Chee Chan B.Sc. (London)

The work described in this thesis was performed in the Radiochemical Laboratory, Sunderland Technical College, during the period from October 1961 to January 1964, under the supervision of G.R. Martin, B.Sc., A.R.C.S, F.R.I.C., Reader in Radiochemistry, University of Durham.

This thesis contains the results of some original work by the author, and no part of the material offered has previously been submitted by the candidate for a degree in this or any other University. Where use has been made of the results and conclusions of other authors in relevant studies care has been taken to ensure that the source of information is always clearly indicated, unless it is of such general nature that indication is impracticable.

C. C. Chan

AN ACKNOWLEDGEMENT

The author wishes to express his gratitude to:

Mr. G.R. Martin, Reader in Radiochemistry, University of Durham, for general supervision during the course of this work.

Dr. D. Hall, Senior Lecturer in Inorganic and Radiochemistry, Sunderland Technical College, for suggesting the topic of this work.

Dr. E.P. Hart, Vice Principal, Sunderland Technical College for his encouragement.

Mr. E. Lewis, and the laboratory staff, Sunderland Technical College for their invaluable cooperation.

The Governors of the Sunderland Technical College for the award of a Research Studentship during the tenure of which this research was performed.

SUMMARY

A study is made of the application of the method of non-dispersive X-Ray fluorescence spectroscopy to problems of chemical analysis. The use of two types of radioactive source, i.e. Pm^{147} - aluminium brehmsstrahlung and Co^{57} low energy gamma rays, to excite fluorescent X-Rays is described.

The method is applied to systems consisting of a single heavy element, or binary mixtures of heavy elements (niobium - tantalum and zirconium - hafnium). dispersed in media of low average atomic number. Calibration curves of fluorescence intensity against element concentration for a wide range of elements are presented. Detection limits for these elements are established, and suggestions made for further work in this field.

CONTENTS

CHAPTER 1

INTRODUCTION

Historical Introduction.

Following the discovery of X-rays by Roentgen, Barkla and his co-workers showed that an element exposed to the radiation emitted fluorescent X-rays having a characteristic wavelength which was longer than that of the exciting radiation. The relation between the frequency of the characteristic radiation and the atomic number of the element was shown by Moseley (1913) to be of the form;

$$U = A(Z - S)^2$$

where U = the frequency of the characteristic radiation.
Z = the atomic number of the element.
A and S are constants.

This direct relation between the frequency of the fluorescent X-ray and the atomic number of the emitting element provides the basis of a method of chemical analysis for the element.

In the years immediately following this discovery the method of analysis consisted of placing the sample to be analysed on the target of an X-ray tube. The resulting fluorescent radiations were dispersed using a flat calcite crystal, the spectra produced being detected photographically. Early notable successes of the method were the discovery of the element hafnium by von Hevesey and Coster(1),

and of the element rhenium by Noddack (1). However the method of producing the fluorescent radiation was cumbersome, and its detection relatively insensitive. The difficulties in application are illustrated by Noddacks claim to the discovery of masurium (Z = 43, technetium) which in the light of later evidence must be regarded as erroneous. (2).

The development of the modern X-ray tube with stable high intensity emission has removed the need to place the sample to be analysed on the tube target. Large single crystal dispersion systems allow more efficient collection of the fluorescent X-rays, and the use of modern nucleonic instruments ie. geiger, proprtional, and scintillation counters, greatly increases the sensitivity of detection. X-ray flouresceonce analysis is now a powerful method for trace element analysis(3). Development in the field continues, recent advances being the use of well-focused electron beams to excite the fluorescent X-rays, a method now referred to as Electron probe microanalysis. (4)

In 1955 reports first appeared on the use of radiation from radioactive isotopes to excite the fluorescent X-rays (5,6,7). The systems based on this method dispense with crystal dispersion elements, the radiation being detected directly by proportional or scintillation counters, and energy resolution of the fluorescent X-rays is made by analysis of the pulse height spectrum from these detectors. The method is generally referred to as non-dispersive X-ray fluorescence analysis.

Discussion of the methods of X-ray fluorescence analysis.

One of the main tasks of X-ray fluorescence analysis is to establish the relationship between the fluorescence intensities of the characteristic X-rays of an element and the concentration of that element in sample to be analysed. Although the present work is concerned with the establishment

of the above relation for the non-dispersive method, a discussion of the dispersive method is included for purposes of comparison.

Dispersive method.

A. Instruments:

X-ray tubes of the Coolidge type (8) with a tungsten or molybdenum target are in common use as a source of primary X-radiation. Power supplies to the tube are required to be of high stability to ensure reproducible emission intensity from the tube. Dispersion of the fluorescent radiations is usually achieved with the use of calcite crystals. The crystals used are of two types, plane and curved surfaces (9). In the case of plane surface crystals a parallel beam of X-rays is required and a collimation system usually of the Soller slit type (9) is used. Detection of the fluorescent X-ray is achieved by the use of Geiger counters.

B. Calibration.

The relation between fluorescent intensity and concentration of an element can be derived (See appendix I). For a sample having infinite thickness exposed to monochromatic X-ray the relation is:

$$I_f = \frac{A\, I_0\, C}{(\mu_p + \mu_f)\rho \operatorname{cosec}\theta} \qquad \text{- - - - - - - - - (1-1).}$$

where A = a constant.

I_0 = intensity of primary X-radiation.

I_f = intensity of fluorescent X-radiation.

C = element concentration in the sample.

μ_p = mass absorption coefficient of the sample for the primary radiation.

μ_f = mass absorption coefficient of the sample for the fluorescent radiation.

ρ = density of the sample.

θ = angle subtended by the X-ray beam at the sample.

For a given sample μ_p and μ_f are the resultant of contributions from all components of the sample, i.e.

$$\mu_p = \mu_{p1} W_1 \rho_1 + \cdots + = \sum_i \mu_{pi} W_i \rho_i \quad \ldots\ldots (1\text{-}2).$$

$$\mu_f = \mu_{f1} W_1 \rho_1 + \cdots + = \sum_i \mu_{fi} W_i \rho_i \quad \ldots\ldots (1\text{-}3).$$

where μ_{pi} = mass absorption coefficient of component i for the primary radiation.

μ_{fi} = mass absorption coefficient of component i for the primary radiation.

W_i = weight fraction of component i.

ρ_i = density of component i.

From relations 1-2 and 1-3 it can be seen that the quantity $(\mu_p + \mu_f)\rho$ of equation 1-1 is dependent on the sample composition this dependence being complex for a multicomponent sample. A two component mixture consisting of a heavy element dispersed in a matrix of low density represents a simple form of sample. For such a sample the quantity $(\mu_p + \mu_f)\rho$ will increase with the concentration of the heavy element, and the curve relating fluorescence intensity to concentration will be convex upwards. Only when the concentration is low and varies over a small range is linear relation obtained (10, 11, 12, 13).

For multicomponent samples a further complication can occur which is readily illustrated by considering a mixture of iron, cobalt, and nickel (see figure 1-1). In figure 1-1, the wavelengths of the Kα radiation of iron, cobalt, and nickel are plotted together with their respective absorption curves. From this it can be seen that Ni Kα radiation is strongly absorbed by iron with the consequence that the fluorescence intensity of Ni Kα will decrease with increasing iron concentration in the sample. On the other hand the fluorescence intensity of Fe Kα will increase with increasing concentration of nickel in the sample because of the increase in the effective I_o for iron. The fluorescence intensity of

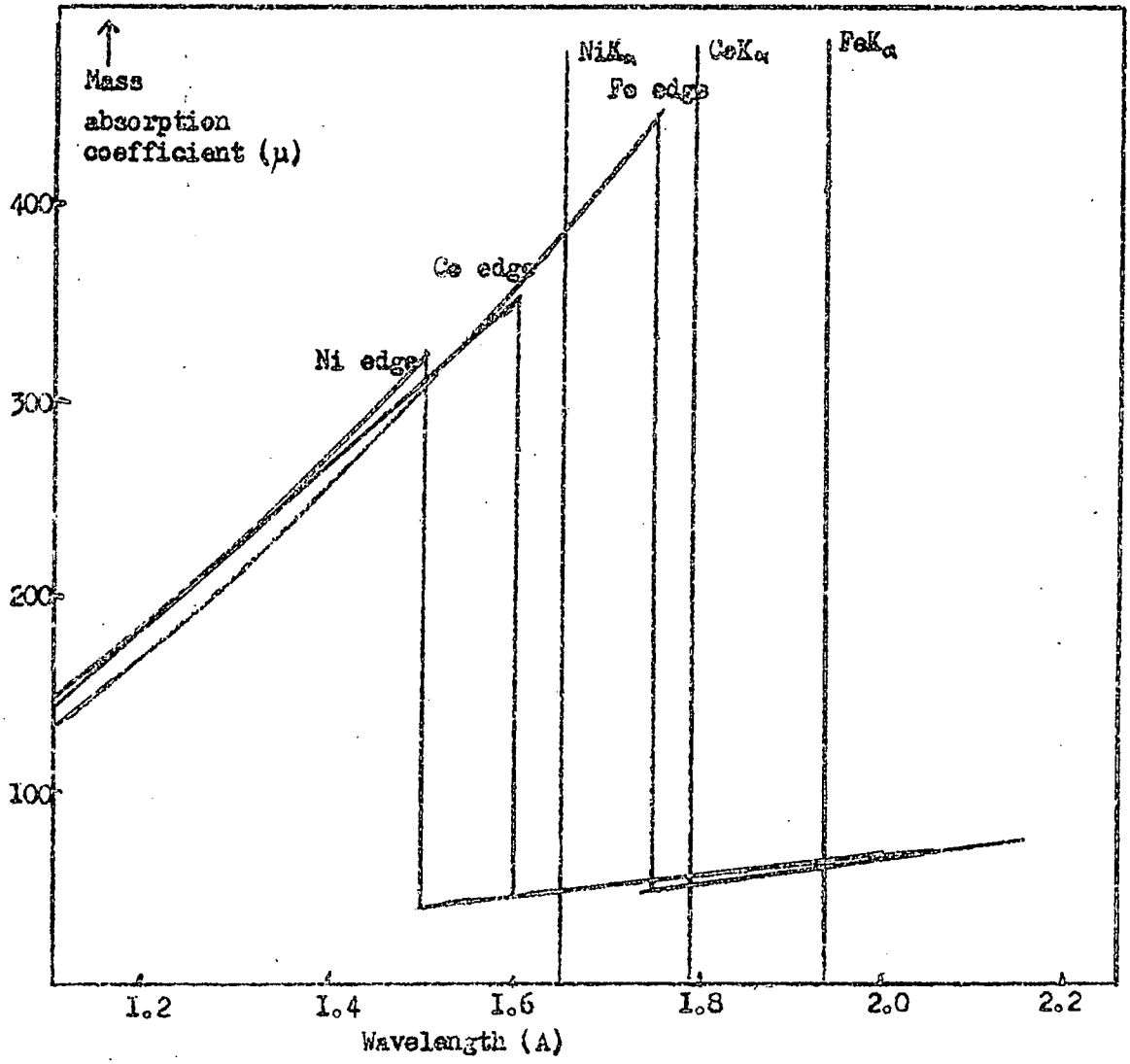

Fig. I-1 Spectral data to illustrate absorption and enhancement effect(variation of u_p ,u_f and effective I_0)

Co K_α will however be little affected by nickel or iron concentration. In a situation of this kind several different values of the fluorescent intensity of an element may be obtained without altering the concentration of the element in the sample. A straightforward calibration of fluorescent intensity against element concentration is then of little value. Such an effect is referred to as the enhancement - absorption or matrix effect (14, 15).

Of the many ways in which to counter the enhancement - absorption effect the most widely used is the internal standard method. A second element is chosen whose characteristic line is affected by the infering element or elements in a similar way to that of the element whose concentration is to be determined. The characteristic energy of this second element should be of roughly the same energy as that of the element to be determined, and since they are affected similarly by interfering elements the ratio of their intensities will be independant of the variation in concentration of the interfering elements. A calibration curve can then be obtained by plotting this ratio against the concentration of the element to be determined. If the effect of the interfering element is one of absorption then the characteristic lines of the internal standard and of the element to be determined must lie in the same side of the absorption edge of the interfering element. If the interference is one of enhancement both absorption edges of the element and internal standard must be overlapped on the same side by the interfering line (see fig. 1-2). A further consideration is that element chosen as internal standard must readily mix with the material of the sample (16,17,18,19,20,21,22,23,24,25,26,27,28,29,30). The use of this method will in general require a knowledge of the composition of the matrix in which the element to be determined is dispersed. Where this knowledge is not available the choice of an element as internal standard is difficult, and cannot be made if the conditions are such

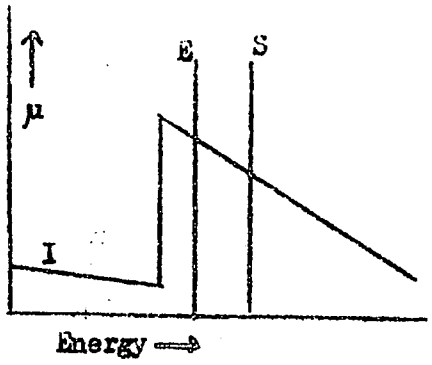

A. Suitable internal standard
(absorption)

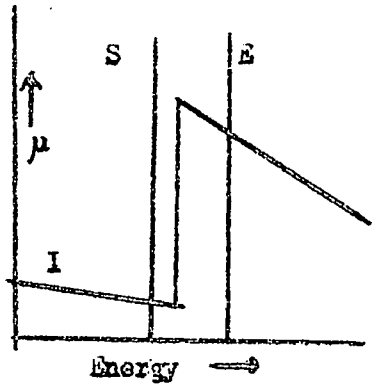

B. Unsuitable internal standard
(absorption)

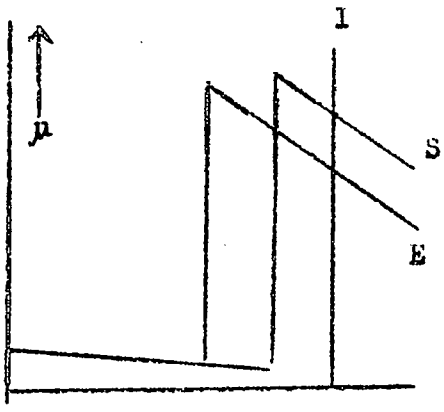

C. Suitable internal standard
(enhancement)

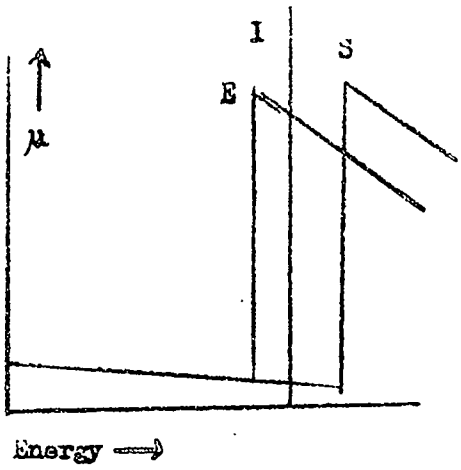

D. Unsuitable internal standard
(enhancement)

Fig. I-2 Relations among absorption edges, characteristic lines of the element, internal standard and interfering element. E represents the element whose concentration is to be estimated.

I is the interfering element.
S is the internal standard

that the matrix composition varies from sample to sample. It is possible that an interfering line falls between the absorption edge of the element and that of the internal standard, or that the absorption edge of the interfering element lies between the fluorescent lines of the element to be estimated and the internal standard. A reliable calibration curve cannot then be obtained. In such cases the addition of an appropriate quantities of the element to be estimated can prove useful. The fluorescence intensity of the element is first determined on the sample. A known amount of the element is then added to the sample, and the fluorescent intensity again determined. Let

x = concentration of element in original sample
a = concentration of element added
I_1 = fluorescence intensity of original sample
I_2 = fluorescence intensity of doped sample.
K = proportional constant.

Then from equation (1-1).

$$I_1 = \frac{K \; I_0 \; x}{(\mu_f + \mu_p)_1 \rho_1}$$

$$I_2 = \frac{K \; I_0 \; (x + a)}{\mu_f + \mu_p)_2 \rho_2}$$

If the ammount added is small enough that we can assume

$$(\mu_f + \mu_p)_1 \rho_1 = (\mu_f + \mu_p)_2 \rho_2$$

then

$$\frac{I_1}{I_2} = \frac{x}{x - a}$$

we have

$$x = \frac{I_1 a}{I_2 - I_1}$$

This method has been applied to the analysis of mixtures of tantalum and niobium oxides (ref. 31). The method just described has relied on neglecting changes in the value of $\mu_f \rho$ and $\mu_p \rho$ due to the addition. A consideration of equation 1.2 and 1.3 shows that the variation in $\mu_f \rho$ and $\mu_p \rho$ can be made small by other means. One method is to dilute the sample for examination in a light matrix so that variations in $\mu_f \rho$ and $\mu_p \rho$ with variation of the weight fraction of heavy elements are small. The light matrix should be transparent to X-rays, and materials chosen have been such things as starch, water, sodium borate, and aluminium powder (32). Such a technique would also reduce absorption - enhancement effect. A further method is to stabilise the value of $\mu \rho$ by the addition of heavy elements such as barium. This has the disadvantage of considerably reducing the fluorescent intensity with consequent loss in sensitivity. (33). Scattered X-rays (background) of suitable energies have also been used to correct for enhancement - absorption effect (30,34,37). These are chosen empirically and are usually near to the fluorescent lines of the elements being estimated. Arithmatical and mathematical methods have been used by other workers (38, 40, 41).

Many types of sample are suitable for analysis by the X-ray fluorescence method. The method has the advantage over conventional methods of chemical analysis that it need not involve destruction of the sample. Samples in the form of metal and alloy turnings can be used for the estimation of elements present by compressing them into a regular shape of reproducible density. Problems arising from the inhomogeneous distribution of elements, and from variation in particle size in the sample can be eliminated by preparing the sample in the form of a liquid or solid solution (30,37). Samples of solid solution can be achieved by fusion with lithuim or sodium borate until the melt is homogeneous then

the melt is poured onto a pre-heated aluminium plate. On slow cooling, the sample is obtained in the form of a flat disc (33,39,). The X-ray fluorescence method has also been used to measure the thickness of metal films (42,43). The method has been applied to the analysis of the impurity of elements having atomic numbers greater than 19, by calibration of the fluorescent intensities of K X-rays against element concentration. When the atomic number of the element is high L X-rays are used instead of K e.g. Ta($z = 23$) (37). For analysis of elements of atomic number less than that of calcium the K X-ray energy is low and absorption of the X-rays by air becomes serious. By the use of vacuum, or displacement of air in the X-ray path by helium or hydrogen, it is possible to do fluorescence analysis with elements of atomic number less than 20, the limit being reached at sodium or magnesium. Because of the longer wavelength of these radiations it is also necessary to use crystals with large lattice spacing e.g. ethylenediamine ditartrate ($d = 4.404$ A) (44,45). Continuous flow counters with very thin windows have been used to minimise losses due to absorption in the counter window. Attempts have been made to adopt windowless flow counter for X-ray fluorescence analysis (46).

C. Statistics and Detection Limit.

The measure of the precision of the results of an analysis by X-ray fluorescence methods is commonly given in terms of the standard deviation expressed in percentage ie.

$$\frac{1}{N^{\frac{1}{2}}} \times 100$$

where N = total observed count.

$N^{\frac{1}{2}}$ = standard deviation of the count.

$\frac{1}{N^{\frac{1}{2}}}$ = fractional standard deviation.

When a background correction is involved the alternative form(47,48).

$$\frac{(N_L - N_B)^{\frac{1}{2}}}{(N_L - N_B)} \times 100$$

is used, where N_L = total observed count

N_B = background count

Expressed in this way, the precision is good, but is found to vary from element to element due to the different energies of the fluorescent X-rays. An important question is that of the definition of the limit of detection, and several different criteria for this definition have been adopted by workers in this field. Of these, the most satisfactory would appear to be that which defines the minimum detectable concentration as that concentration which gives a value of the fluorescent intensity three times the standard deviation of the background. The minimum detectable concentration defined in this way gives a confidence of ninety nine per cent with a standard deviation approaching fifty per cent. The agreement between the results obtained by wet chemical methods and X-ray fluorescence analysis is good (49).

Non-dispersive method.

The non-dispersive method of X-ray fluorescence analysis uses a radioactive material as the source of the primary X-radiation. A radioactive source with radiation emission equivalent to the radiation output of a modern X-ray tube, such as used in the dispersive method, would have a strength from 10 kilocuries up to 1 megacurie (1 curie = 3.7×10^{10} disintegration per second). Work with radioactive materials at such activity levels is extremely hazardous requiring special shielding and remote handling facilities. On the

other hand it is possible to do analysis by the non-dispersive method with as little as 100 microcuries of radioactive material, although the sensitivity with such a sample is very much lower than can be achieved in the dispersive method. In the dispersive method much of the primary radiations and fluorescent radiations is lost in the collimation and dispersion systems, and so with the much lower primary intensity available from usable radioisotope sources such collimation and dispersion systems cannot be used. Instead the fluorescent radiation is detected by making use of the property of a proportional or scintillation counter whereby the voltage output from the counter is proportional to the energy of the radiation incident upon it. The resolution of such counters is very much inferior to that of crystal dispersion systems which are capable of resolving the K_{α_1} K_{α_2} K_{B1} and K_{B2} fluorescent X-radiations from an element.

In view of the lower primary intensity and poorer energy resolution available in the non-dispersive method it is not to be expected that it can compete on equal terms with the dispersive method. There are however a wide variety of possible applications of the non-dispersive method for which some knowledge of its sensitivity in analysis would be useful. The present investigation sets out to examine this for a wide variety of elements, and also its application to the analysis of mixtures of niobium and tantalum.

A. Source of Primary Radiation

The radioactive sources used are of three main types.

(a). Low energy γ - emitters.

(b). Compact combinations of a beta-emitting radionuclide with a target element, which give rise to bremsstrahlung and characteristic X-rays of the elements present.

(c). β - emitters; a magnetic field is usually used with such sources to prevent scattered β - radiation entering the detector.

The use of α-particle sources has been attempted (50) but the production of fluorescent X-rays is found to be many times less efficient than that of β -particles. A summary of the various types of source is given in tables I, II, and III.

Table I (51, 53)

Bremsstrahlung Sources				
Isotope	Half-life	Target Element	Type of Radiation	Useful photon energy
^{3}H	12.3 years	Ti	Bremsstrahlung	4-8 Kev
		zr	Bremsstrahlung	5-9 Kev
^{147}Pm	2. 6 years	Ag	KAg X-rays - Bremsstrahlung	20-40Kev
		Al	Bremsstrahlung	10-40Kev
^{85}Kr	10.7 years	C	Bremsstrahlung	30-80Kev
$^{90}Sr/^{90}Y$	28 years	Al	Bremsstrahlung	70-150 Kev

Table II

Electromagnetic radiation from radio isotope without the use of target (50, 53).

Isotope	Half-life	Type of Radiation	Energy
^{131}Cs	9.7 days	effectively monochromatic X-ray	29.6 Kev
^{55}Fe	2.9 years	Monochromatic	5,9 Kev
^{181}W	140 days	Monochromatic	56.9 Kev
^{241}Am	470 years	γ + X rays	mainly 60 Kev

Table III

Radioisotope provides beta particles to excite characteristic X-rays from elements in sample (52, 53, 54, 55).

Isotope	Maximum beta energy	half life
^{143}Pr	930 Kev	13.8 days
^{204}Tl	770 Kev	4 years
^{147}Pm	220 Kev	2.6 years
$^{90}Sr/_{90}Y$	540 and 2240 Kev	28 years
^{85}Kr	100 Kev	10.6 years

B. Detection and resolution of the Fluorescent Radiations.

The choice of a suitable detection system depends upon a number of factors notably the detection sensitivity and energy resolution required as well as the energy of the fluorescent radiation. The proportional counter has superior resolution to a scintillation counter for low energy radiation but its detection efficiency falls off for radiation of energy greater than 25 kev (56). The low intensity of the primary radiation and the even lower intensity of the fluorescent radiation require that source, sample and detector should be as close together as possible in order to achieve the maximum sensitivity. Typical of the geometrical arrangements chosen by most workers are those shown in fig. 1-3, 1-4. The voltage pulse from the detector after suitable amplification by means of a linear amplifier is fed to a pulse height analyser which records the spectrum of radiation from the sample.

Attempts to improve the resolution of the system have been made by using the balanced filter technique, which also serves to reduce errors due to instability in the associated

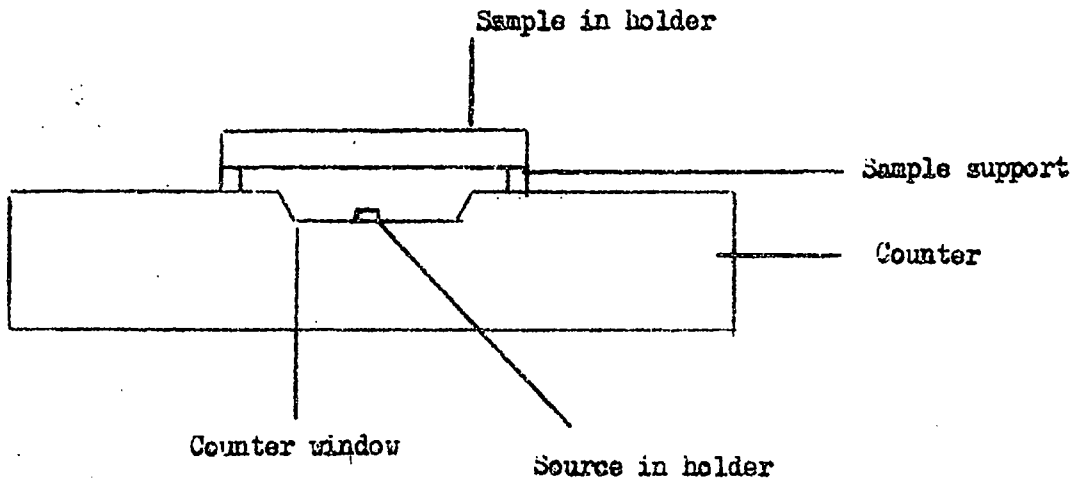

Fig. 1-3 Geometrical arrangement

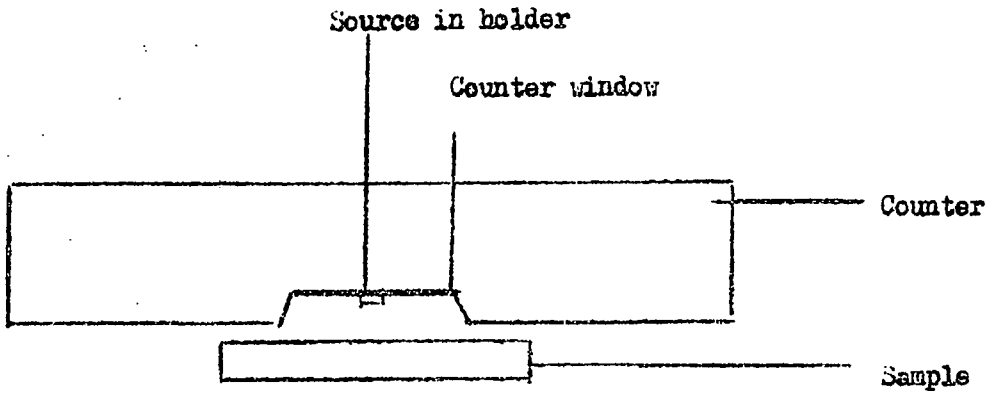

Fig. 1-4 Geometrical arrangement

electronic circuits. The balanced filter technique takes advantage of the difference in energy of the absorption edges of elements with a small difference between their respective atomic numbers. Two such elements give a filter system. The transmission of each filter for X-rays is made equal over the whole energy range except inbetween their absorption edges. (See fig. 1-5). In actual experiment, one filter is placed upon the counter window, then count rate is taken. With the filter replaced by the other filter, the count rate is taken again. The difference in transmission then represents the intensities of fluorescent X-rays whose energies lies between the two absorption edges e.g. Co K_α radiation (6.93 kev) can be isolated using the Mn K_α absorption edge (6.54 kev) together with the Fe K_α absorption (7.11 kev).

In case where the neighbouring fluorescent peaks are only partially resolved the individual fluorescent intensities can be determined by a method due to Dolby (58).

Let Y_A = resultant peak intensity for element A
Y_B = resultant peak intensity for element B
I_A = actual peak intensity for element A
I_B = actual peak intensity for element B
a_B^A = contribution constant for element B at peak position A
a_A^B = contribution constant for element A at peak position B

Then

$$Y_A = I_A + a_A^B I_B$$
$$Y_B = a_B^A I_A + I_B$$

Hence the constants can be evaluated and all I_A, I_B for mixtures of elements A and B calculated.

With the exception of the methods adopted to counter the absorption - enhancement effect, the discussion given in the section of dispersive systems can be carried over to

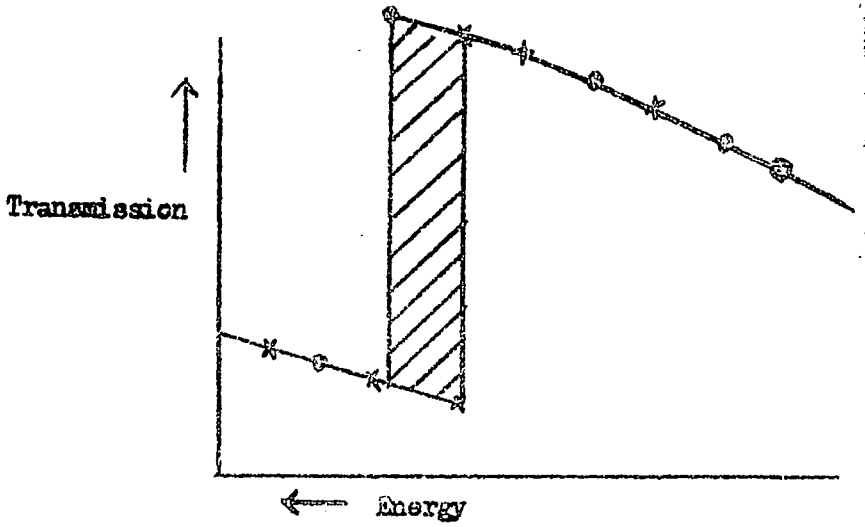

Fig. I-7 Transmission of filters when they are made balanced The shadowed portion represents the intensities of the selected radiations

the non - dispersive method. The low resolution of the detection system is such that the requirement for the characteristic radiation of the internal standard to be close to that of the element to be determined cannot be met, and this is true also for the use of scattered radiation. The low intensity of the fluorescent radiation means that the amount of the same element which must be added to produce significant change in the observed fluorescent intensity is such that one can no longer regard $(\mu_f \rho + \mu_p \rho)$ as being constant. These factors restrict the use of the non-dispersive method to simple systems, at the most binary mixtures of elements. For binary systems, the fluorescent intensity is calibrated against the respective weight percentage or weight fractions of the elements rather than their concentrations.

C. Advantages of non-dispersive method and some of the results obtained.

In spite of the afore mentioned limitations, the non-dispersive method can achieve useful results at considerably less cost than the dispersive method. The source is robust, portable and compact and lends itself readily to a wide variety of arrangement. The emission of X-rays from a given source is stable and reproducible over long periods, its only variation being that of the decay of the radioactive isotope for which correction can readily and accurately be made. The use of the proportional counter makes the resolution of long wavelength radiations easier than by using crystals which are difficult to obtain with the large lattice spacing required.

The method has been applied to alloy composition analysis (54,59) iron ore (60), glass (54), solution containing uranium (61) and cobalt in hydrocarbon (62). Large samples

have been examined by moving a specially designed detection system over the sample surface (63) the concentration either being expressed as an average, or as individual analysis for each part of the surface.

CHAPTER 2
Introduction to the Technique of Isotope method

Sources

These isotopes which emit alpha, beta, low energy gamma, and monochromatic X-rays can be used to excite the characteristic X-rays of elements. Monochromatic X-rays from these isotopes which decay by electron capture (eg. Fe^{55}, W 181) can excite very efficiently the characteristic X-rays of elements whose absorption edge energies lie at slightly lower energy than that of the monochromatic X-ray. For the excitation of the characteristic X-rays of a wider range of elements a bremsstrahlung source is more suitable. Bremsstrahlung sources are readily prepared by forming suitable combinations of a beta emitting isotope with a target element, the deceleration of the beta particles in the target matrix giving rise to bremsstrahlung. Suitable combinations are formed by mechanical mixtures eg. Pm 147 and aluminium powder; by adsorption eg. Kr^{85} on active charcoal; or by chemical combination, eg. H3 with titanium or zirconium metal.

The choice of a suitable source depends upon the energies of the characteristic X-rays which it is required to excite. The energies of the primary X-rays from the source should not be very much higher than required to bring about the excitation of the fluorescent X-rays, since higher energy radiation will cause an increase in background due to Compton

scattering and escape peak production without any increase in the intensity of the fluorescent X-ray. In analytical applications it is usual to excite the K X-rays of elements of low atomic number. For elements of high atomic number the fluorescent yield for K X-rays increases slowly with atomic number (64) whilst the photoelectric cross section for K electrons decreases rapidly (65) with the result that the fluorescence efficiency for K X-rays is not much better than that for elements of low atomic number. The available data on L X-ray fluorescent yields (66), and L electron photoelectric cross sections (67) shows that for elements of higher atomic number the fluorescence efficiencies for both K and L X-rays are similar. In such cases the use of a source which excites only the L X-rays is therefore preferable since it will result in a lower background due to less Compton scattering and elimination of escape peak production. A smaller biological hazard will also result with the use of lower energy source. Therefore the source chosen to excite X-rays over a wide range of elements should have a maximum energy no greater than 60 kev, sufficient to excite L X-rays from all elements, and K X-rays from elements lighter than thulium.

A wide choice exist in the physical size and shape of the source. The best shape is one designed to fit the perimeter of the counter window since this permits the maximum amount of fluorescent radiation from the sample to enter the counter, but unfortunately technical difficulties in the preparation of such sources greatly increase their cost. A more usual arrangement is that of a disc shaped source placed at the centre of the counter window. The source is mounted on a backing material of high atomic number of sufficient thickness to prevent access of primary X-rays to the counter.

COUNTERS

Geiger counters can be used to detect the fluorescent radiation. However since they are unable to discriminate between photons of different energies, Geiger counters must be used in combination with balanced filter systems for energy selection. The long "dead time" of such counters also makes them less suitable for high intensities of X-rays.

Proportional and scintillation counters can be used for direct energy selection since in both cases the voltage output is proportional to the energy of the incident photon. X-ray proportional counters are generally filled with Argon-methane or Xenon-methane gas mixtures the choice of filling being determined by the photon energy it is required to detect or the positions of escape peaks if they should occur. The counter is fitted with a thin beryllium window with as large an active area as is possible consistent with mechanical stability. To minimise loss by absorption in the case of low energy X-rays a gas flow proportional counter which permits the use of extremely thin windows is used. A hydrogen or helium optical path between the sample and counter window is also used to further reduce absorption losses. The scintillation counter uses a crystal of sodium iodide activated with thallium, and optically coupled to a suitable photomultiplier tube. The window consists of a thin layer of beryllium metal to minimise absorption of the X-rays.

ENERGY SELECTION

The selection of the fluorescent X-rays is made by measurement of the output pulse from a proportional or scintillation counter.

In the case of the proportional counter the size of the output pulse is determined by the energy deposition within the counter this latter being determined by the energy of the X-ray photon. The size of the output pulse from the

counter is strongly dependent on the high voltage applied to the anode, and this voltage pulse from the counter is small and must be amplified considerably before detection. In order to avoid attenuation and distortion of the pulse in connecting cables a pre-amplifier with cathode follower output is placed as close to the counter as possible, the pulse being then fed to a high gain amplifier. It is desirable that amplification of the output pulse should be linear in order to differentiate pulses arising from X-ray photons of different energies. After amplification selection of pulses is made electronically by means of a pulse-height analyser which has one or more channels of variable threshold energy. The number of pulses in a given voltage range is then recorded by means of a scaler or ratemeter.

The requirements for the scintillation counter are similar to those of the proportional counter, except that the initial amplification is provided by the photomultiplier tube, the pulses being fed via a cathode follower output directly to the linear amplifier.

The fluctuation in the total number of ion pairs formed in the proportional counter by absorption of photons of the same energy gives rise to Gaussian pulse height distribution with a standard deviation nearly equal to 1.6 times the square root of the number of electrons in the initial ionisation (68). This combined with the fluctuations in the associated electronic circuits gives an overall standard deviation considerably greater. For the scintillation counter the distribution in pulse height arises from fluctuation in fluorescent yield in the crystal, in amplification by the photomultiplier, together with that of the associated electronic circuits.

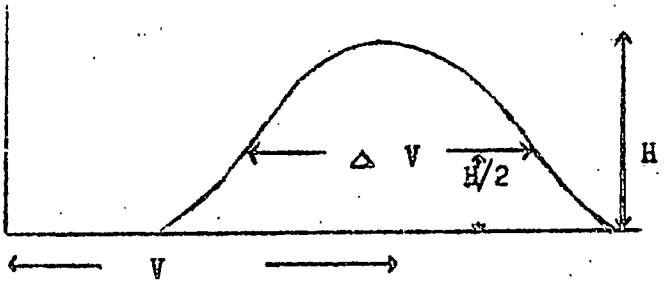

A measure of the extent of the fluctuation is given by the ratio

$$\frac{\text{Width at half height of distribution}}{\text{Mean amplitude of pulse}} = \frac{\Delta V}{V}$$

This ratio is referred to as the resolution of the counter. The behaviour of different systems can be compared by examining their resolution for a given radiation eg. Cu K_α (68)

Detector	Resolution
Proportional counter	20%
Scintillation counter	50%
Li F system (dispersive)	1.5%

A further method of energy selection is that using filters. In practice it is difficult to make filters completely balanced over the whole energy range (69) especially that far away from the absorption edges of the filters. Thus one finds that energy discrimination with a proportional counter is still necessary, but the use of such filters allows an increase in the channel width of the pulse analyser with a consequent increase in sensitivity and resolution. It has recently been claimed that selective filters can be made balanced over the whole energy range making further energy selection with a proportional counter unnecessary (70). In such case a geiger counter can be used as a detector.

CHAPTER 3

Preliminary Work

Sources

In the present work the use of two different types of source was investigated

(a) Bremsstrahlung source.

(b) γ-emitting source.

The radioisotope source used to produce bremsstrahlung was the pure β - emitting isotope Pm^{147} (71).

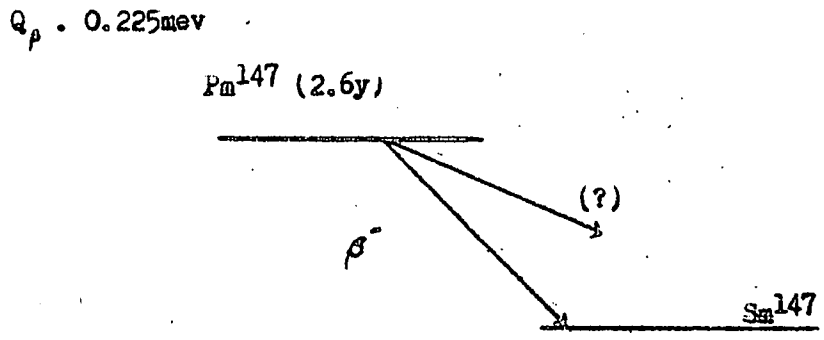

The source, prepared by the Radiochemical Centre, Amersham, consisted of 1 curie of Pm^{147} bonded in aluminium as target element placed on a backing of metallic gold (see fig 3.1). Two such sources were obtained the first being considerably contaminated with Eu^{154}. This latter isotope has a half life of sixteen years and gives high energy γ-rays.(72)

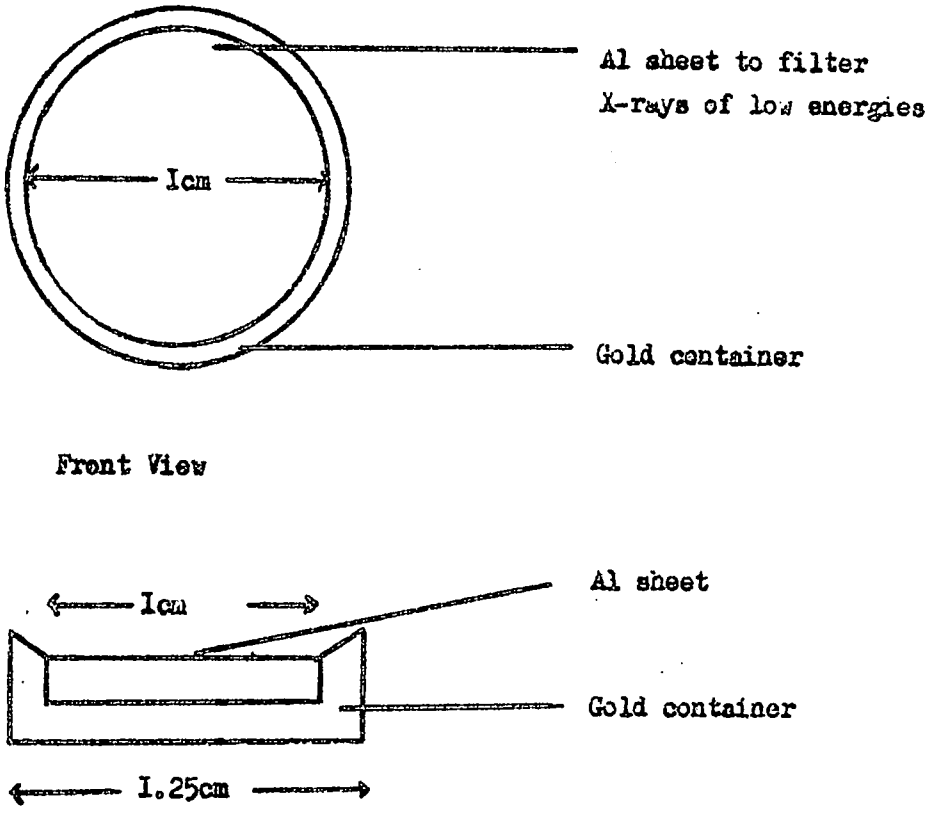

Fig. 3-1 Pm^{147}/Al Source

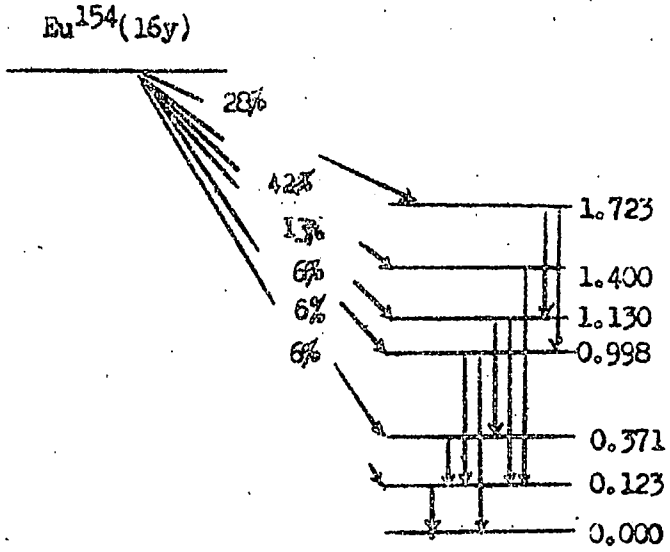

The γ - emitting source consisted of Co^{57} (72)

$Q_{EC} = 0.57$mev

All energy level in mev

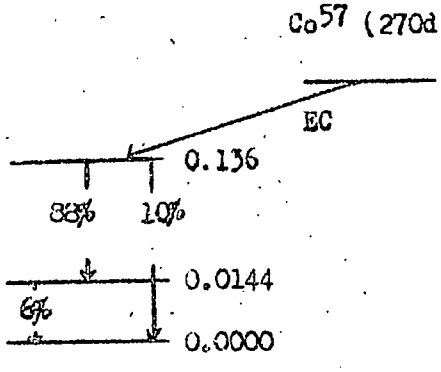

1 millicurie of Co^{57} as cobalt chloride in dilute hydrochloric acid was obtained from the Radiochemical Centre, Amersham. The source was prepared by evaporation of the solution in a platinum cup 0.4 cm. in diameter after which the deposit was covered with a thin layer of vinylite resin, the latter being prepared by addition of a dilute solution of V.Y.N.S. (1 part resin: 30 parts solvent) resin in cyclohexanone and allowing the solvent to evaporate.

Instruments

A commercially available proportional counter was used throughout this work. Manufactured by 20th Century Electronics limited, the counter (type Px 130B/XE) was filled with a Xenon - methane mixture and fitted with a thin beryllium window 3.5 cms in diameter. The remaining units of the assembly were standard nucleonic instruments manufactured by Dynatron Radio Ltd. A block schematic diagram of the layout is shown in fig. 3-2.

Instrument Settings

Optimum instrument settings were selected. The most important of these were the high voltage applied to the counter and the pulse integration and differentiation time constants of the linear amplifier.

(a) Counter voltage

With both amplifier time constants arbitrarily set at 0.32 microseconds and the pulse analyser discriminator threshold set at 10 volts, observation of the background noise level of the counter was made for various applied voltages. A noticeable increase in noise level began at an applied field of 2500 volts and increased rapidly for applied voltages in excess of 2900 volts (see fig. 3-3). The counting efficiency for a fixed source counter - geometry (selected so that the counting level was not too high) was determined as a function of counter voltage (see fig. 3-4). The best condition was found for an applied voltage of 2000 volts.

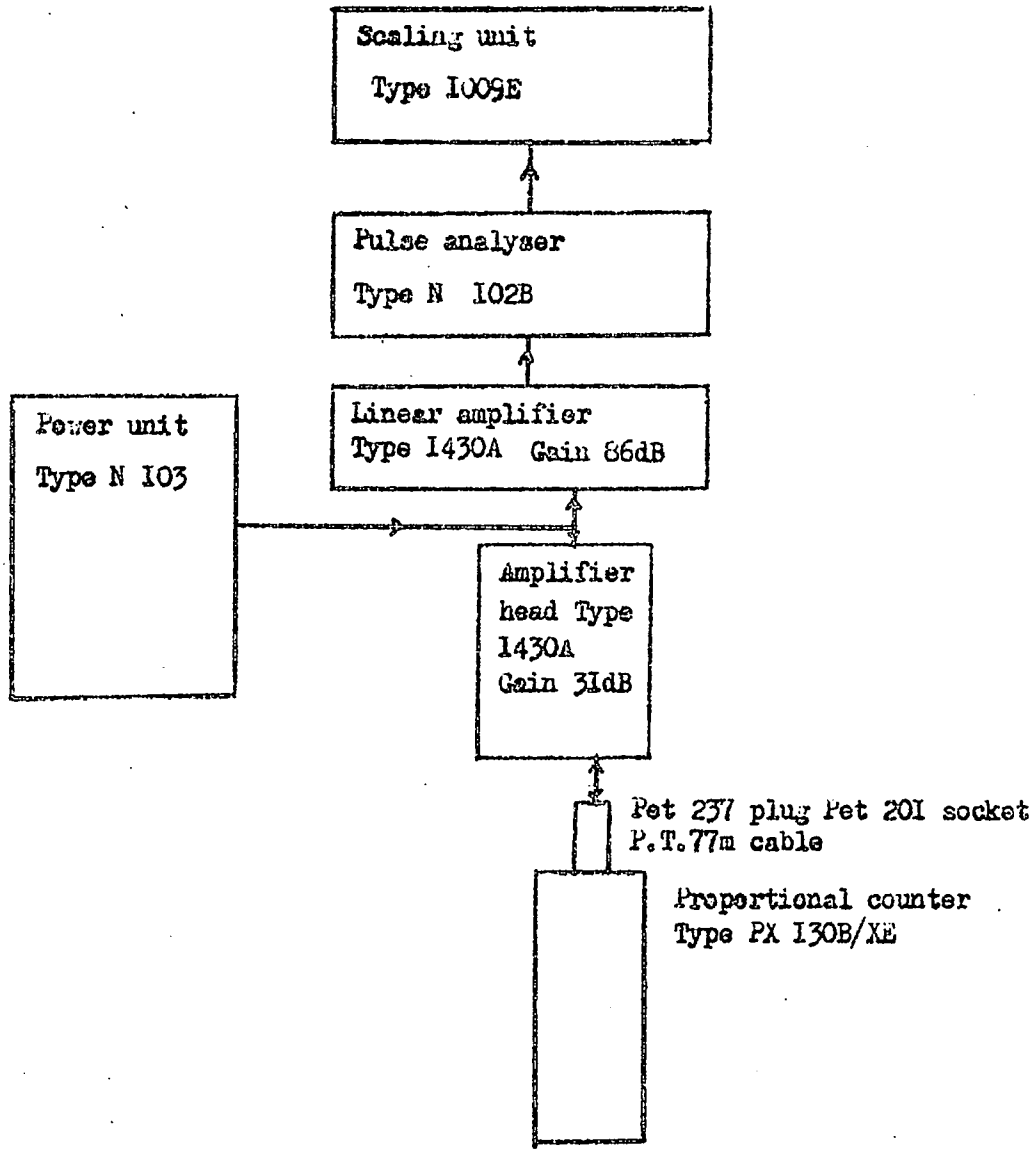

Fig. 3-2 Schematic diagram of instruments

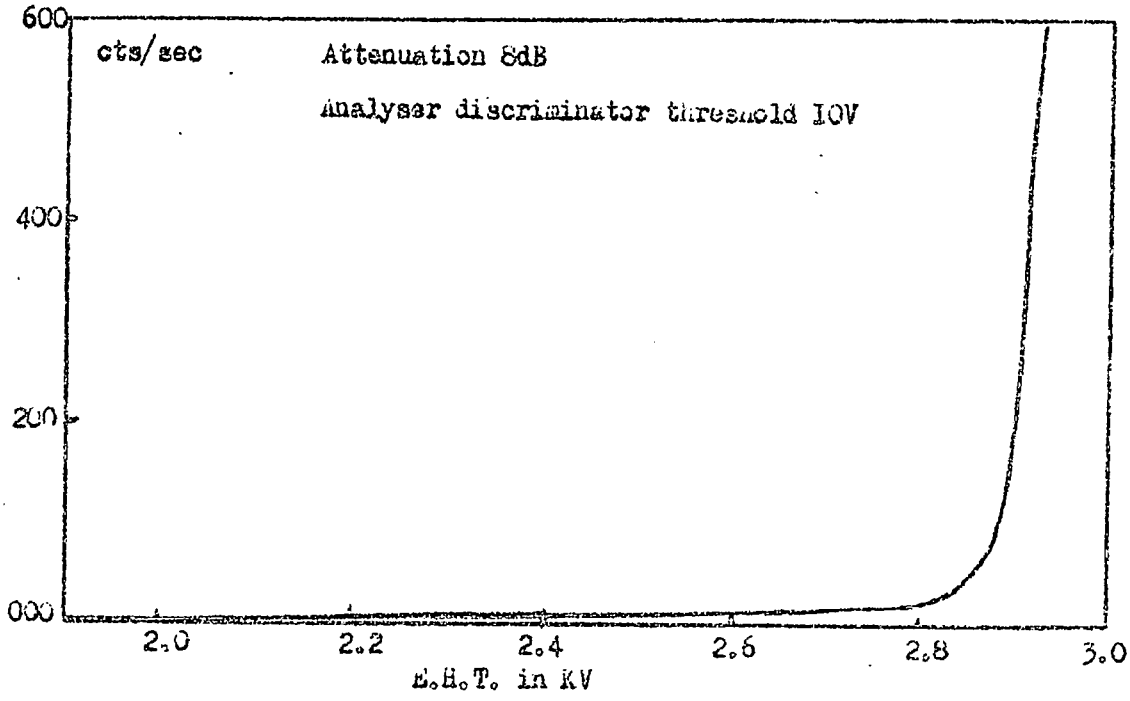

Fig. 3-3 Background noise of the instruments with E. H. T.

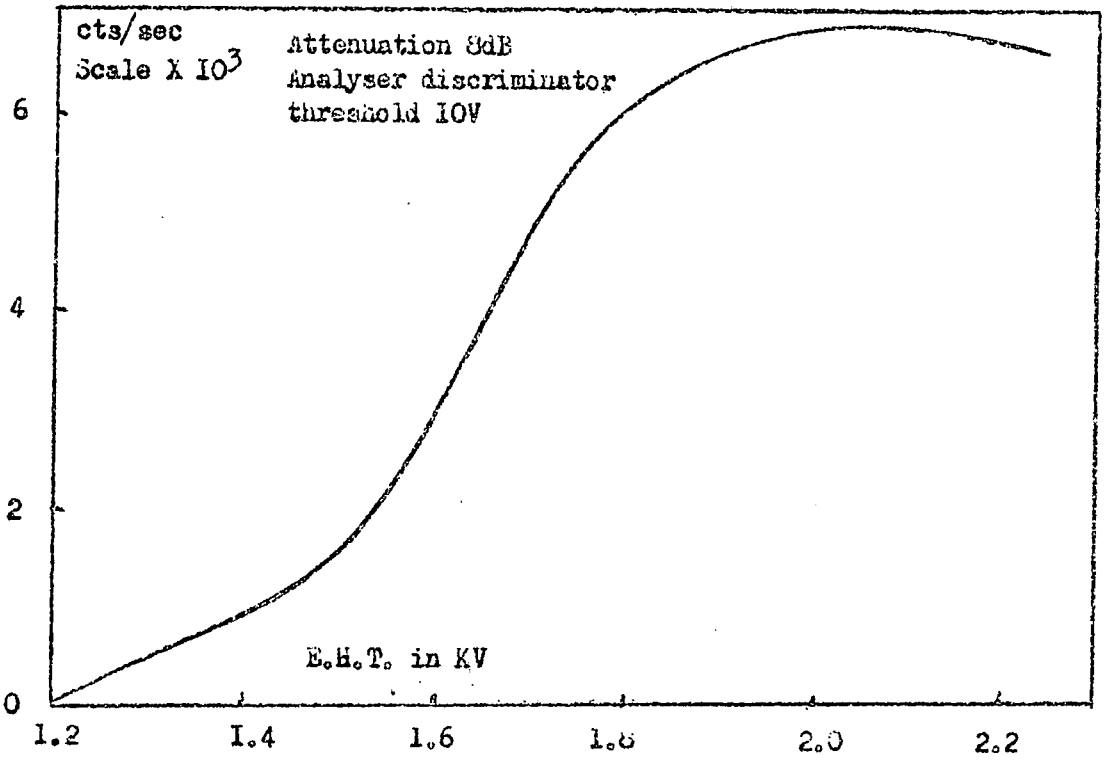

Fig. 3-4 Counting efficiency and E.H.T.

Measurements were also made of the variation in peak position of the Cu K radiations with applied counter voltage (fig. 3-5). The high voltage supply unit was said by the manufacturers to have a stability of 0.0 5% for a variation in mains voltage of 10%. Such a variation would shift the peak position by 0.8% with the applied voltage at 2000 volts, and in order to avoid this a main stabiliser (Servomex Controls Ltd., type A.C. 2 Mark II A) was used to supply the H.T. unit.

(b) Amplifier time constants.

Using Cu K X-rays as standard the resolution of the instrument was determined as a function of the integration and differentiation time constants of the linear amplifier. With instrument settings;

Counter voltage : 2000 v

Amplifier attenuation: 18 dB.

Pulse analyser channel width 1.0 volt the results were as follows.

Diff^{n}. time constant (μ secs)	0.08	0.16	0.32	0.80	1.60
Int^{n}. time constant (μ secs)	0.08	0.16	0.32	0.80	1.60
Resolution in percentage	50	33	26	32.4	42.5

The best resolution was obtained with both time constants at 0.32 secs. A percentage resolution of 20% has been claimed by Parish and Kohler (73) using Cu K_{α} radiation, but in the present work no attempt has been made to separate the K_{α} and K_{β} radiations which may account for the lower resolution.

Calibration.

The fluorescent X-ray of an element is determined by observing the counter response for a fixed pulse analyser channel width with variation of the channel threshold voltage. The channel threshold voltage at the maximum of the peak is characteristic of the element. Profiles of counter response for a number of elements are shown in fig. 3-6. It will be

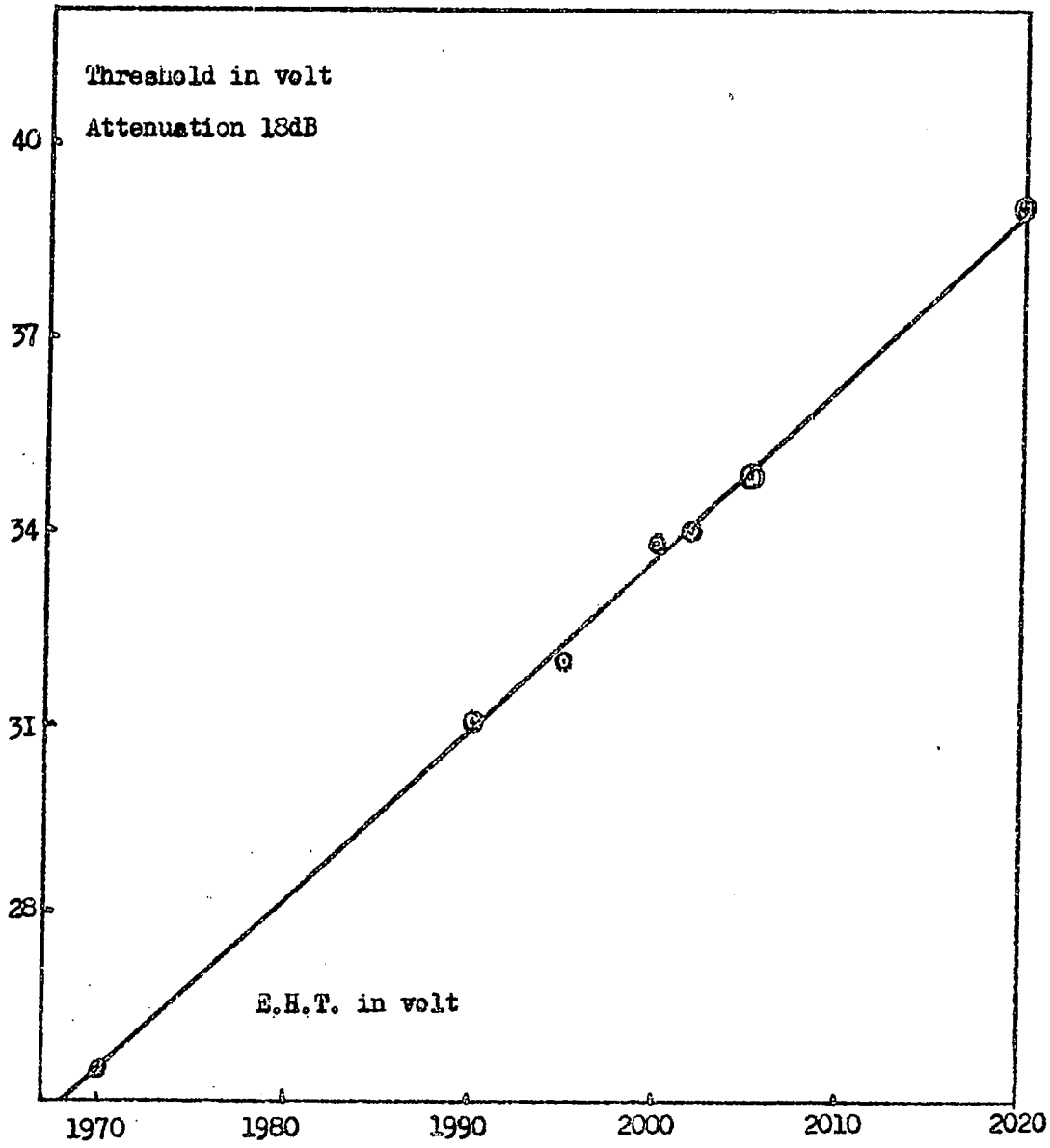

Fig. 3-5 Variation of peak(CuK) position with E.H.T. The slope value is 0.268V threshold per vold change in E.H.T.

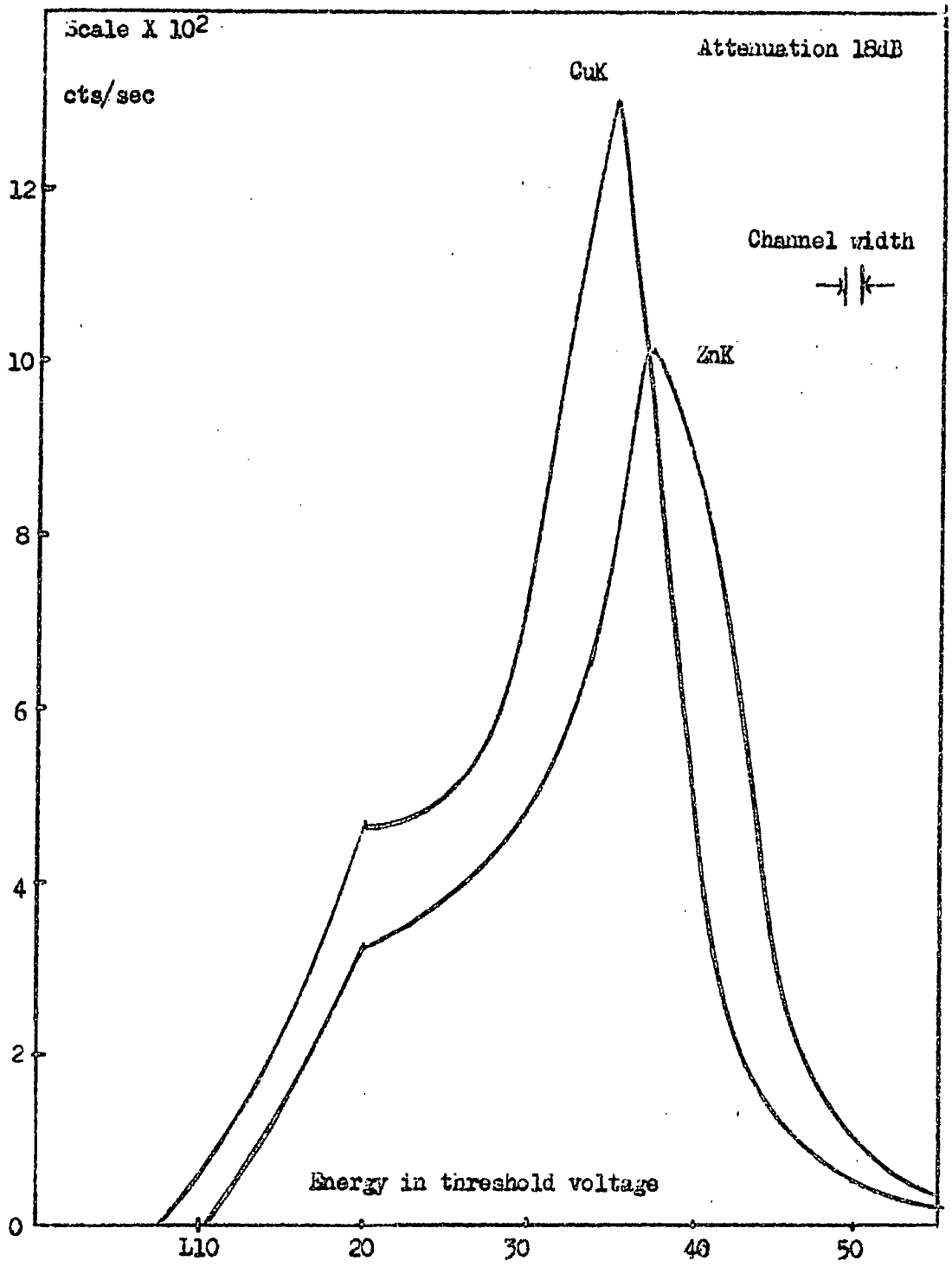

Fig. 3-6 Profiles of counter response for Cu and Zn strips

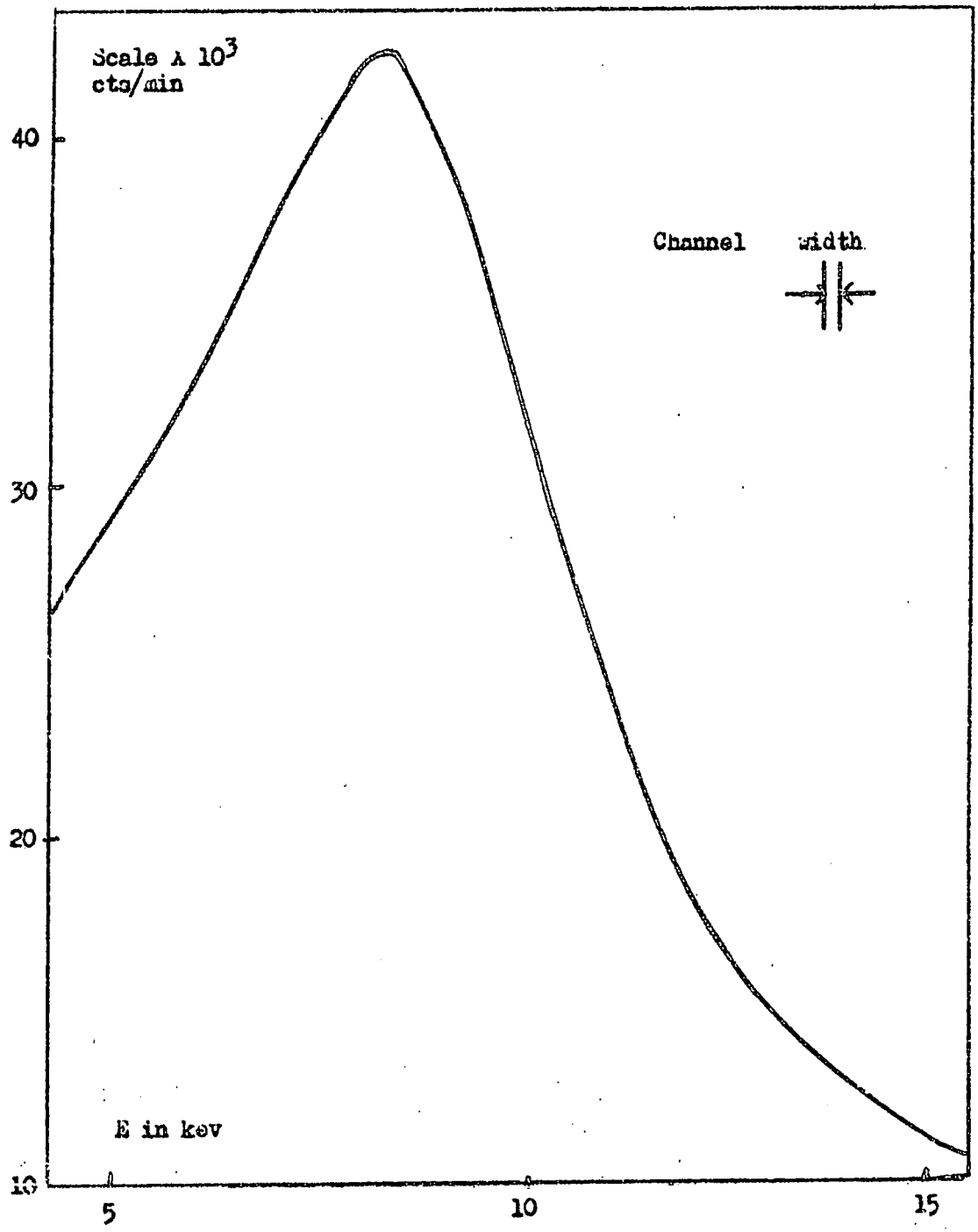

Fig. 3-6a Spectrum from tantalum metal.

observed that the distortion is not of the gaussian form expected the profiles being distorted on the lower energy side. From the observation that this distortion appeared to move with the element's peak it was at first thought to be due to escape peak production. As more results were obtained however it became clear that this apparent movement was due to the changing shape of the profile, and that the distortion was a feature of the primary X-ray spectrum, the separation between the fluorescent peak and the distortion increasing with atomic number.

The mean amplitude of the pulses from the counter should be proportional to the energy of the X-ray photon producing the pulses. This was confirmed by plotting the peak position in volts against the known energy of the characteristic X-rays (see fig. 3-7). From these graphs the approximate mean pulse amplitude in volts can be determined for X-rays of any energy, and conversely the energy of X-rays can be determined from the mean pulse amplitude.

Some comment is necessary on the choice of energy value for the fluorescent X-ray peak. The low resolution of the counter does not allow the K X-rays to be split into the components $K_{\alpha 1}$, $K_{\alpha 2}$, $K_{\beta 1}$, and $K_{\beta 2}$ radiations, and so all will make a contribution to the observed peak. The relative intensities of the component radiations are (74):

$K_{\alpha 1}$	100
$K_{\alpha 2}$	50
$K_{\beta 1}$	21
$K_{\beta 2}$	3

In assigning an energy value to the fluorescent peak that of the $K_{\alpha 1}$ radiation has been chosen since it makes the greatest contribution to the resultant peak height.

The mean pulse amplitude for a given X-ray can also be varied by variation of the pulse attenuation, a control for

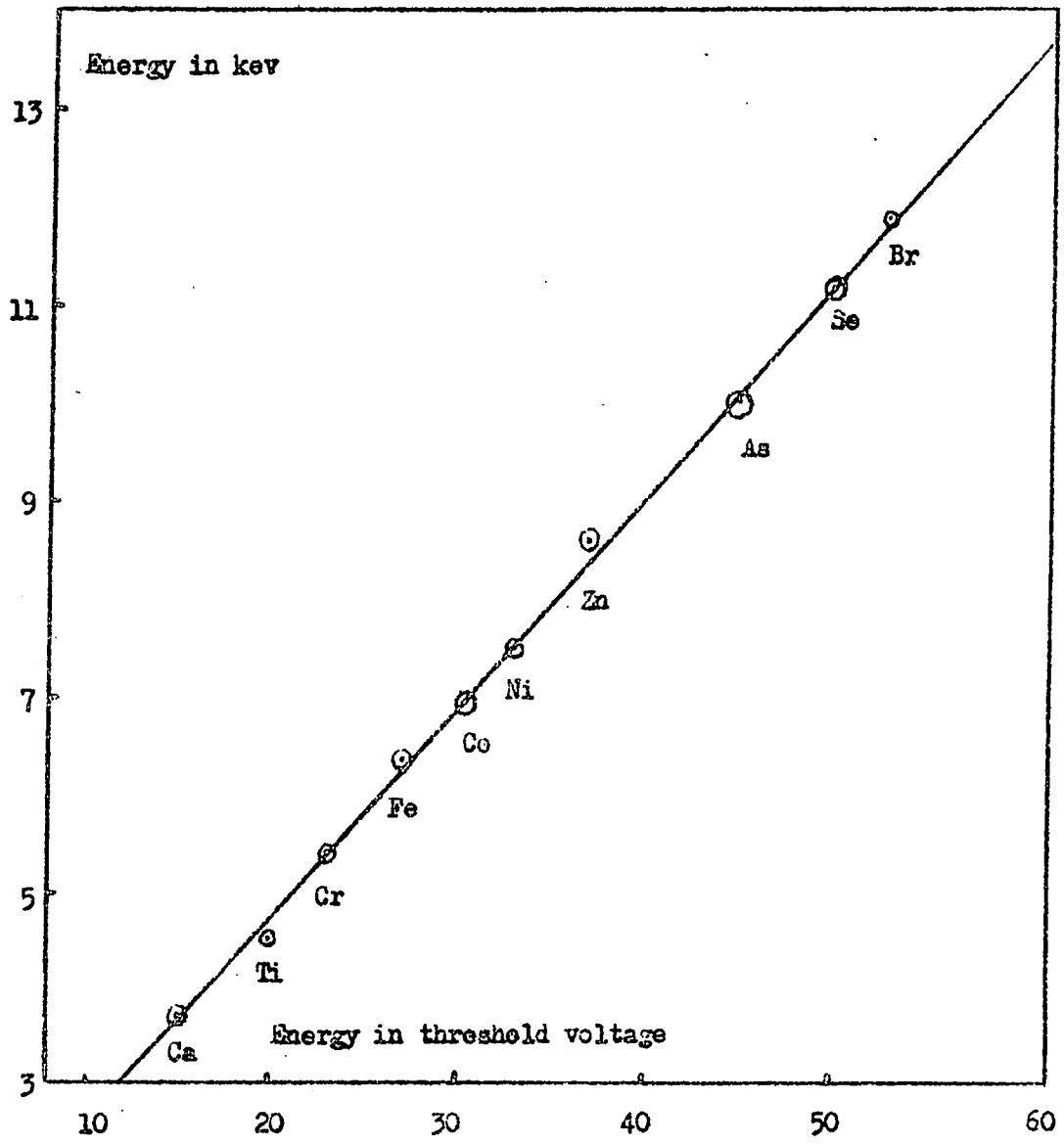

Fig. 3-7 Calibration of the instruments at 18dB
Energy in kev against threshold voltage

which is a feature of the amplifier. Provided that the input and output impedances of the amplifier are equal, the pulse amplitude measured at different attenuation can be related to a standard attenuation using the relation.

$$\text{Attenuation value in decibels} = 20 \log \frac{(V_1)}{(V_2)}$$

Where V_1 = pulse amplitude at attenuation value 1

V_2 = pulse amplitude at attenuation value 2

After correction to a standard attenuation value the square root of mean pulse amplitude for K X-rays was plotted as a function of atomic number, the relation being linear as expected from the Moseley relation (fig. 3-8). From such a graph the peak position for K X-rays for any element can be determined for the standard attenuation value.

Determination of counter "Dead time".

The "dead time" of a proportional counter is normally only a few microseconds and can be neglected for all but very high values of count rate. It was considered however that the associated electronic circuits might make a significant contribution to "dead time" and so a determination was made by the method of Martin (75). This is based on the equation

$$ne^{\lambda t} = No - n No\tau$$

where n = observed count rate.

λ = disintegration constant of isotope observed.

No = True count rate.

τ = "dead time".

t = time

A sample of Mn^{56} ($t_{\frac{1}{2}}$ = 2.576 hrs), was prepared by the reaction Fe^{56} (np) Mn^{56}, and after allowing one hour for the decay of short lived species the decay was observed with the counting set. A plot of $ne^{\lambda t} \sim n$ gives a linear relation for which the slope is $No\tau$. The intercept then gives No and τ

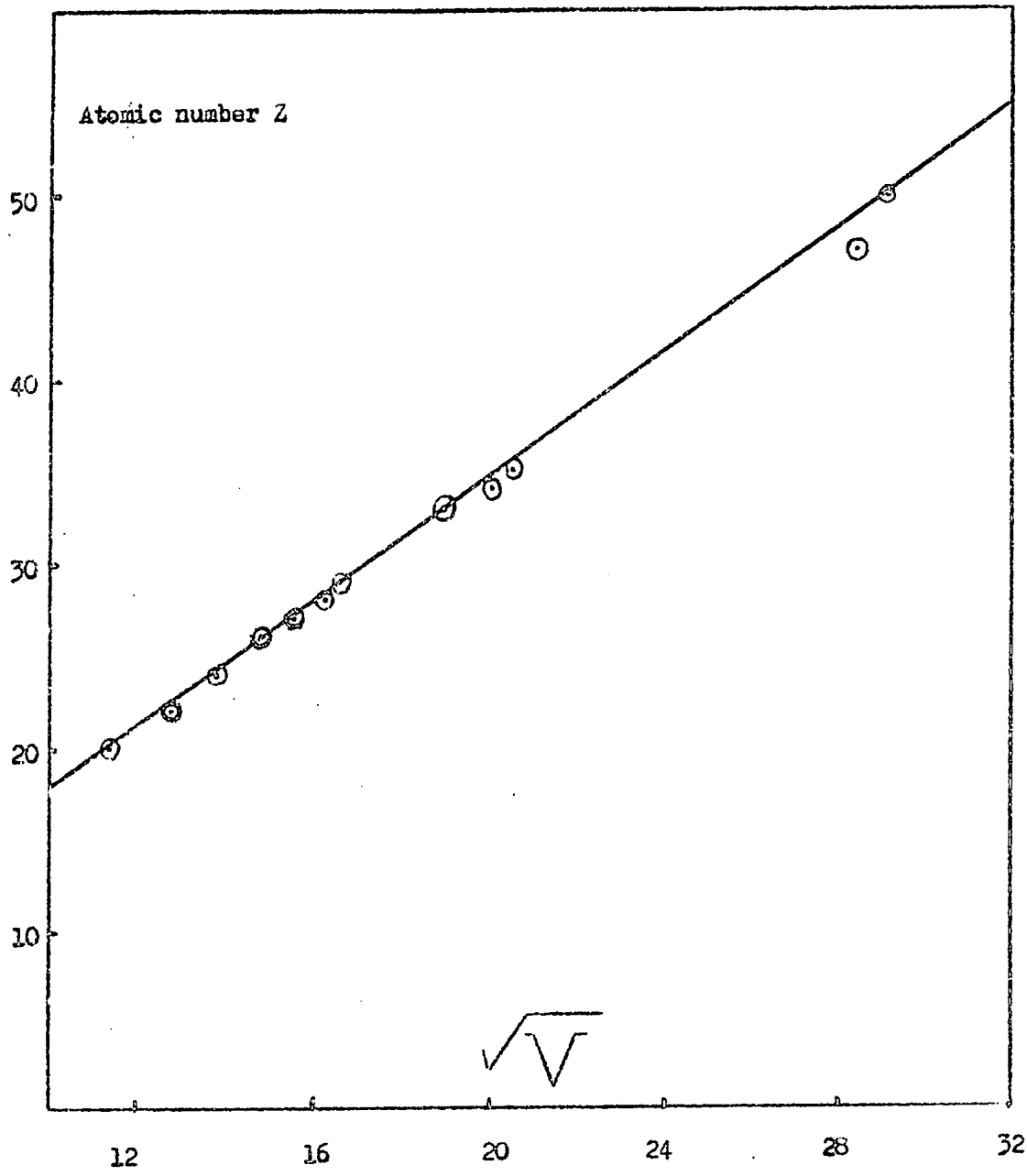

Fig. 3-8 Atomic number Z against square root of mean amplitude of pulses produced by K X-rays (after correction for attenuation)

is determined. Results are shown in fig. 3-9, and give a value for dead time of 101 μ seconds. This value was used to correct the observed data where necessary.

Primary X-ray spectra of Sources.

(a) Co^{57} spectrum.

The spectrum of the Co^{57} source measured with the proportional counter is shown in fig. 3-10, and is considerably different from that expected on the basis of its decay scheme (page 22). Assuming linearity of the energy scale above the highest energy of fluorescent X-ray measured (Ce K:- 34.7 kev) no peak is found for the γ -ray of 122 kev energy, but instead a broad distribution is obtained. Some factors contributing to the observed spectrum may be:-

(1) the low photoelectric cross section of Xenon (the principal component of the counter filling gas) for radiation of 122 kev energy.

(2) the high energy photoelectrons arising within the counter from the photoelectric interaction are neutralised by the counter wall before losing all their energy by ionisation of the counter gas. Such an effect would give rise to a lower pulse output than would be expected for 122 kev energy, and a broad distribution of pulse heights would be obtained.

(3) at an energy of 122 kev the Compton scattering cross section will be comparable with the photoelectric cross section, again giving continuous pulse height distribution.

(4) since the source decays by an electron capture process the associated inner bremsstrahlung effect would make a contribution to the spectrum.

(b) Pm^{147} spectrum

Two sources (I and II) were purchased from the Radiochemical Centre, Amersham, both nominally containing 1 curie of Pm^{147}. The spectra of the sources measured with

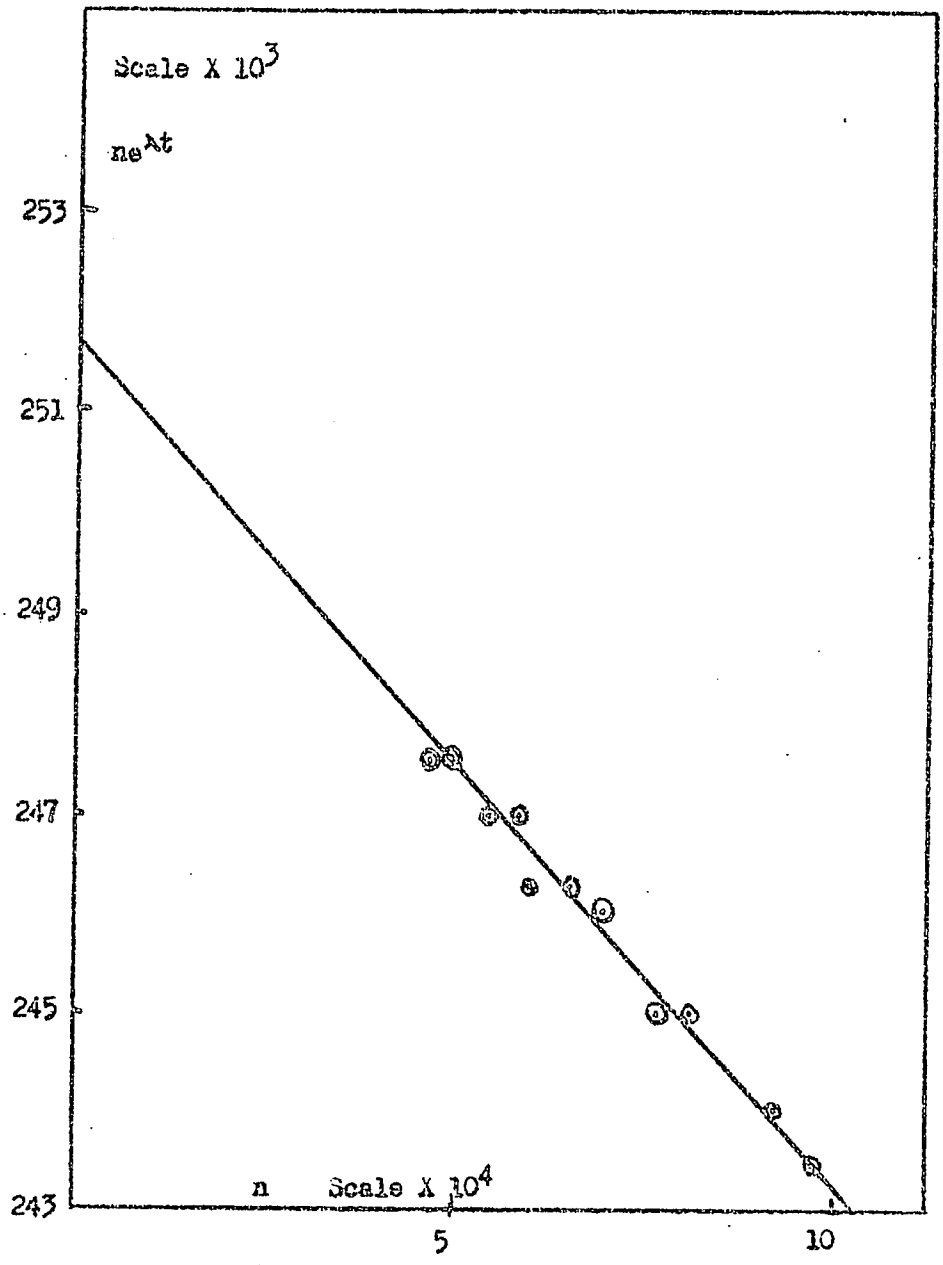

Fig. 3-9 $ne^{\lambda t}$ against n to find the "dead" time of instruments
n is counts/300seconds from ^{56}Mn t is equal to time
λ the decay constant

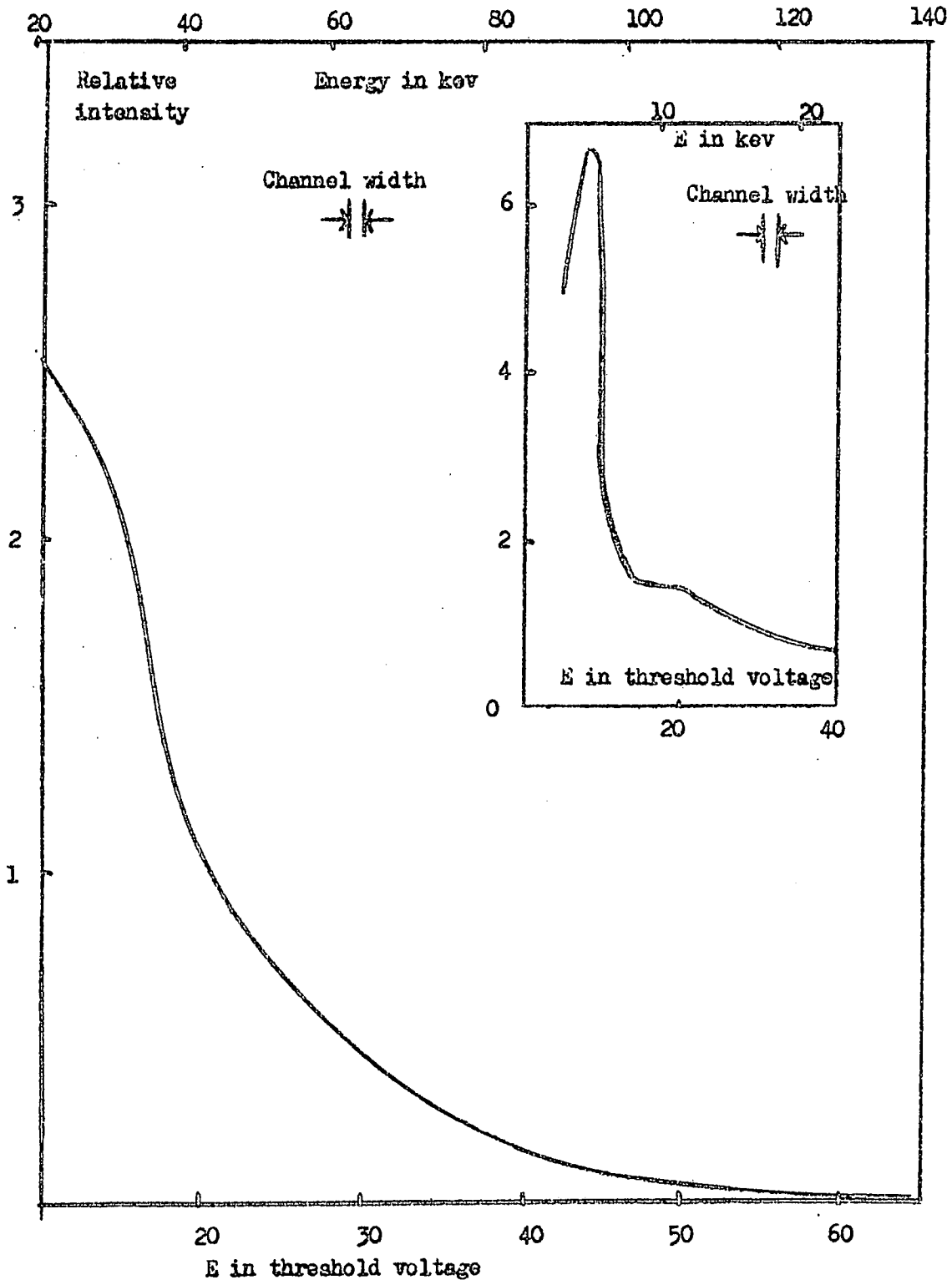

Fig.3-10 Primary spectrum of Co^{57} Relative intensity against threshold voltage (the inserted diagram is the lower energy portion of the spectrum at lower attenuation value)

the proportional counter are shown in fig. 3-11, and were obtained by exposing the counter to the direct radiation from the source which was placed at a sufficient distance from the counter to give a reasonable value of the count rate. The spectra shown are similar in shape to the published spectrum (76). However there is some doubt as to whether these spectra truly record the bremsstrahlung intensity as a function of energy. The experience with the Co^{57} source shows that the counter is less sensitive to the higher energy radiation and some at least of the fall off at high energies must be attributed to this cause. Again, with the geometry adopted to give reasonable values of the count rate, a disproportionate attenuation of the lower energy bremsstrahlung is to be expected due to air absorption.

Although nominally of the same strength it can be seen from fig. 3-11 that the intensity of radiation from the sources is not the same. This could be due to a difference in the degree of mixing of the Pm^{147} with the aluminium matrix. When the sources were examined with a geiger counter using a lead absorber to remove bremsstrahlung both sources showed the presence of high energy γ-rays. A consultation with the makers of the sources confirmed the presence of radioactive isotopes of europium. The level of contamination of the two sources is different, a lead absorber experiment using a geiger counter as detector showing that one source had 50 times as great a contamination (see Fig. 3-12).

The presence of the high energy γ-ray contamination will also make a contribution to the observed spectra of the sources. By the method used to measure the spectra the effect of the γ-ray contamination will be magnified by the fact that the whole body of the proportional counter will be sensitive to the γ-rays whereas only the relatively small windows will allow the bremsstrahlung to enter. A further measurement of

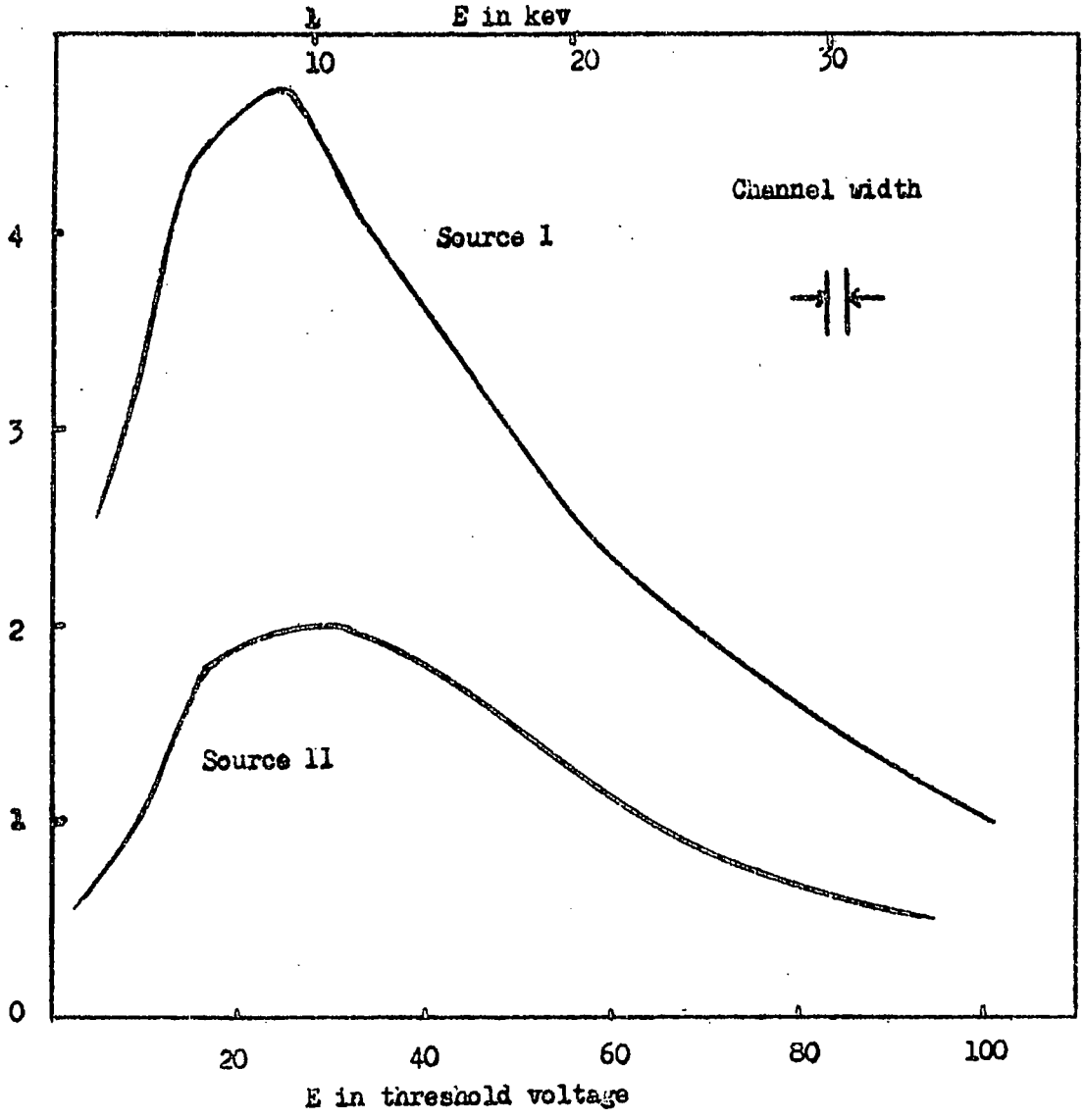

Fig. 3-11 Spectra of two Pm^{147} sources (relative intensity against energy)

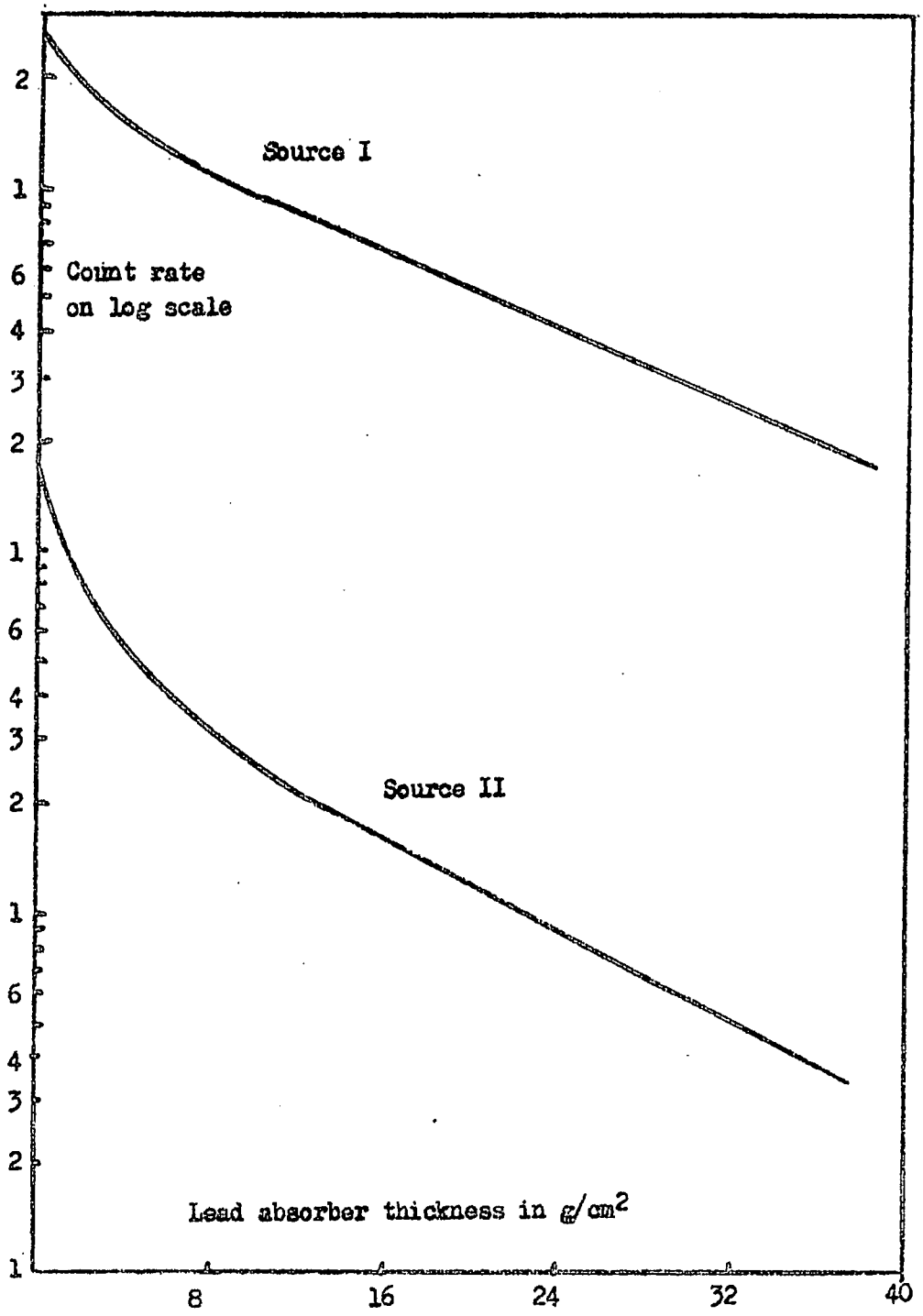

Fig.3-12 Count rate on log scale against absorber thickness using source I and II

the source spectra was made in which the body of the counter was covered in layers of lead sheet to stop the γ-rays, the counter windows being left free. The results are shown in fig. 3-13, and indicate that the γ-rays have made a considerable contribution to the primary spectrum in the bremsstrahlung region.

The foregoing discussion suggests that for the present only valid method for comparison of the two sources is one of comparing the intensity of fluorescent radiation which they produce in the same sample of material. In the present case because of the very much higher γ-ray level in one of the sources it was not possible to do this comparison in the same geometry.

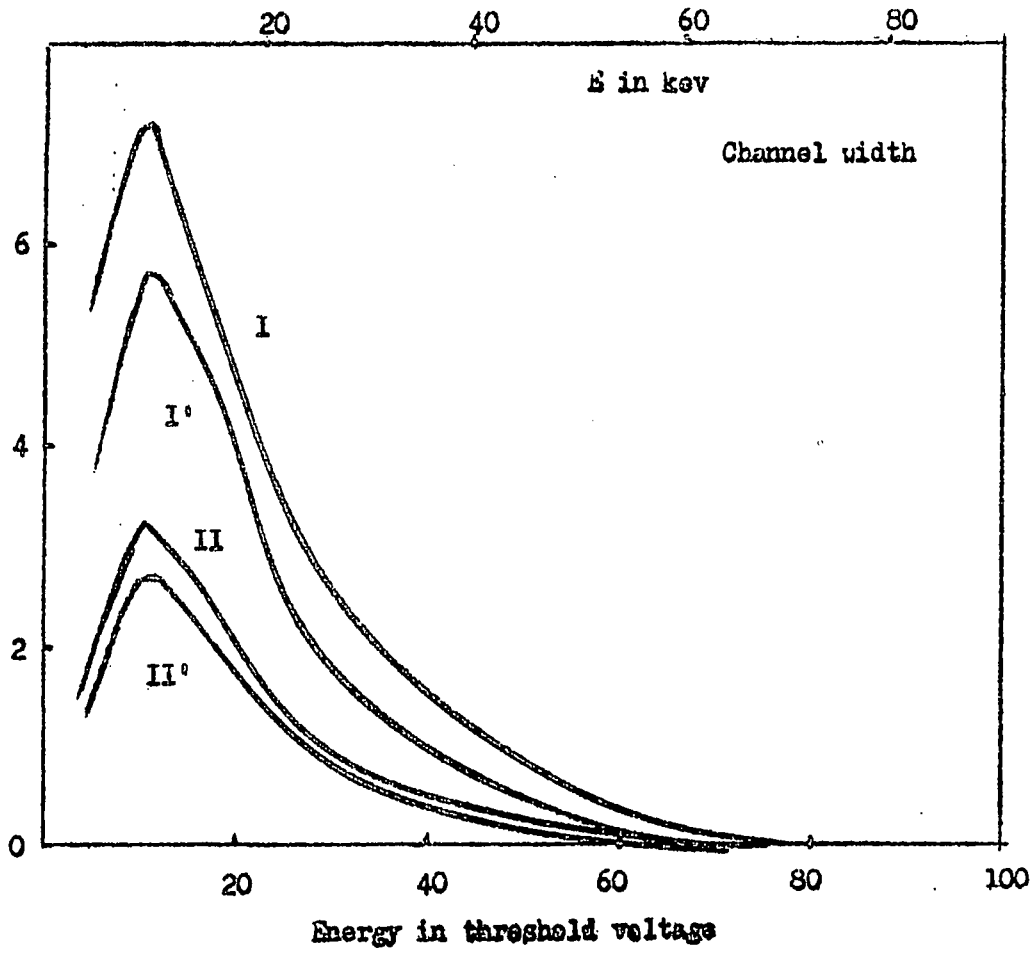

Fig.3-13 Relative intensity of source I and II (I' II' are spectra obtained with the counter body covered with lead plates) against energy

CHAPTER 4

Liquid Solutions (Pm^{147} source)

The use of solutions has the advantage of providing a readily reproducible homogeneous sample form, thus reducing the number of variables to be considered. The liquid solutions used in the present work usually involved water or dilute acid as the solvent.

Because a wide range of elements was to be investigated for which the optimum conditions (e.g. sample-source distance) required to give the highest ratio of peak fluorescent intensity to background intensity are not always identical, it was decided to select these conditions for one element whose characteristic X-ray energy represented an average value, and then use the same conditions for all elements. The element chosen was bromine, solutions of the element being prepared by dissolving potassium bromide in water.

Experimental arrangement

Three different arrangements of source, sample and counter were investigated, these being depicted in fig 4-1 and labelled A, B, and C.

A:- In this arrangement the sample cell consisted of a plastic cup which was filled to a measured volume with the solution to be determined. A number of shelf positions were available to alter the source sample distance. In practice the arrangement gave a lower fluorescent peak to background ratio than could be achieved with other arrangements. This

The three Geometrical Arrangements tested (Fig. 4-1)

A Front View

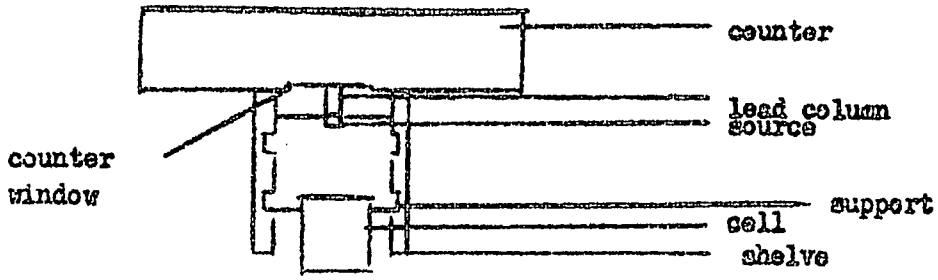

B Front View

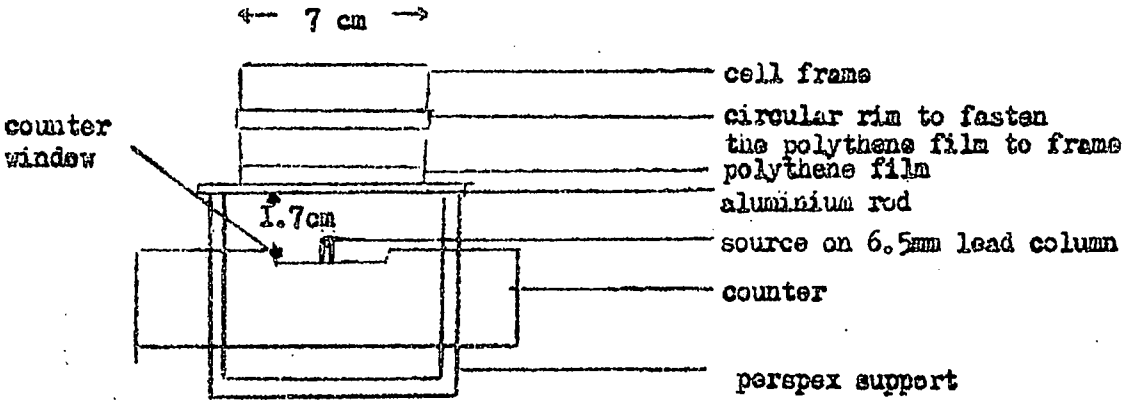

C Side View

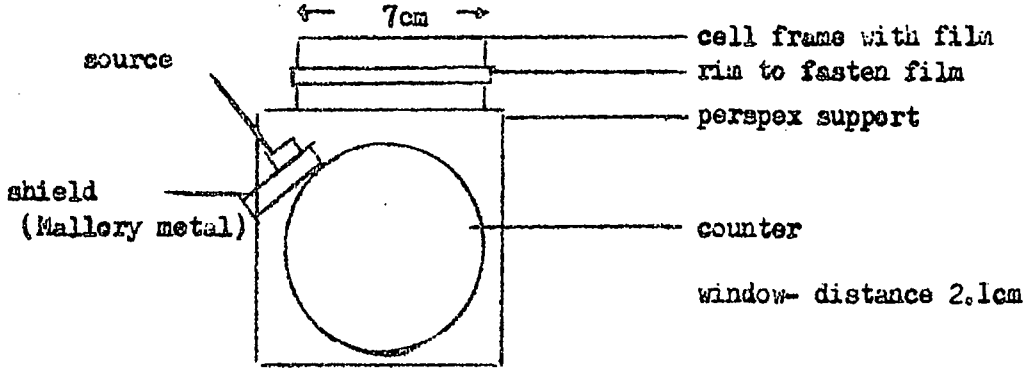

could be attributed to scattered radiation, from the sample support and bench, entering the counter. The fluorescent intensity was found to be very sensitive to small changes in level of the sample surface such as might occur through inaccuracies in the measurement of sample volume. For the above reasons A was replaced by the arrangements B and C.

B:- The sample cell consisted of a polythene cylinder one end of which was closed with a thin film of polythene. The polythene film was stretched over the end of the cylinder and then held in place by a ring of polythene. The cell was supported over the source and counter window on two aluminium rods.

C:- This was adopted when using the source with the higher europium contamination (source I), the counter window being shielded from direct radiation by a shield of high density tungsten - copper alloy (mallory metal). The cell arrangement was identical with that in B.

The arrangements B and C gave better reproducibility and were also much more tolerant to small displacements of the sample cell. However B is to be preferred when possible.

Sample size

According to equation 1.1 the fluorescent intensity from the sample varies with concentration and with the factor $(\mu_p + \mu_f)\rho$ for a sample having an infinite thickness. Determination of the fluorescent intensity as a function of sample depth for various concentrations of reference sample are given in fig. 4-2, and show that the condition of infinite thickness is satisfied for sample depths of a few centimetres. A consideration of the results for a sample concentration of 10 gms. KBr/ litre shows a rise of fluorescent intensity with increasing depth up to a maximum at a sample depth of 2.4 cms. and is constant at higher values of the depth. The background level, increases with increasing depth. A sample depth of 2.8 cms. was chosen as providing an adequate

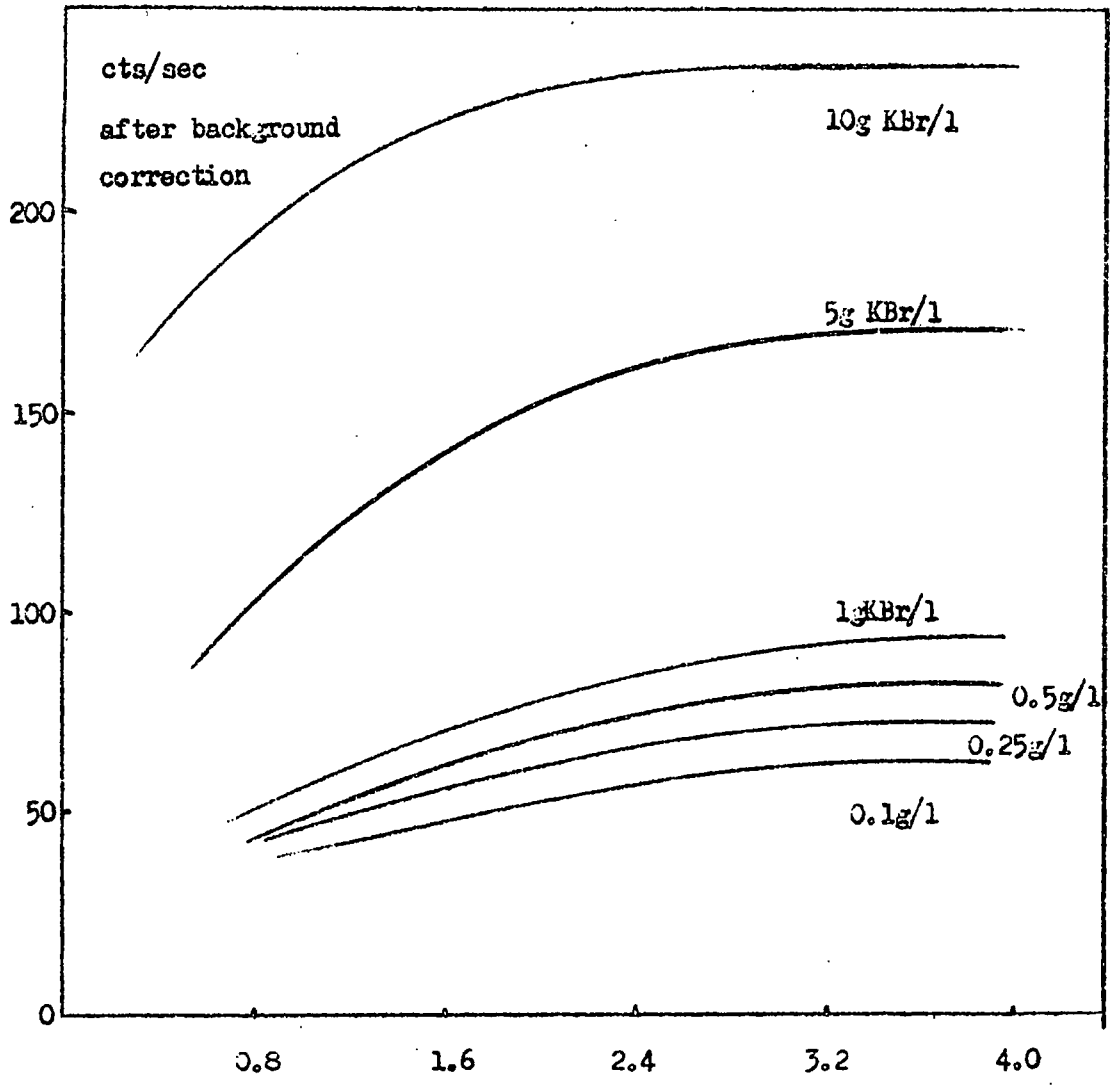

Fig.4-2 Line intensity (BrK X ray) against depth of solution to the critical thickness of liquid sample.

fluorescent intensity with an acceptable background level, and for the cell diameter available gave a sample size of 90 c.cs.

Background Correction

The correction of the observed results for background level presents a difficult problem particularly for multicomponent samples. If the background were constant with respect to concentration the correction could readily be made using a blank determination. For samples containing a single heavy element it seemed reasonable to assume that the radiation intensity at some position higher in energy than the fluorescent radiation from the sample would be due to background only, and that its variation would be similar to that of the background radiation at the fluorescent peak position. For an arbitrarily chosen off-peak position the variation of intensity was studied as a function of concentration for a range of elements. The results, expressed as the ratio of intensity at concentration x ($B.G_x$) to intensity at zero concentration (B.Go) plotted against concentration, are shown in figs 4-3 and 4-4 and indicate that the background level varies with concentration.

With the assumption that the variation in background was mainly due to absorption by the only heavy element present a somewhat less arbitrary method of correction was arrived at. Figure 4.5 shows a typical plot of the mass absorption coefficient of an element as function of X-ray energy, the position of the characteristic X-ray of the element also being shown (a). It can be seen that there exists a second energy value (b) for which the mass absorption coefficient is the same as that of the characteristic energy. Thus at (a) and (b) the variation in intensity due to absorption by the element should be identical. The background intensity as a function of energy determined on a blank sample allows the

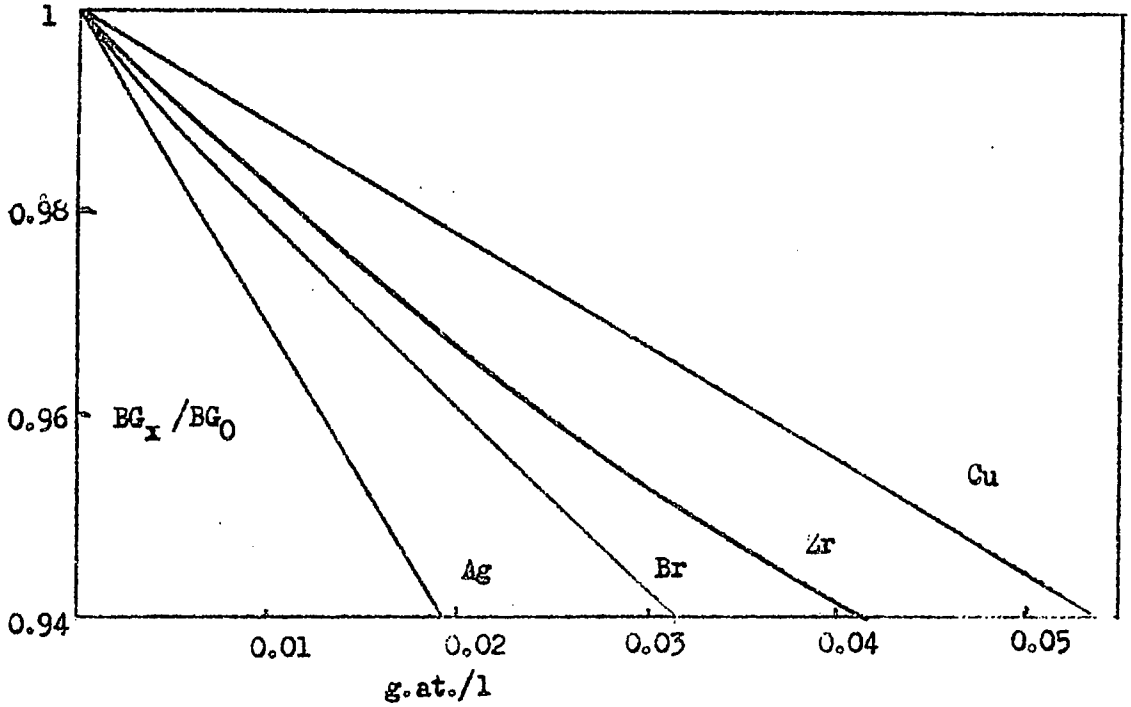

Fig.4-3 Fractional variation of background with respect to concentration in gram atom per litre

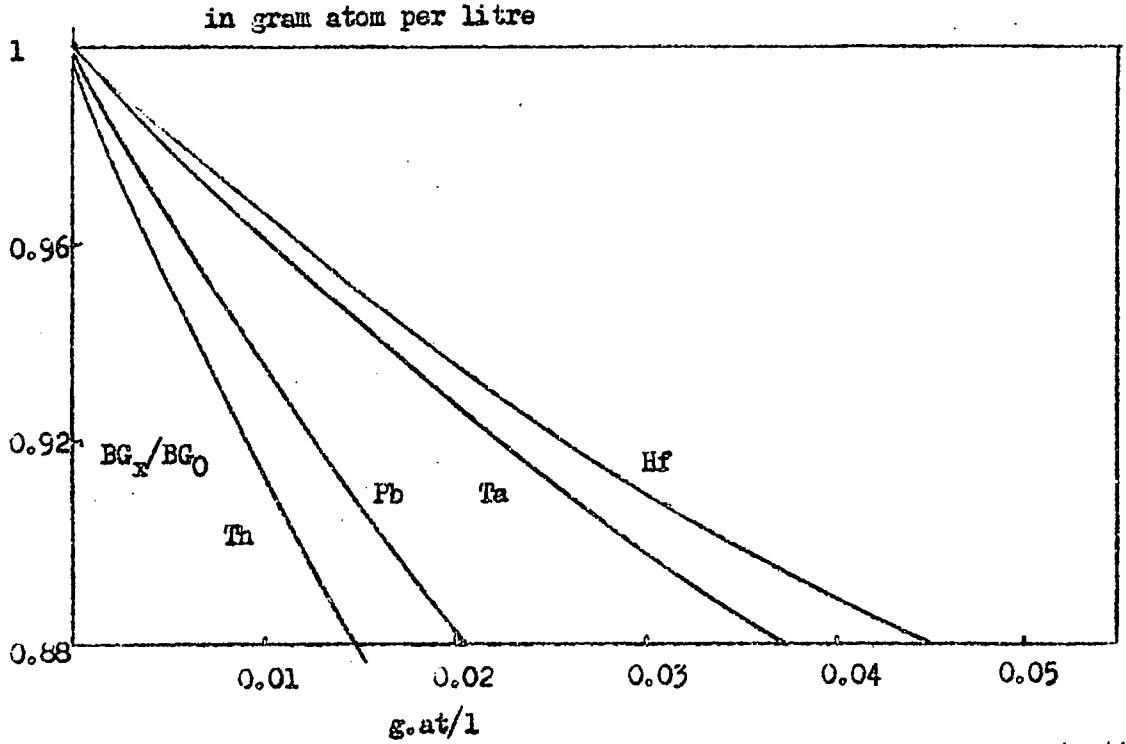

Fig.4-4 Fractional variation of background with respect to concentration in g at/l

intensity ratio R = A/B to be obtained (see Fig. 4-6). If the initial assumption is correct R should be constant, and hence the background contribution to the observed fluorescent peak can be determined from observation of the intensity of radiation at the reference position (b).

In practice the heavy element will always be associated with other elements in the solution, and their presence should be taken into account when choosing the background reference position. A first choice of reference position was made from the mass absorption curves for the heavy element. Consideration of the absorption of the other elements at this energy allows a semi-quantitative correction to be applied to the first choice to give a final reference position.

Counting time.

The choice of counting time is inevitably a compromise. Long counting times reduce the fractional statistical error, but rely on a long term stability of the counting system. On the other hand short counting times reduce the time required for analysis, but with sacrifice in precision.

In this particular work no automatic timing device was used, and in order to minimise errors arising from manual control a relatively long counting time of 5 minutes was adopted. Three or four observations were made at each concentration.

Results.

Calibration curves of fluorescence intensity against element concentration for solutions containing one heavy element were prepared for a wide range of elements, the results being illustrated in Figures 4-7, 4-8, 4-9, 4-10, 4-11, 4-12, 4-13, 4-14. All measurements were made with a pulse analyser channel width of one volt, and for the purpose of comparison were converted to a standard amplifier attenuation of 26 decibels. All observed counts were corrected for counter dead time, and for background by the method outlined. Due

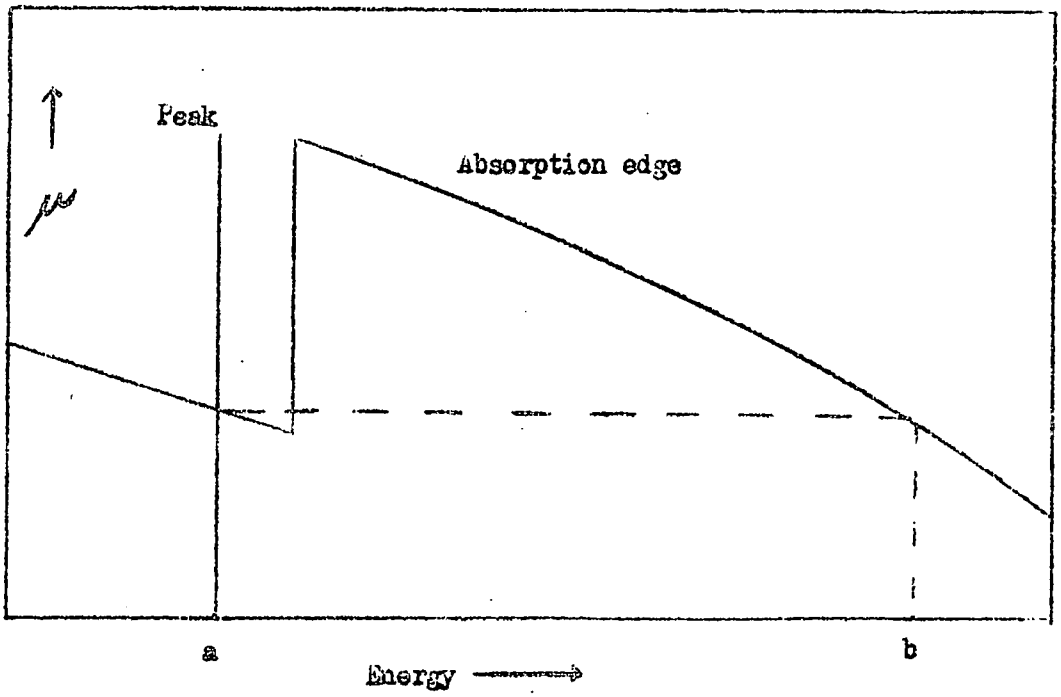

Fig.4-5 Typical relationship between absorption edge and fluorescent peak of an element .a represants the position of the fluorescent peak . b represents another position where the element has the same mass absorption coefficient as at position a.

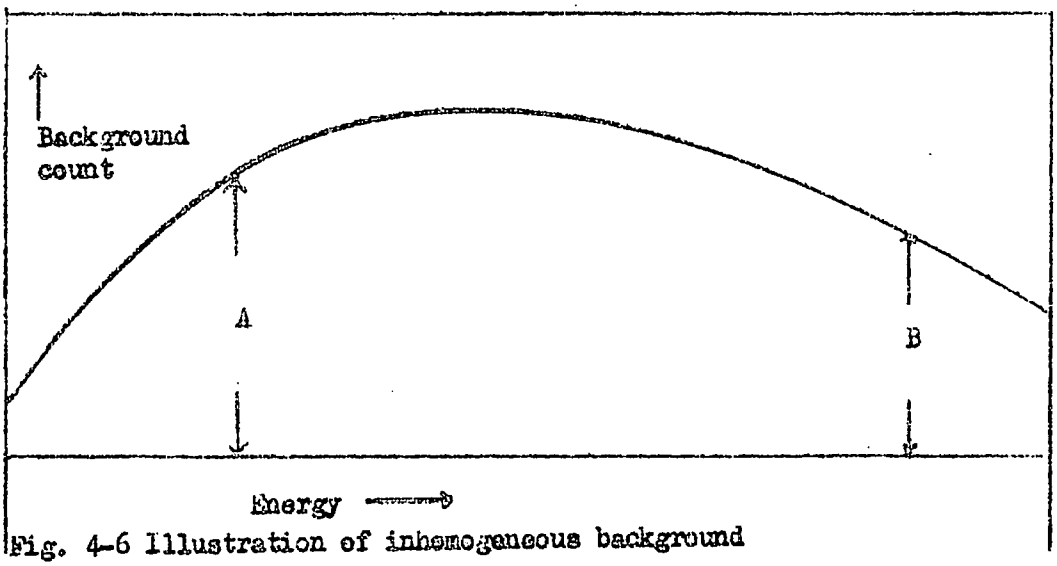

Fig. 4-6 Illustration of inhomogeneous background

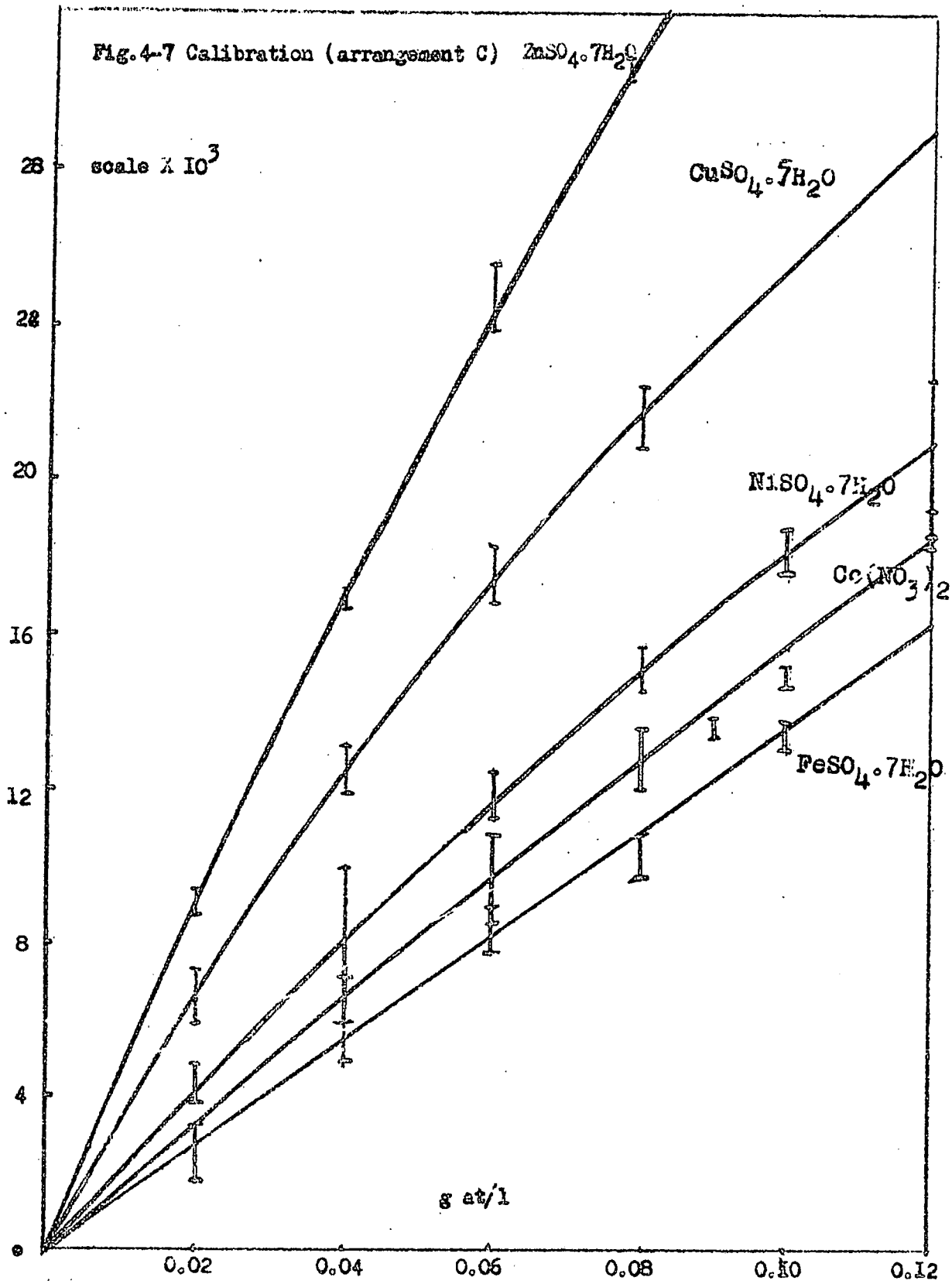
Fig.4-7 Calibration (arrangement C) $ZnSO_4 \cdot 7H_2O$
scale X 10^3
28
24
20
16
12
8
4
0
$CuSO_4 \cdot 7H_2O$
$NiSO_4 \cdot 7H_2O$
$Co(NO_3)_2$
$FeSO_4 \cdot 7H_2O$
g at/l
0.02
0.04
0.06
0.08
0.10
0.12

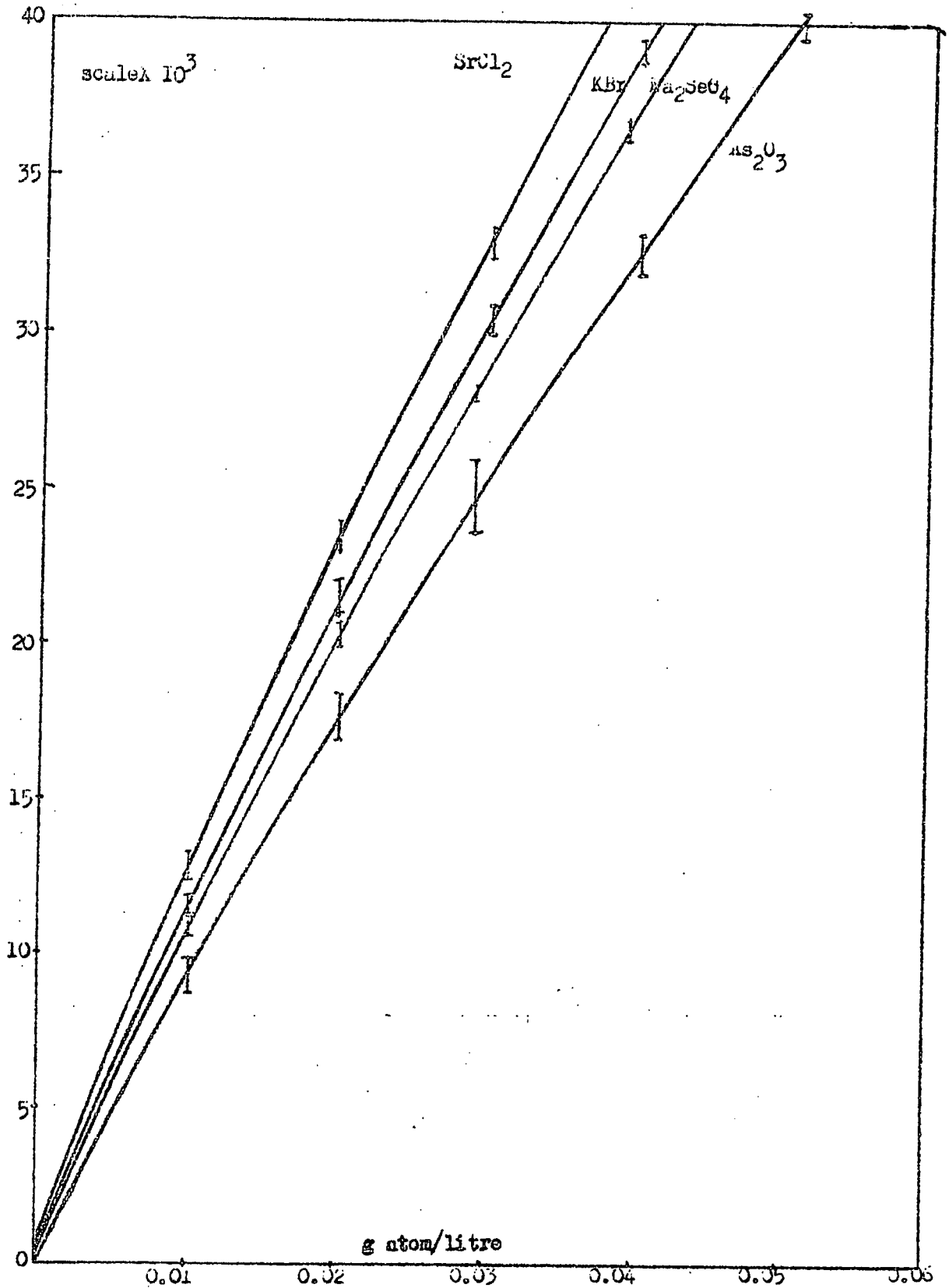

Fig.4-8 Calibration of single element (arrangement C with source I)

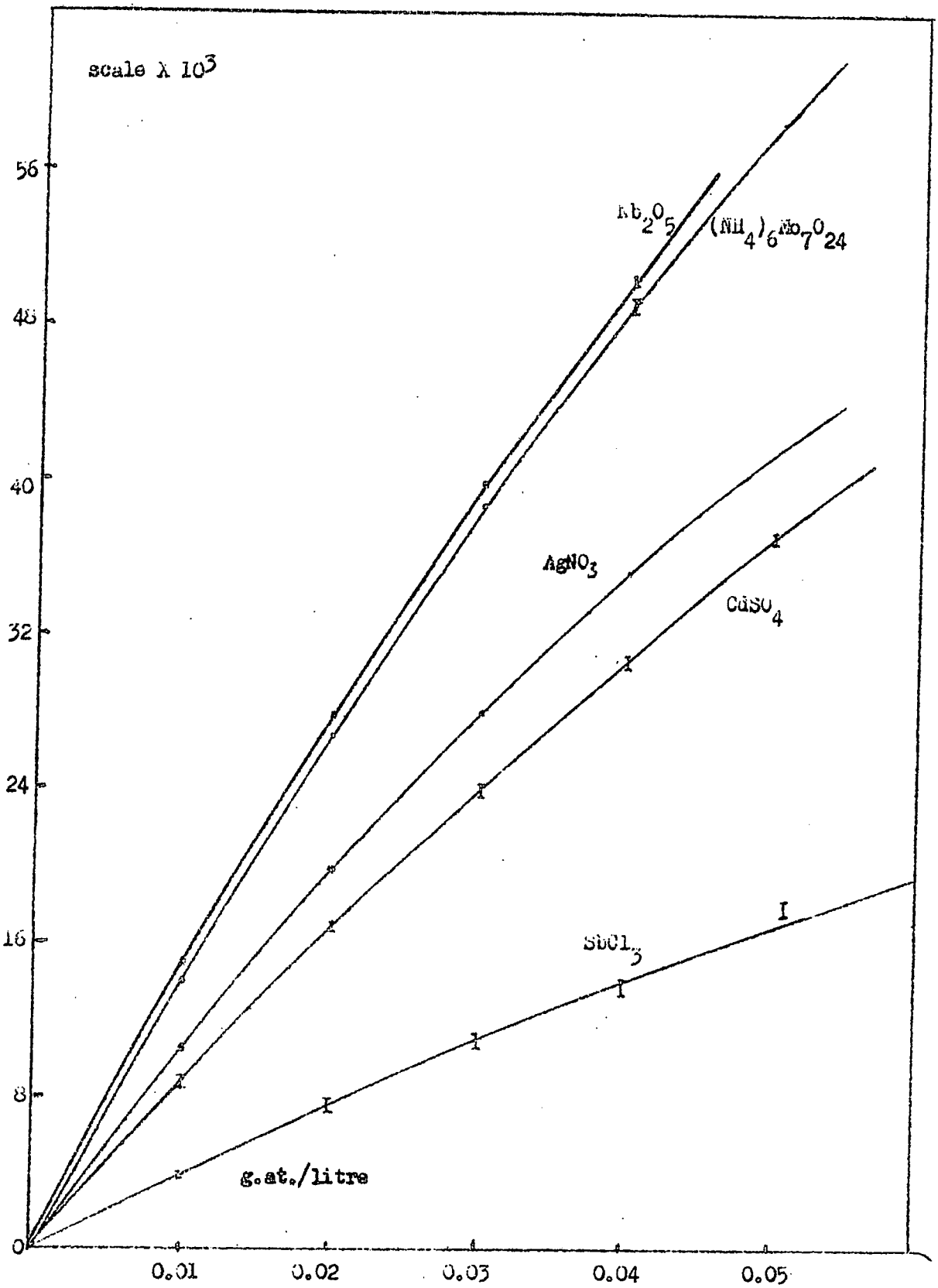

Fig.4-9 Calibration of single element (arrangement C with source I)

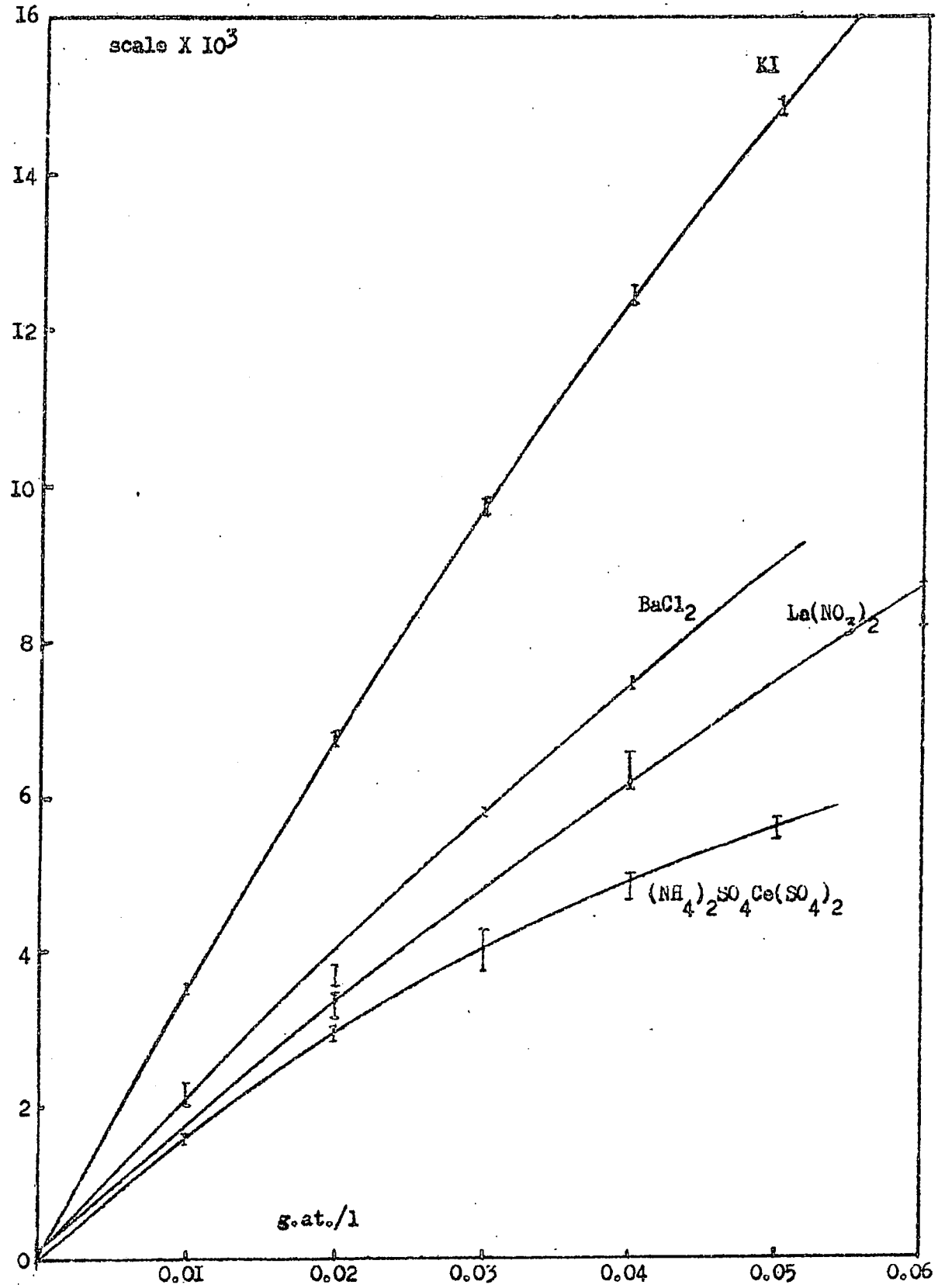

Fig.4-10 Calibration of single element (arrangement C with source I)

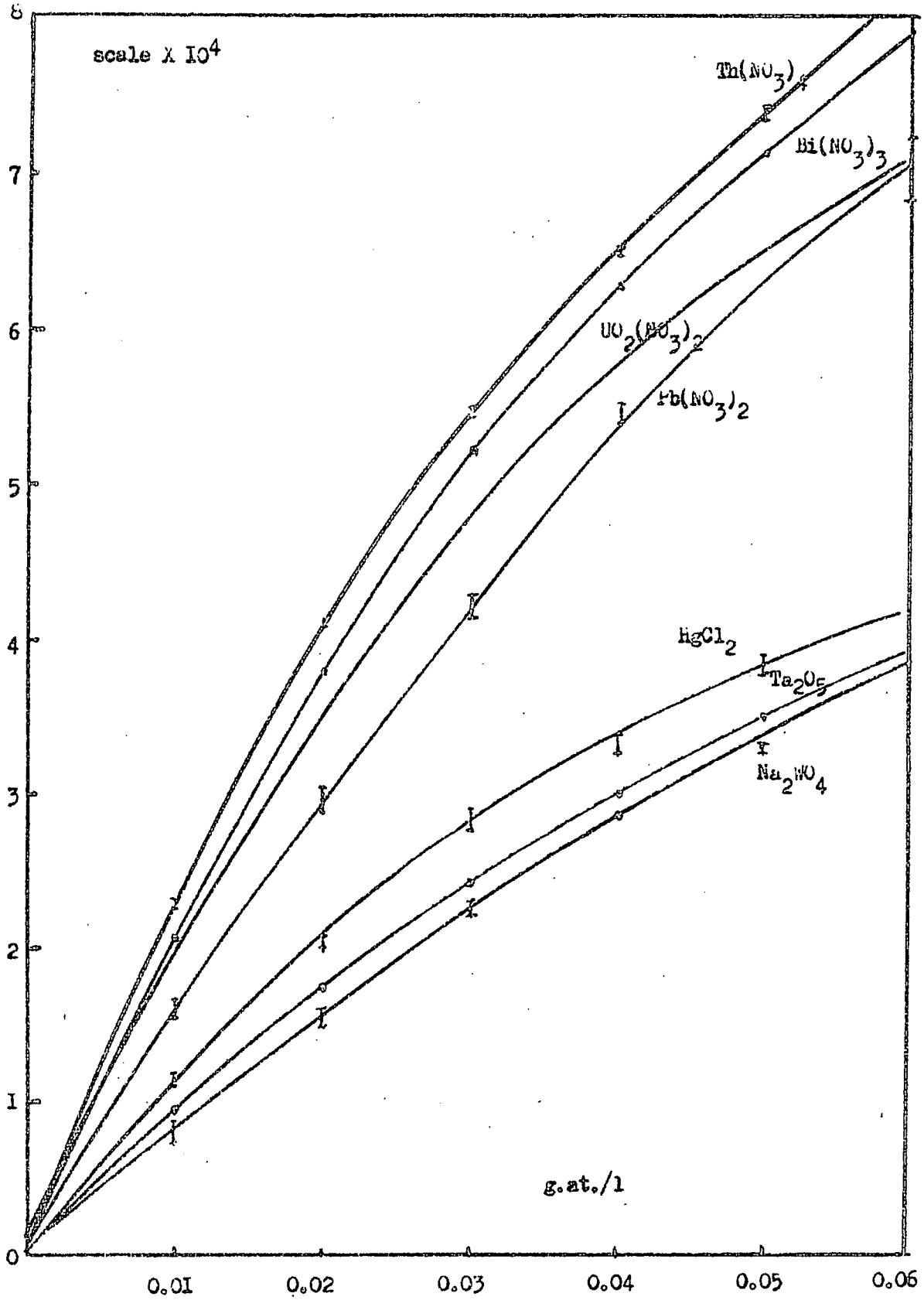

Fig.4-11 Calibration of single element (L-x ray, arrangement C, source I)

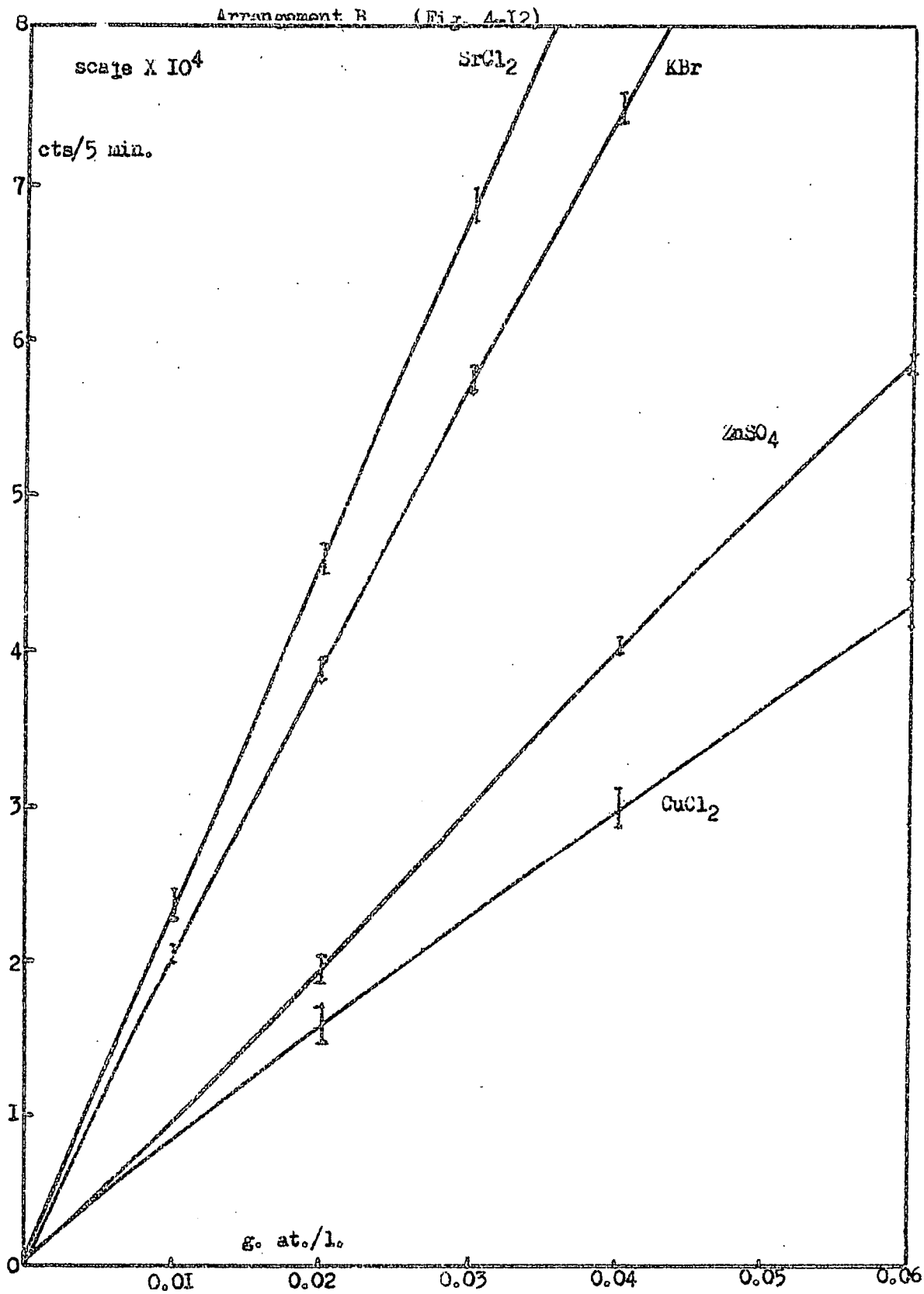
Arrangement B (Fig. 4-12)
scale X 10^4
cts/5 min.
$SrCl_2$
KBr
$ZnSO_4$
$CuCl_2$
g. at./l.
0
1
2
3
4
5
6
7
8
0.01
0.02
0.03
0.04
0.05
0.06

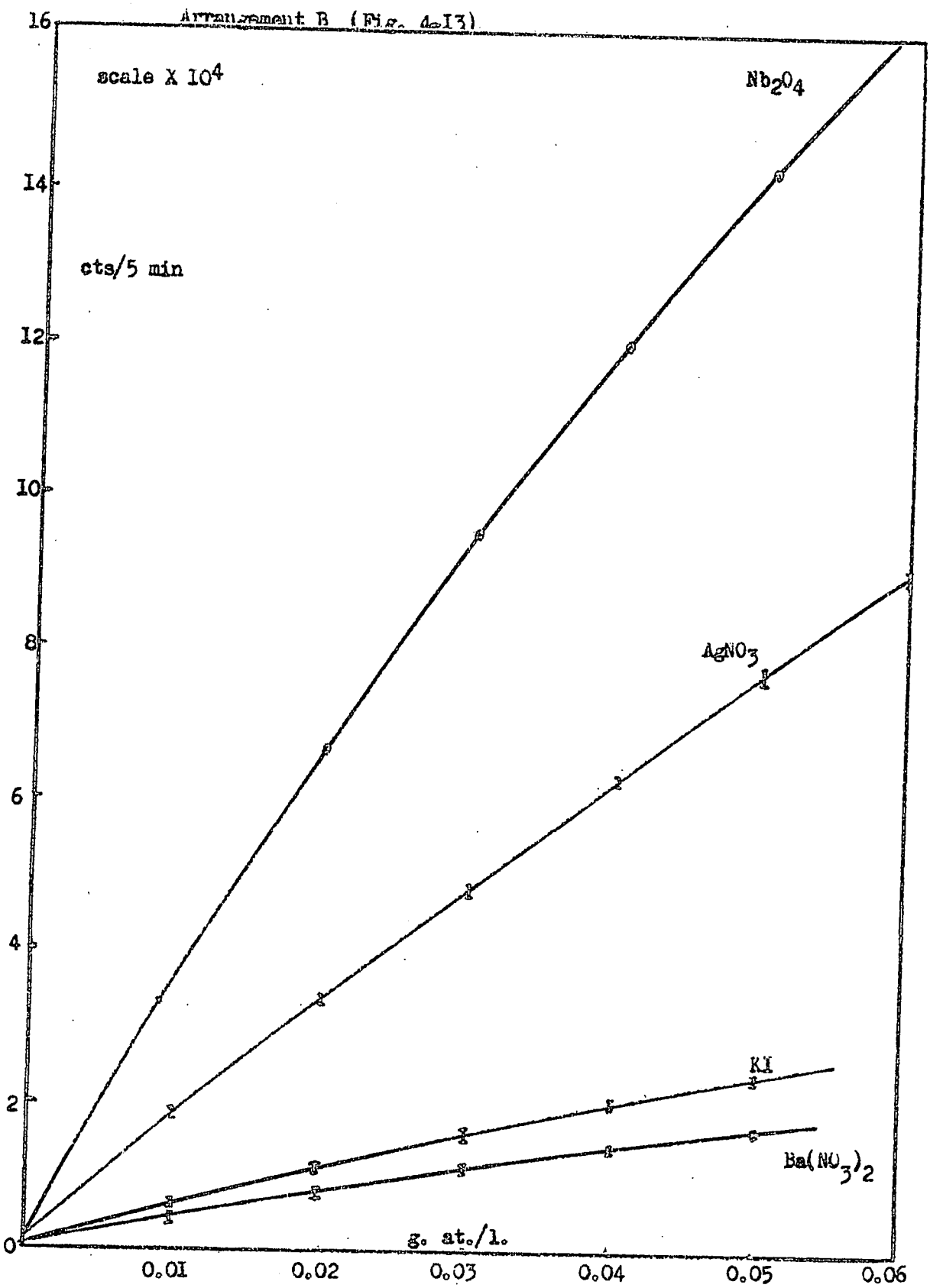
Arrangement B (Fig. 4-13)
scale X 10^4
cts/5 min
Nb_2O_4
$AgNO_3$
KI
$Ba(NO_3)_2$
g. at./l.
16
14
12
10
8
6
4
2
0
0.01
0.02
0.03
0.04
0.05
0.06

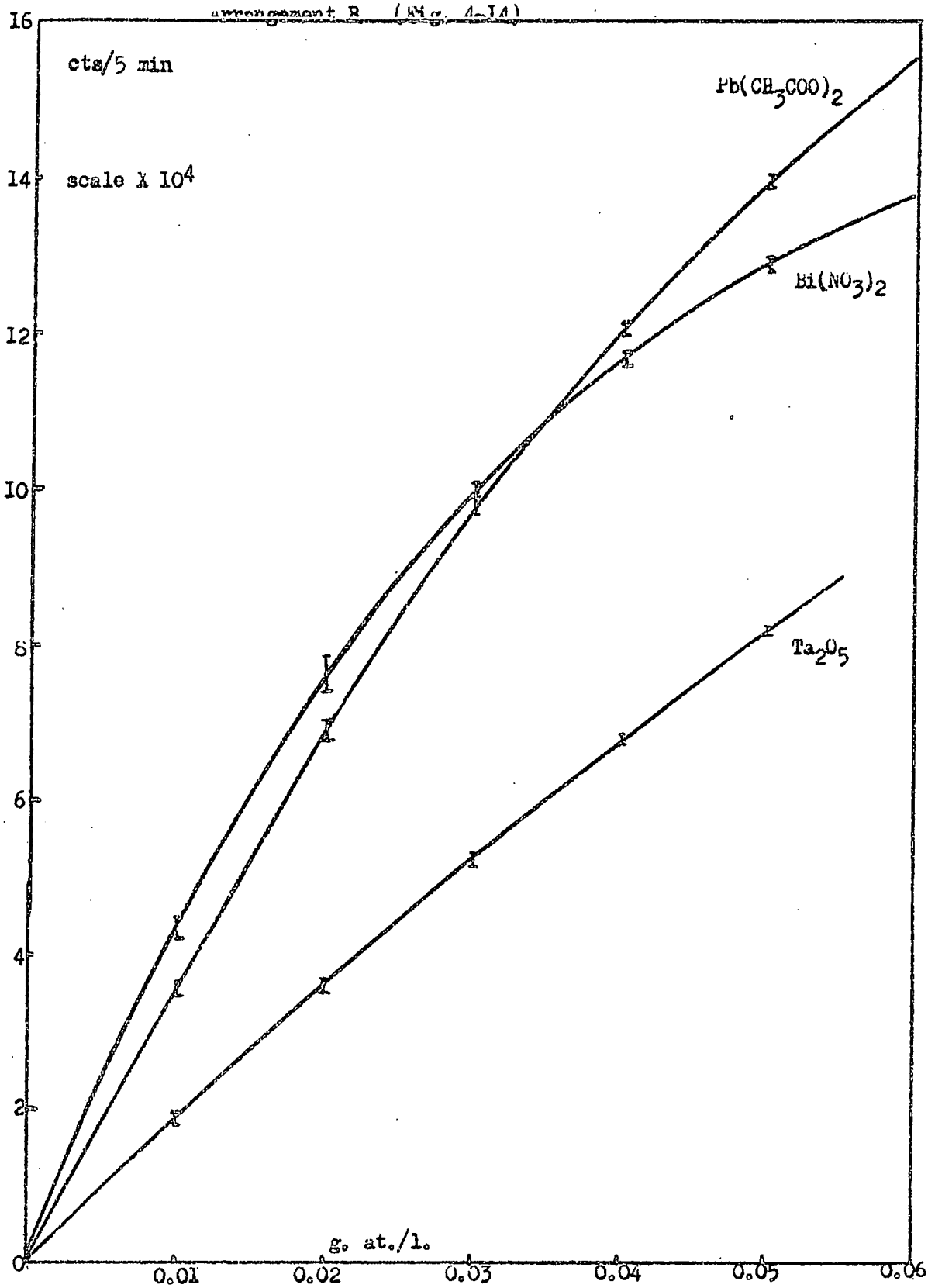
arrangement B (Fig. 4-14)
cts/5 min
scale X 10^4
16
14
12
10
8
6
4
2
0
$Pb(CH_3COO)_2$
$Bi(NO_3)_2$
Ta_2O_5
g. at./l.
0.01
0.02
0.03
0.04
0.05
0.06

to the high background and low fluorescent intensity in the region of 6 kev energy, no results were obtained for elements of atomic number lower than iron with arrangement C (source I), or for elements of atomic number lower than nickel for a arrangement B (source II). The calibration curves show the expected convex upwards shape due to self-absorption of th characteristic radiation of the sample at the higher element concentrations. Some curves show a slight concave upwards shape at low concentration due to error in the choice of reference position for the background. As mentioned earlier the choice of reference position is only semi-quantitative. All calibration curves were drawn by the method of least squares.

The minimum detectable concentration was defined as that concentration which gave a count at least three times the standard deviation of the background above the background. All concentrations were expressed in gram atoms/litre of solvent. The minimum detectable concentration as a function of atomic number is illustrated in Figure 4-15 for both K and L X-rays, and for both arrangements B and C. In Figure 4-16 the peak to background ratio for a fixed concentration of 0.01 gm. atoms/litre of solvent are given in a similar way as a function of atomic number.

The count rate per 0.01 gram atoms/l at the concentration 0.01 gram atoms/l is given as a function of atomic number in Figure 4-17; In general better results are achieved with the geometrical arrangement B (source II) than with arrangement C (source I). The best results are obtained for those elements with characteristic peaks in the region of NbK (16.6 kev), and for heavy elements those with characteristic peaks near to UL (13.5 kev).

The expected standard deviation of a determination expressed as a percentage is given by,

$$\sigma = \frac{(N_T + N_B)^{\frac{1}{2}}}{N_T - N_B} \times 100$$

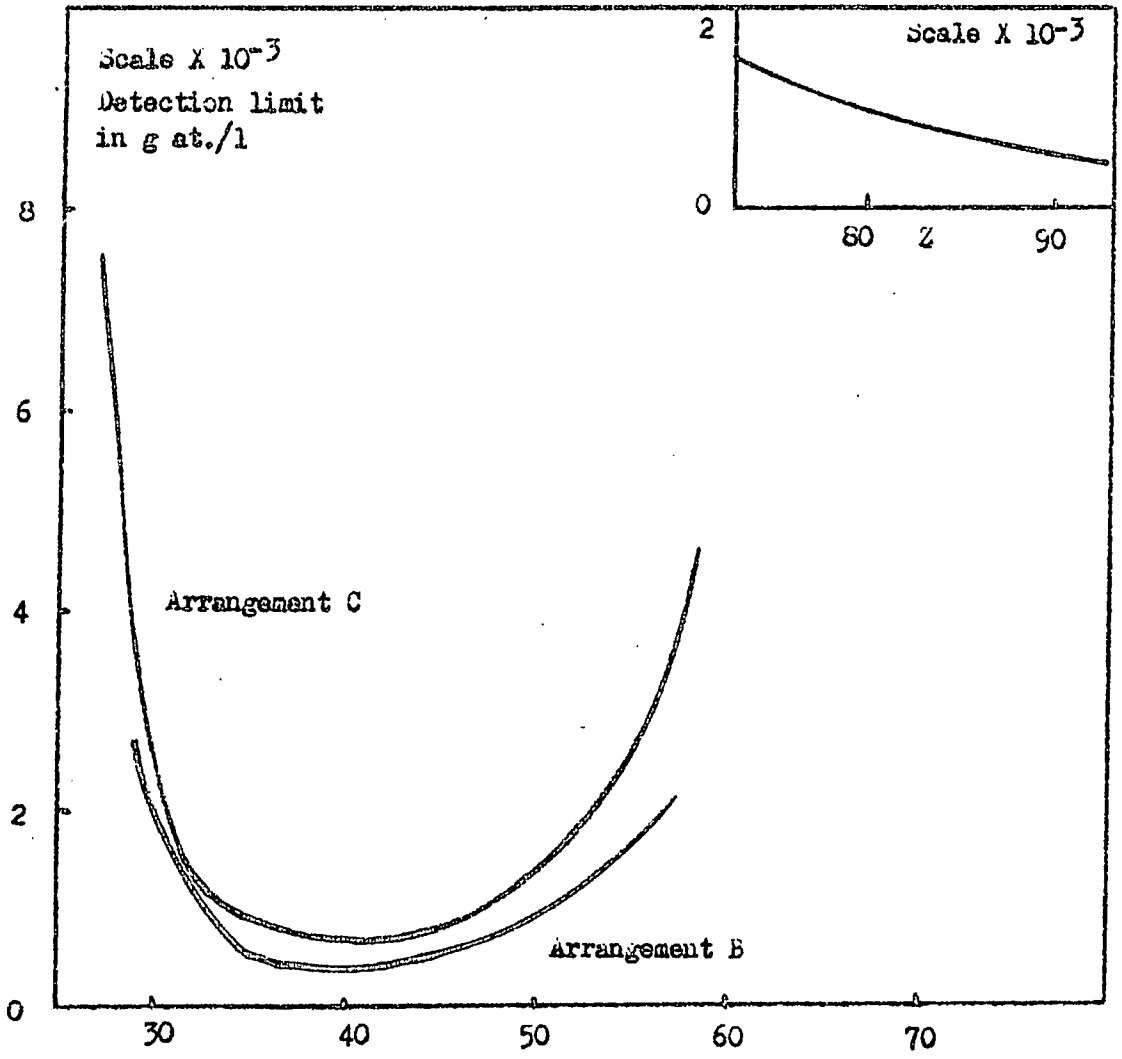

Fig.4-15 Detection limit against atomic number Z. The inserted diagram is the detection limit when a L-X ray is used for calibration

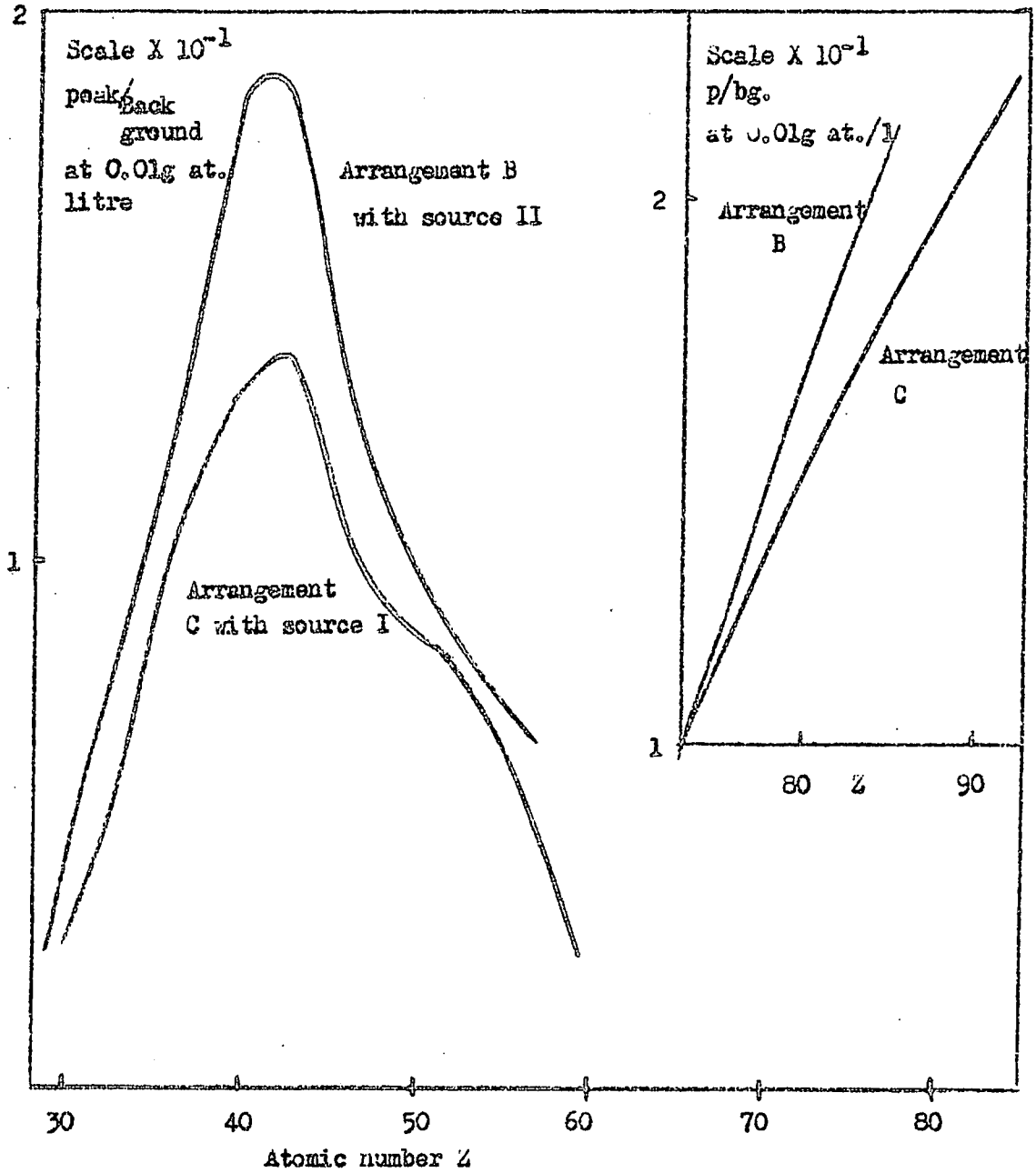

Fig.4-16 Peak to background ratio against atomic number. The inserted diagram is peak/background against Z when L x ray is used in the calibration.

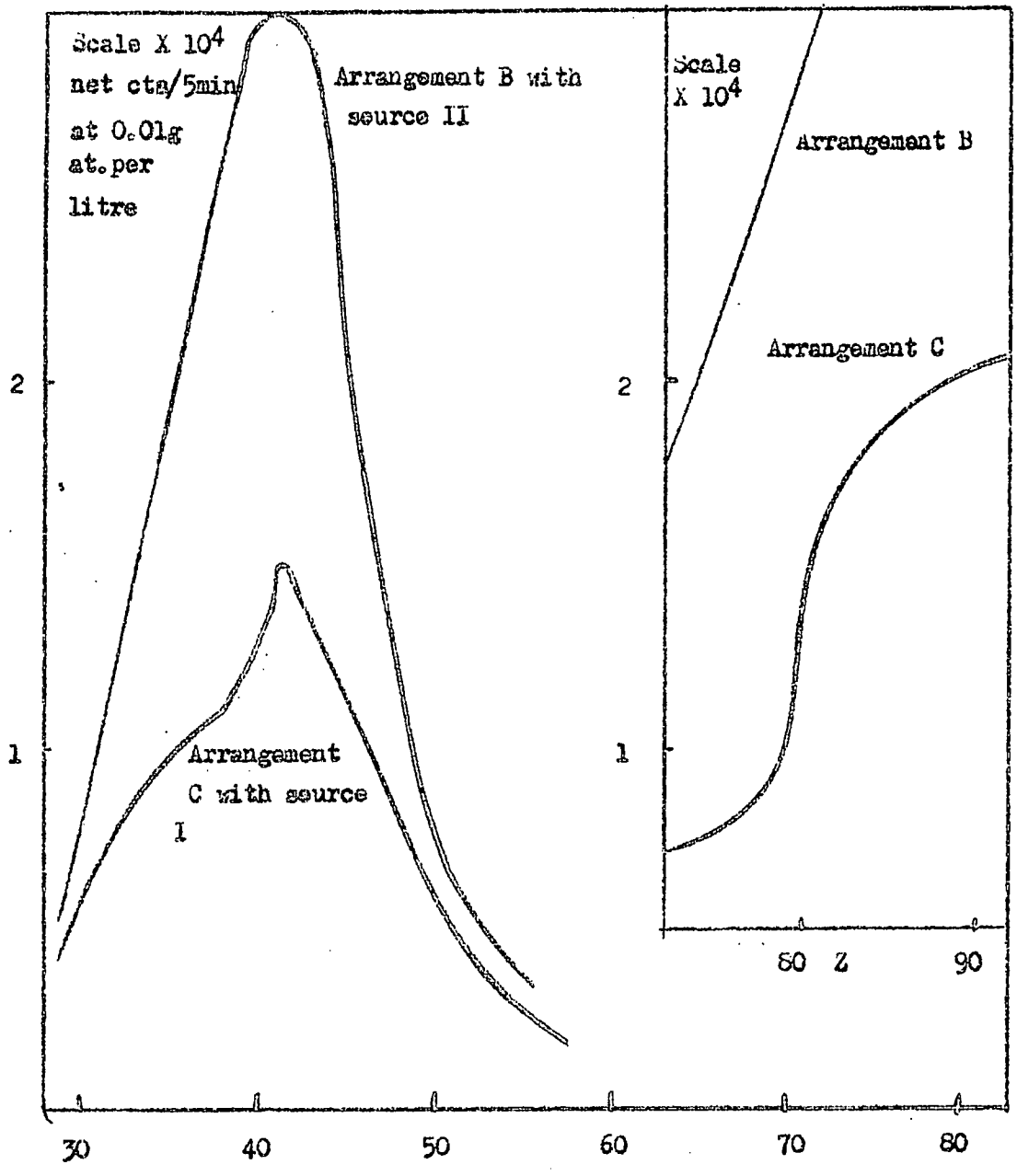

Fig.4-17 Count/5min at 0.01 g atom /litre against atomic number
The inserted diagram represents results obtained when L-x ray used.

and will have a maximum value of 40% for the minimum detectable concentration using the criterion $N_T = 3N_B^{\frac{1}{2}} + N_B$. The value of σ' varies with atomic number as well as with concentration, the variation with atomic number at a fixed concentration (see Fig. 4-18) being similar to the variation of the detection limit. For a concentration of 0.01 gm atom/litre the value of σ' has a minimum value for Nb (1 to 2%) and approaches its maximum value for iron where this value is almost equal to 10%. The value of σ' is found to be 10-20% better for arrangment B than for arrangement C.

Having regard to the small number of observations taken for each element and concentration value (3 or 4) the actual spread of results is in good accord with σ', with the exception of some results for higher values of the atomic number. This exception for higher atomic number elements is almost certainly due to the criterion adopted for background correction. As the atomic number increases the background reference position (b) (see Fig 4-5, 4-6) moves further away from the fluorescent peak position (a) with the result that the ratio R increases due to the rapid fall off of the primary spectrum with energy. For the element cerium R has the very unfavourable value of 40, which means that the statistical fluctuations in intensity at the reference position (b) are multiplied by this factor in the background correction. Thus large errors may appear in the background correction. It would seem in such cases that better results would be achieved by adopting as background correction the intensity level for zero concentration.

Binary mixtures of heavy elements in solution.

For a binary mixture of elements the fluorescent intensity of a particular element will vary not only with the amount of that element present, but also with its percentage ratio to the second element. One or other of these quantities must be fixed in order to set up a calibration curve. The most covenient method is to study the variation in fluorescent

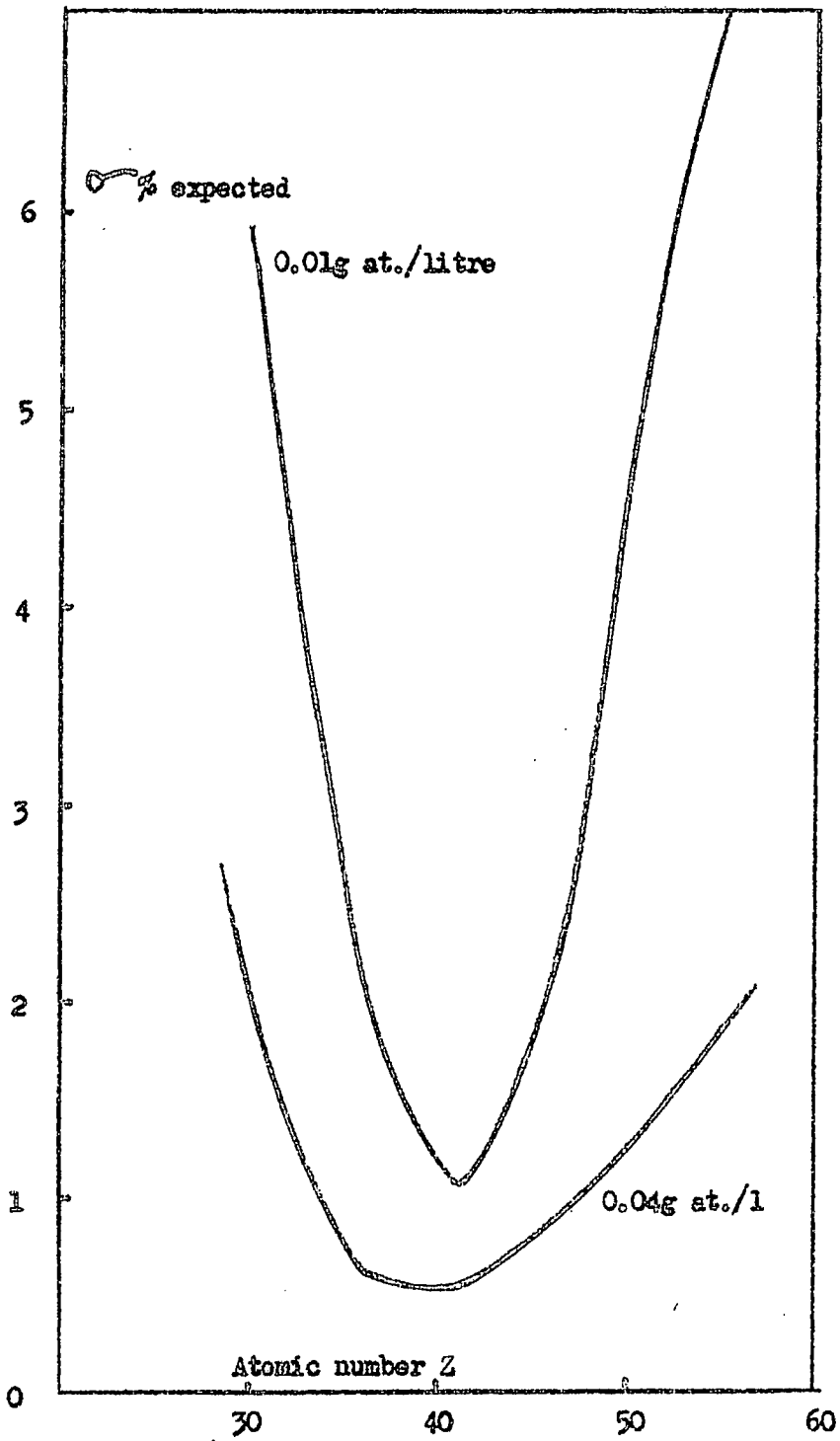

Fig.4-18 σ% standard deviation in percentage expected against atomic number.

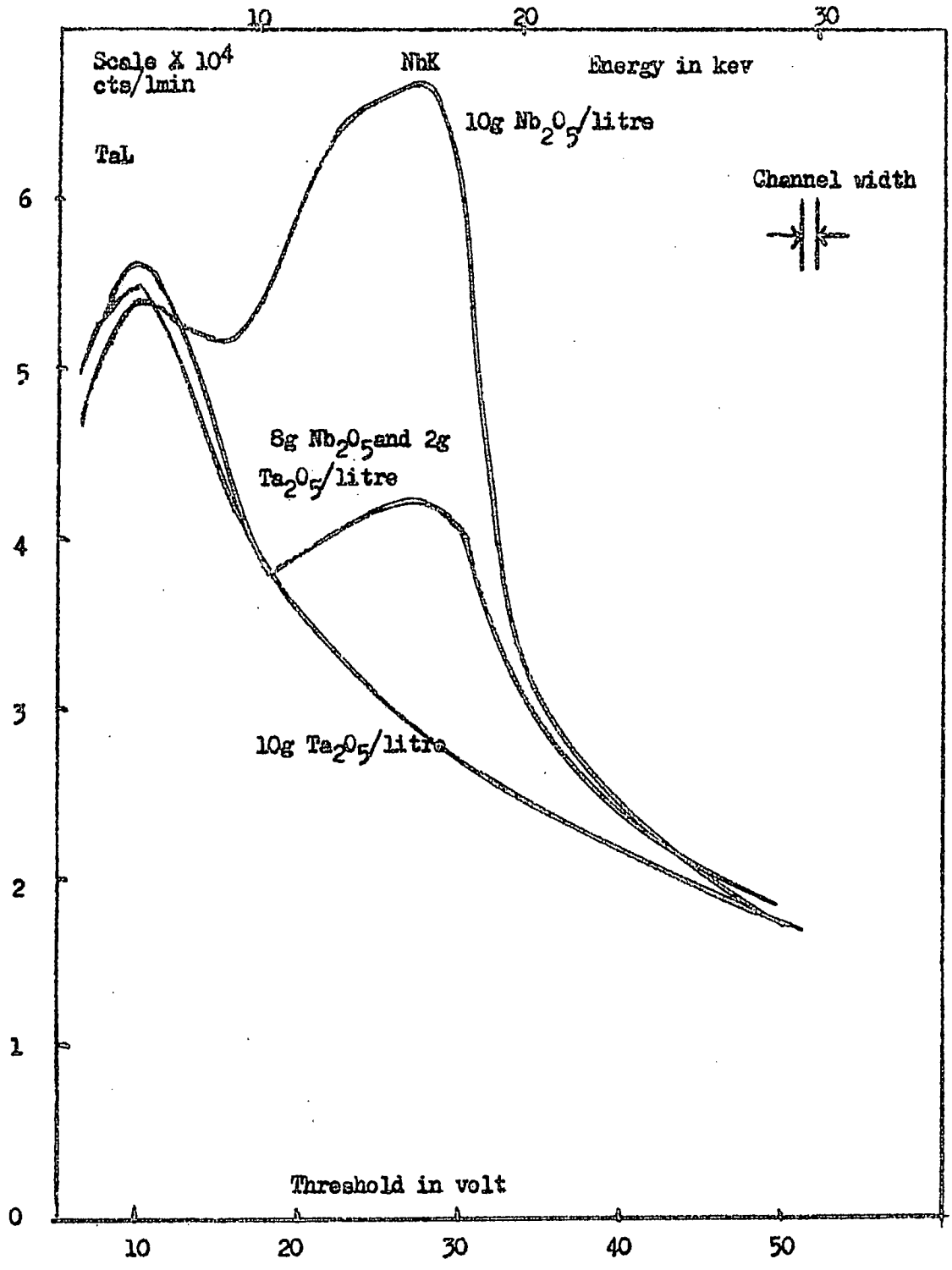

Fig.4-19 Oxides of niobium and tantalum in diluted HF.

intensity as a function of the weight percentage and this requires that a fixed total quantity of the mixture be taken. In this particular case the fluorescent intensity of the elements was studied as a function of the weight percentage of the mixed oxides, the binary mixtures of interest being niobium-tantalum and hafnium - zirconium.

Mixtures of the appropriate oxides were prepared by weighing and then dissolved in dilute hydrofluoric acid, the resulting solutions being further diluted to give a series of samples containing ten grams of the mixed oxides per litre. The fluorescent intensity of the elements was measured the results being given in table.

Table 4-1

Mixture	Arrangement B with source II	Arrangement C with source I	Arrangement C with source I
	10g Nb_2O_5 and Ta_2O_5/litre	10g Nb_2O_5 + Ta_2O_5/litre	10g ZrO_2 + HfO_2/litre
Detection limit	0.4wt.% of Nb_2O_5	1.6wt.% of Nb_2O_5	2.66 wt. % of ZrO_2
Error at 20 wt.%	2.8 %	3%	14%

The shapes of all the calibration curves for niobium in tantalum and zirconium in hafnium are more or less concave upwards (see figs 4-20, 4-21) irrespective of the particular geometrical arrangement adopted in the determination. This is to be expected since the absorption of Nb K and Zr K by tantalum and hafnium respectively is very serious according to the data available (77), hence the term $(\mu_f + \mu_p)$ in equation 1.1 decreases as the weight percentage of niobium or zirconium increases. No reliable calibration could be obtained for hafnium in zirconium or tantalum in niobium due

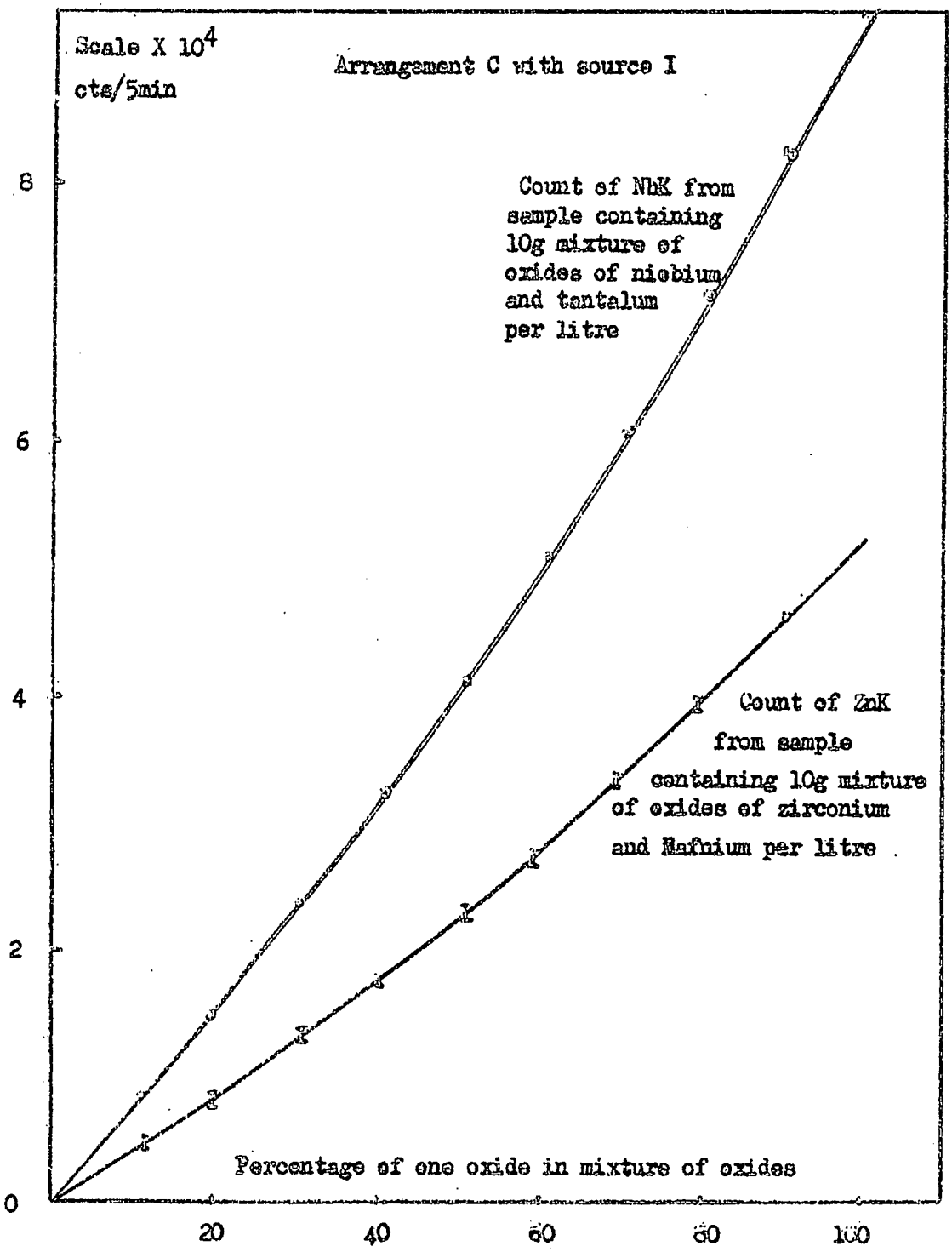

Fig.4-20 Count of NbK and ZnK against mixture of oxides of niobium and tantalum and mixture of zirconium and hafnium (respective weight percentage)

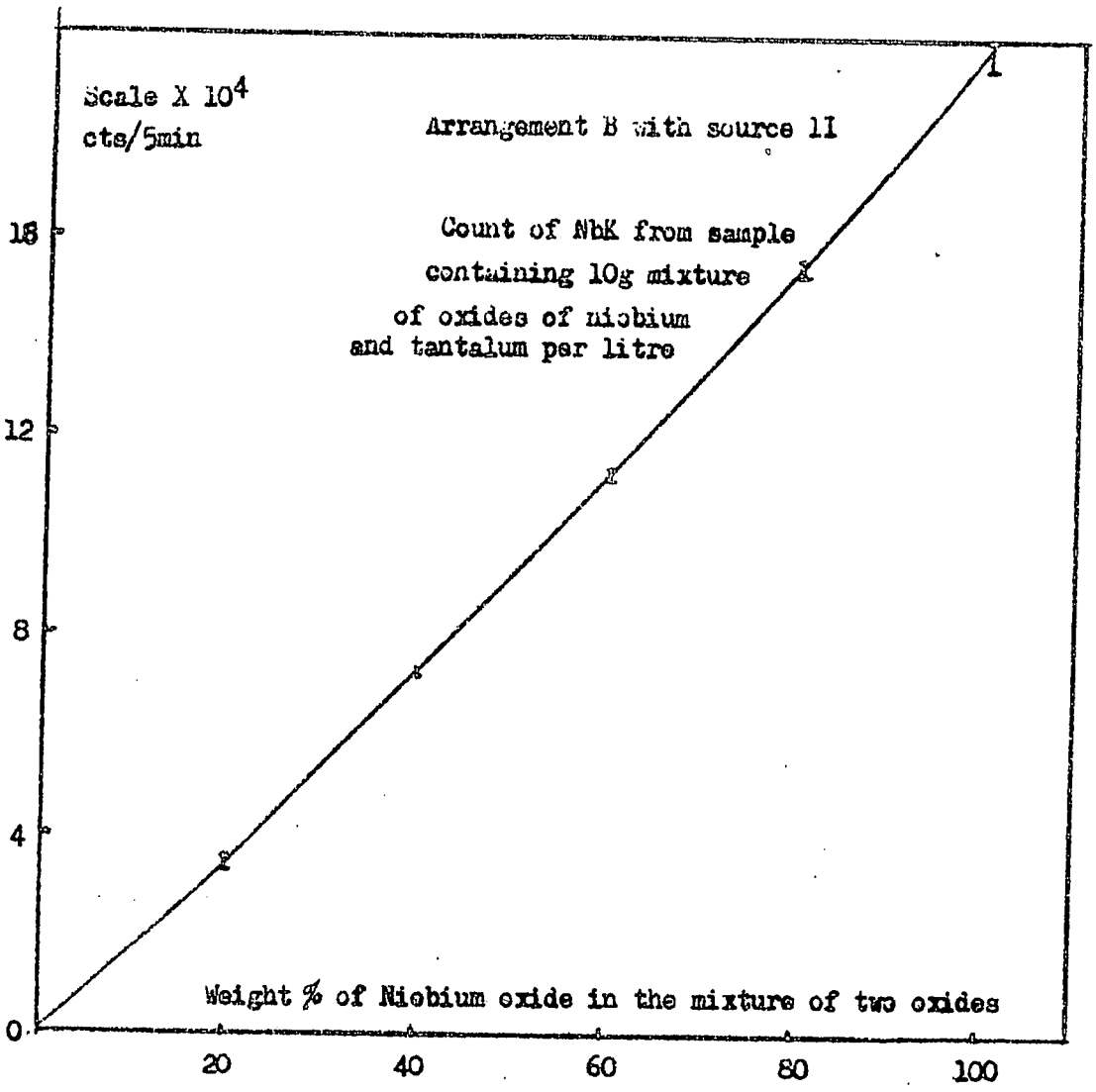

Fig. 4-21 Calibration of niobium oxide in mixture of niobium and tantalum oxides.

to the low intensities of Hf L and Ta L. In addition the background was high and varied a great deal because of variation in the composition of the mixtures, and the fact that suitable background reference positions for hafnium and tantalum were occupied by Zr K and Nb K respectively (See Fig 4-22). The attempt to calibrate the mixtures at lower total concentration to reduce the absorption effect gave poor results. Methods to counter the absorption effect such as calibrating the peak to background ratio against concentration, a device commonly used in the dispersive method (30, 34), were also investigated but met with little success due to difficulty in the choice of background reference position.

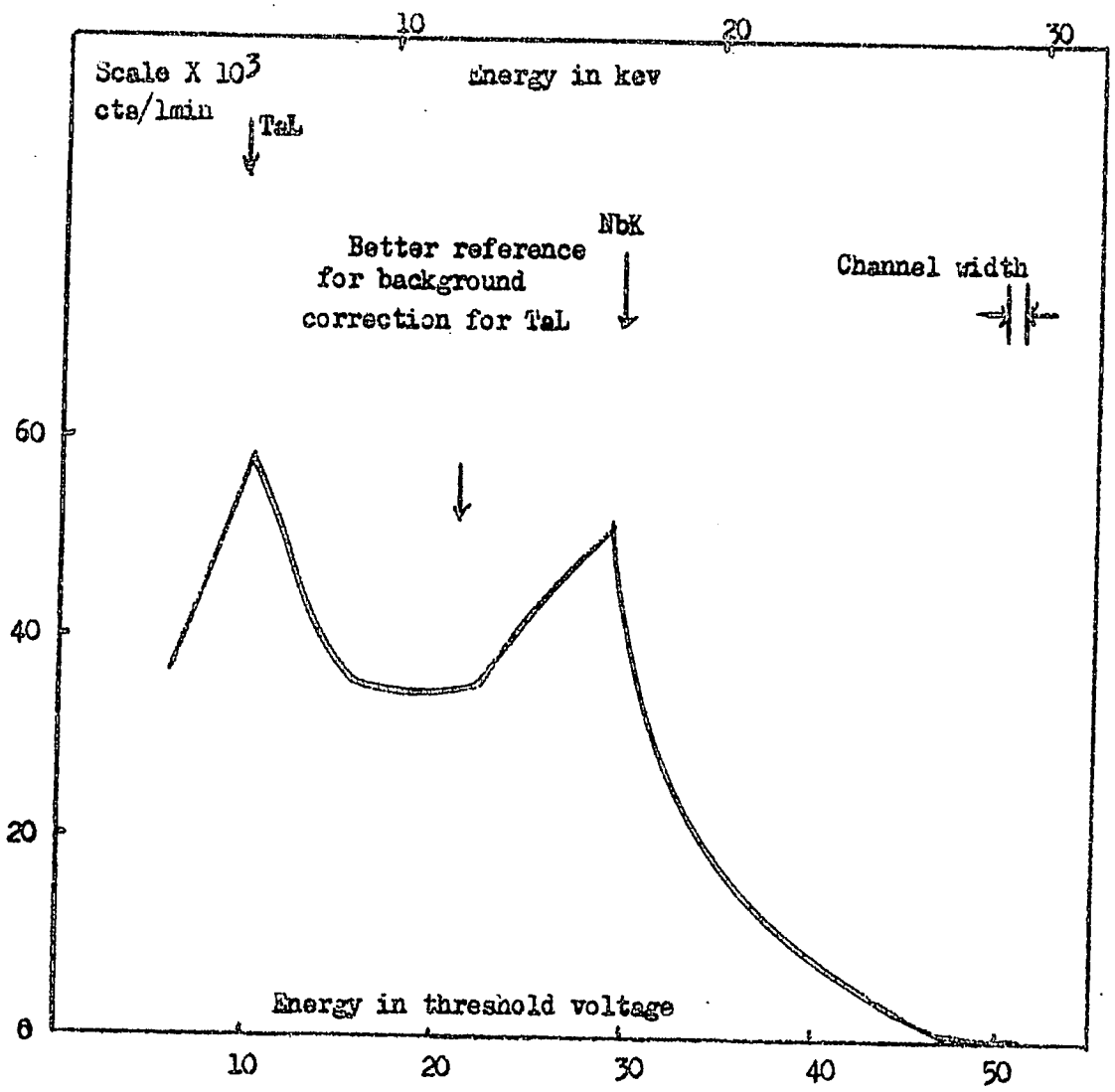

Fig.4-22 Spectra of Nb and Ta to show the better reference position for TaL background correction is occupied partially by NbK

CHAPTER 5

Solid Samples

The use of two different solid sample systems for the analysis of niobium - tantalum mixtures was investigated. One system consisted of a homogeneous solution of tantalum and niobium oxides in anhydrous sodium borate, and the second a suspension of the finely ground oxides in perspex.

Borate solution system.

Samples were prepared in the following way. 0.2 grams of oxide or mixed oxides and 20 grams of anhydrous borax were heated in a platinum dish at 1000°C until complete solution was attained. This process usually required about one hour for completion. A mould made from a piece of thick aluminium plate with a circular depression 0.15 cms. in depth and diameter 4 cms was placed in the furnace for a few seconds. The fused borax was poured into the mould which was then moved to the mouth of the furnace to prevent melting of the aluminium plate. The borax was allowed to cool slowly over a period of minutes to avoid cracking of the solid. The sample was obtained as a transparent disc having one face flat and the other face curved.

The freshly prepared sample was transparent, but developed a milky appearance on the surface after a few days. This effect could be prevented by storing the sample in a dessicator, but in practice had no observable effect on the

fluorescence intensity from the sample. Measurement of the fluorescence intensity of the sample was always made on the flat surface.

(a) Sample reproducibility

Four samples each containing 0.2 gms of niobium oxide per 20 gms of anhydrous borax (set I), and three samples each containing 0.16 gms of niobium oxide, 0.04 gms of tantalum oxide, per 20 gms of anhydrous borax (set II) were prepared. Several determinations of the fluorescence intensity of NbK and TaL were made together with observations of the intensity at the appropriate background reference positions. In Table 5.1 the percentage standard deviation from the mean fluorescence intensity (σob) is compared with the appropriate value of the expected standard deviation (σ exp).

Table 5.1

Sample set	Line	ob	exp
I	NbK	0.96	0.4
II	NbK	0.60	0.5
	TaL	7.8	6.6

The results suggest that the sample reproducibility is good having regard to the fact that they will include errors in timing of the count and the instrumental stability.

(b) Calibration

A range of samples at various concentrations of niobium and tantalum were prepared in order to set up calibration curves.

A:- Niobium oxide in borax

B:- Tantalum oxide in borax

C:- Mixture of niobium and tantalum oxides 0.2 grams of mixture in 20 gms of borax).

The sample concentrations used were of the same order as those used in the hydrofluoric acid solutions. The spectra

obtained on the samples of mixture are shown in Figure 5-1, and the calibration curves for all samples in Figures 5-2 and 5-3. Compared to the sample solutions in hydrofluoric acid a reduction in background of approximately 30% for niobium and 40% for tantalum is obtained. This results in a more favourable peak to background ratio and hence better calibration curves for the mixed oxide systems.

The calibration curve for niobium in fused borax (Figure 5-2) and for tantalum in borax (Figure 5-2) have the expected convex upwards shape. That for niobium in the niobium - tantalum mixture (Figure 5-3) shows a linear relationship which can be explained in terms of the efficient absorption of NbK radiation by tantalum at low concentration of niobium. This can be seen by comparing the fluorescence intensities at equivalent concentrations in Figures 5-2 and 5-3, eg. the fluorescence intensity at 20% weight of niobium oxide in Figure 5-3, and at 0.04 gms of niobium oxide in Figure 5-2. The convex upwards shape of the calibration curve for tantalum in niobium oxide (Figure 5-3) is in part due to the enhancement effect (Chapter I) especially when the percentage of tantalum is low, and also to the choice of background reference position which must lie at a higher energy value due to the ideal position being occupied by NbK.

The observed percentage standard deviation (σob) was within the expected standard deviation (σexp) with the exception of those results obtained at low element concentrations for the single species (sample types A and B) and low percentage ratio for the mixtures of elements (sample type C). The latter results, representing the worst situation observed, are shown in Table 5-2 where they are compared with the expected standard deviation.

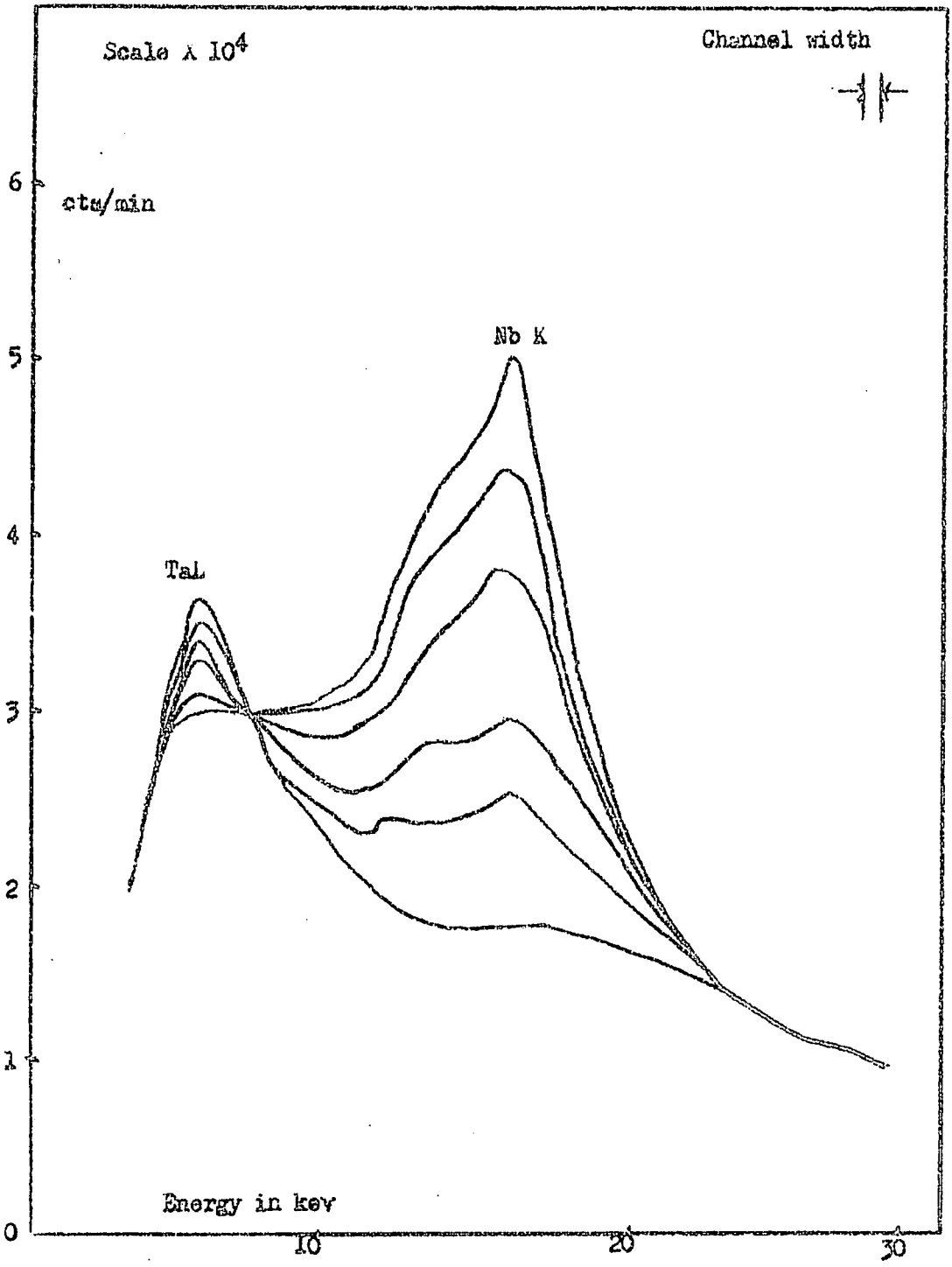

Fig. 5-I Mixture of Ta_2O_5 and Nb_2O_5 in 20 g sodium borate, the percentage of 0.2g mixture varies from 100 per cent Nb_2O_5 0 per cent Ta_2O_5 to 0 per cent Nb_2O_5 100 per cent Ta_2O_5 at 20 per cent interval

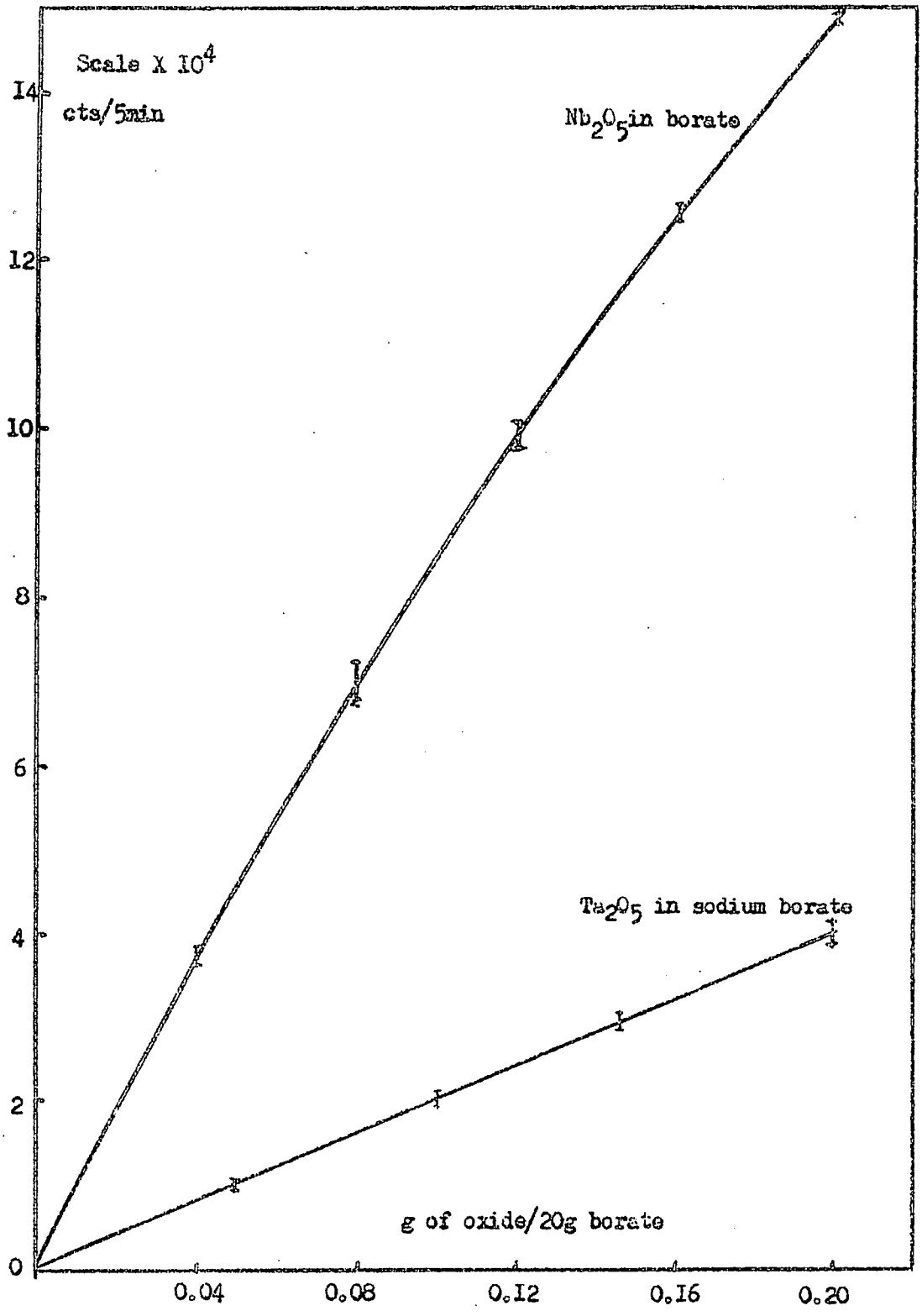

Fig. 5-2 Single oxide in sodium borate

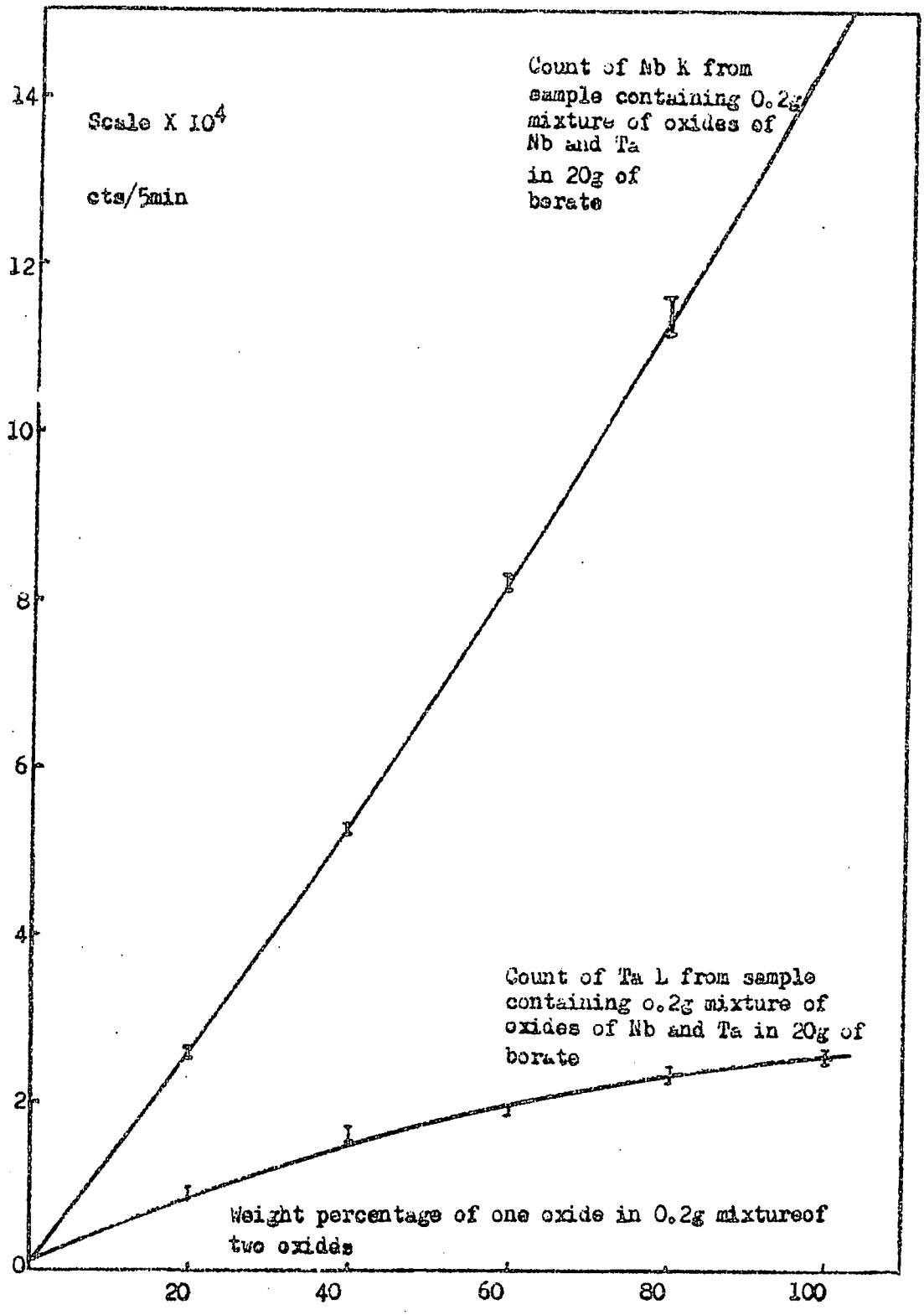

Fig. 5-3 mixture of oxides of Nb and Ta in sodium borate

Table 5.2.

Sample type	A	B	C	
	Nb_2O_5 2 gm/1000 gm	Ta_2O_5 2 gm/1000gm	Nb_2O_5 20% wt.	Ta_2O_5 20%wt.
σ exp	1.5	4.8	1.3	4.4
σ obs	4.5	3.5	3.7	18

The results for tantalum show a greater deviation than those for niobium. This arises in part from the difficulty in selecting a suitable background reference position, and also from the fact that the concentration used represents a lower atom concentration than that of niobium because of the higher atomic weight of tantalum.

(c) Detection limit

The detection limit defined according to the criterion already adopted is expressed in terms of grams of oxide in 1000 gms of anhydrous borax for the single element systems, and in terms of the minimum weight percentage of the element oxide in a system containing 0.2 grams of mixture in 20 grams of anhydrous borax in the case of mixtures. These values are given in Table 5.3.

Table 5.3.

Sample	A	B	C	
Element	Nb	Ta	Nb	Ta
Detection limit	0.03	0.31	0.67	2.67

(d) Element mixtures in unknown matrix

When the mixture to be analysed consists of the oxides of niobium and tantalum together with one or more other components the above method is no longer applicable. A study was therefore made of the method of addition described earlier (page 6, chapter I). In this method we have the relation:

$$x = \frac{I_1 a}{I_2 - I_1} \text{ - - - - - -(1).}$$

where x = element concentration to be determined.
a = concentration of element added.
I_1 = fluorescent intensity for original sample.
I_2 = fluorescent intensity from "doped sample.

A set of four samples was prepared in the usual way with the addition of a quantity of sodium silicate to simulate an unknown matrix. Details of the samples are given in Table 5.4.

Table 5.4.

Sample	Ta 0 (gms)	Nb 0 (gms)	Sodium silicate(gms)
1	0.08	0.12	0.1058
2	0.08	0.14	0.1058
3	0.10	0.12	0.1000
4	0.08	0.13	0.1000

The fluorescence intensity from each sample was measured. If the samples are then considered in sets of two, one of the samples being regarded as the unknown and the second as the "doped" sample, sufficient data is available to use equation 1 to estimate the "unknown", and allow an assessment of the method to be made.
The results of this examination are given in Table 5.5, and represent the mean values of several determinations. Variations about the mean values were of the order of 1%.

Table 5.5.

Sample sets	1 + 2	1 + 4	1 + 3
x_w (by weight)	0.12 gm Nb_2O_5	0.12gm Ta_2O_5	0.08 gm Ta_2O_5
a (by weight)	0.02 gm Nb_2O_5	0.01gm Nb_2O_5	0.02 gm Ta_2O_5
x_c (calculated)	0.1145	0.1299	0.065
$\frac{(x_c - x_w)}{x_w} \times 100$	- 4.6%	+ 8.3%	- 18%

The deviation from the true value can be explained as being due to two effects.

(1). The assumption of a linear relationship between fluorescence intensity and concentration is not valid when the weight fraction, a, is large (compare sample sets 1 + 2 with 1 + 3).

(2) When the weight fraction a is small the quantity $I_2 - I_1$, in equation 1 becomes a small difference between two large quantities with a resulting increase in error (compare sample sets 1 + 2 with 1 + 4).

These two effects will work against one another.

Perspex system

This method represents an attempt to extend the application of a standard technique for the examination of metallurgical specimens to samples for X-ray fluorescence analysis. The sample in the form of a fine powder is dispersed in a metallurgical mounting powder which is then compressed into a standard shape in a mounting press. The mounting powder is melted under pressure to form a coherent mass.

(a) Sample preparation

0.1 gram of oxide or mixed oxides was weighed accurately and then together with 10 grms of a perspex mounting powder (1385 AB Transoptic powder) was transferred to a grinding mill (A10 electric mill, Janke and Kunbel). The mixture was ground and thoroughly mixed in the mill, after which it was transferred to a metallurgical mounting press. All remaining residue in the mill was carefully transferred to the press using a small camel hair brush. The mixture was heated to 170°C under a pressure of 2000 lbs/sq. inch, and then allowed to cool to 40°C when the sample was removed.

Samples prepared in this way were cylindrical in shape with a diameter of 3.2 cms and a thickness of 1.03 cms.

After several preparations a thin deposit on the bottom of the mill became noticeable. At the same time an increase in fluorescence intensity from samples with the same nominal element concentration was observed in order of sample preparation. This was thought to be due to the element oxide adhering to the surface of the mill more readily than the mounting powder thus altering the weight ratio in the sample. As the deposit thickened the properties of the mill surface changed so that element oxide adhered less readily, and increased its weight ratio in the sample. This view was strengthened by the great improvement in sample reproducibility which occurred when the mill was cleaned between each preparation with powdered glass. This practice was adopted for all subsequent sample preparation.

(b) Sample reproducibility

The sample reproducibility expressed as the percentage standard deviation on the mean fluorescent intensity of several samples, for samples containing niobium oxide only, and tantalum oxide only is given in Table 5.6

Table 5.6.

Sample	% age Standard deviation
Nb_2O_5	0.65 %
Ta_2O_5	1.86 %

(c) Sample thickness

Samples prepared as above had a thickness of 1.08 cms. In order to determine whether this thickness represented a value near to the critical thickness (see Page 31) the following experiment was performed.

A sample was prepared containing 0.1 gms of niobium oxide in 10 gms of mounting powder. Successive layers of 1 mm thickness were removed from the sample by turning in a lathe, and determinations of the fluorescence intensity made at each sample thickness. Each determination was accompanied by a similar determination on a blank sample of the same thickness

for background correction. The plot of fluorescence intensity against sample thickness (Figure 5-4) shows a marked levelling off above 0.9 cms thickness. The value of 10.8 cms obtained with the sample quantities used in the preparation therefore represents a suitable sample size.

(d) Calibration

Comparative measurements of fluorescence intensity taken on both faces of the sample were found to differ, in some cases the difference being quite considerable. This was thought to be due to gravitational settling of the oxides in the molten perspex mounting powder during the formation of the samples since that surface which was lower in the mounting press gave the higher fluorescence intensity. The effect was most serious with samples containing tantalum oxide which has a higher density than niobium oxide, and in the worst case observed the fluorescence intensity from the two surfaces of the same sample differed from their mean value by $\pm$ 44% ($\pm$ 5% for samples containing niobium oxide). In the calibration of the fluorescent intensity of tantalum oxide samples the mean value of the results from both surfaces was taken (Figure 5-6). For samples containing a mixture of niobium and tantalum oxides the Nb K fluorescent intensity was smaller for the lower surface than for the upper surface. This could be due to a higher tantalum concentration at the lower surface with a consequent higher absorption of NbK radiation.

The calibration curves are illustrated in Figs. 5-6, 5-7, and in general have the same shape as for the corresponding samples in borax. An assessment of the errors is rendered difficult by the inhomogeneity of the samples, and it is clear from a consideration of the error limits on the calibration curves that these arise from the sample preparation. This point will be discussed further in Chapter 6.

(e) Detection limit

The detection limit is expressed in the same way as for

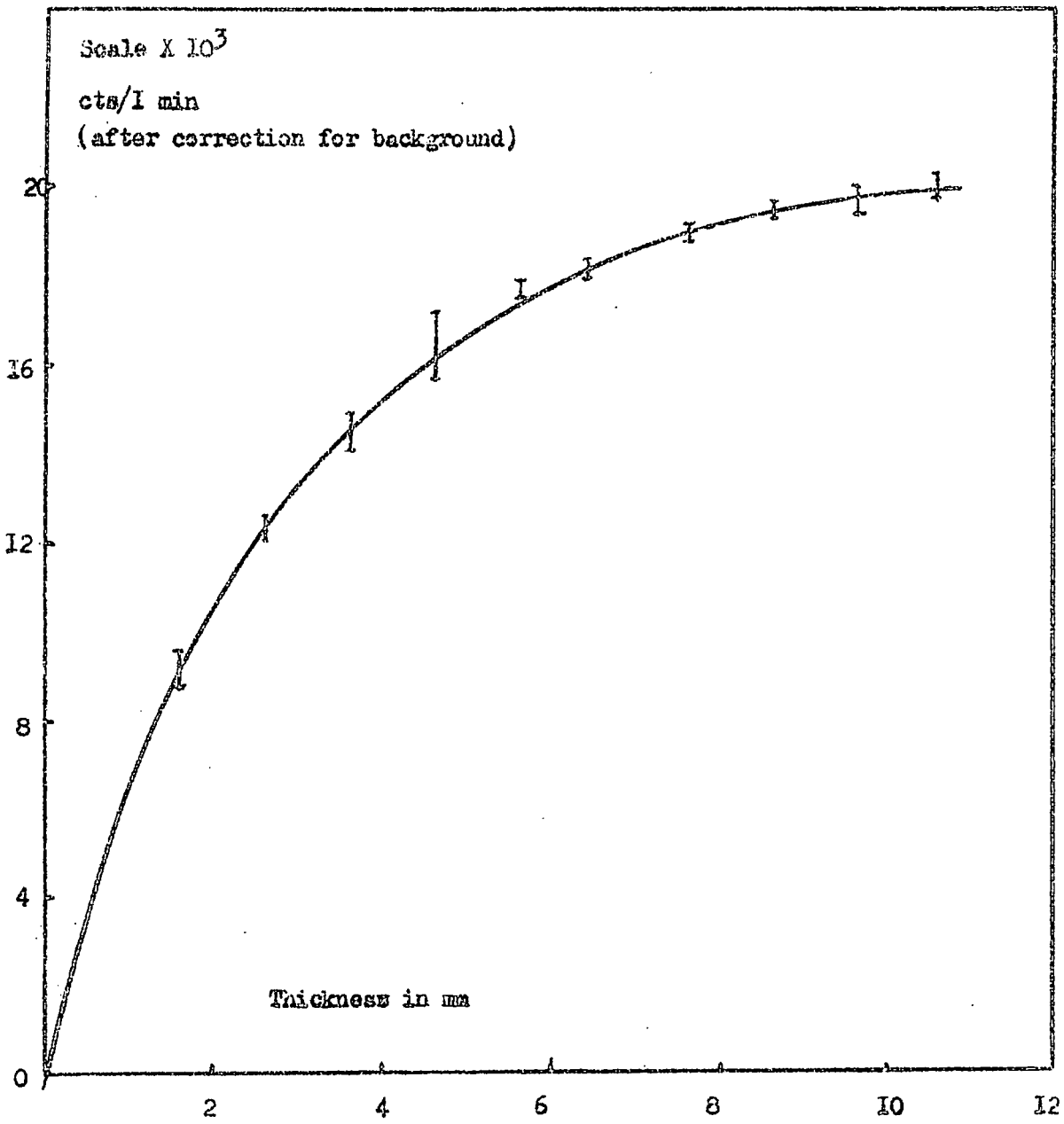

Fig. 5-4 Variation of fluorescent intensity of Nb K against thickness of sample (Nb_2O_5 in perspex)

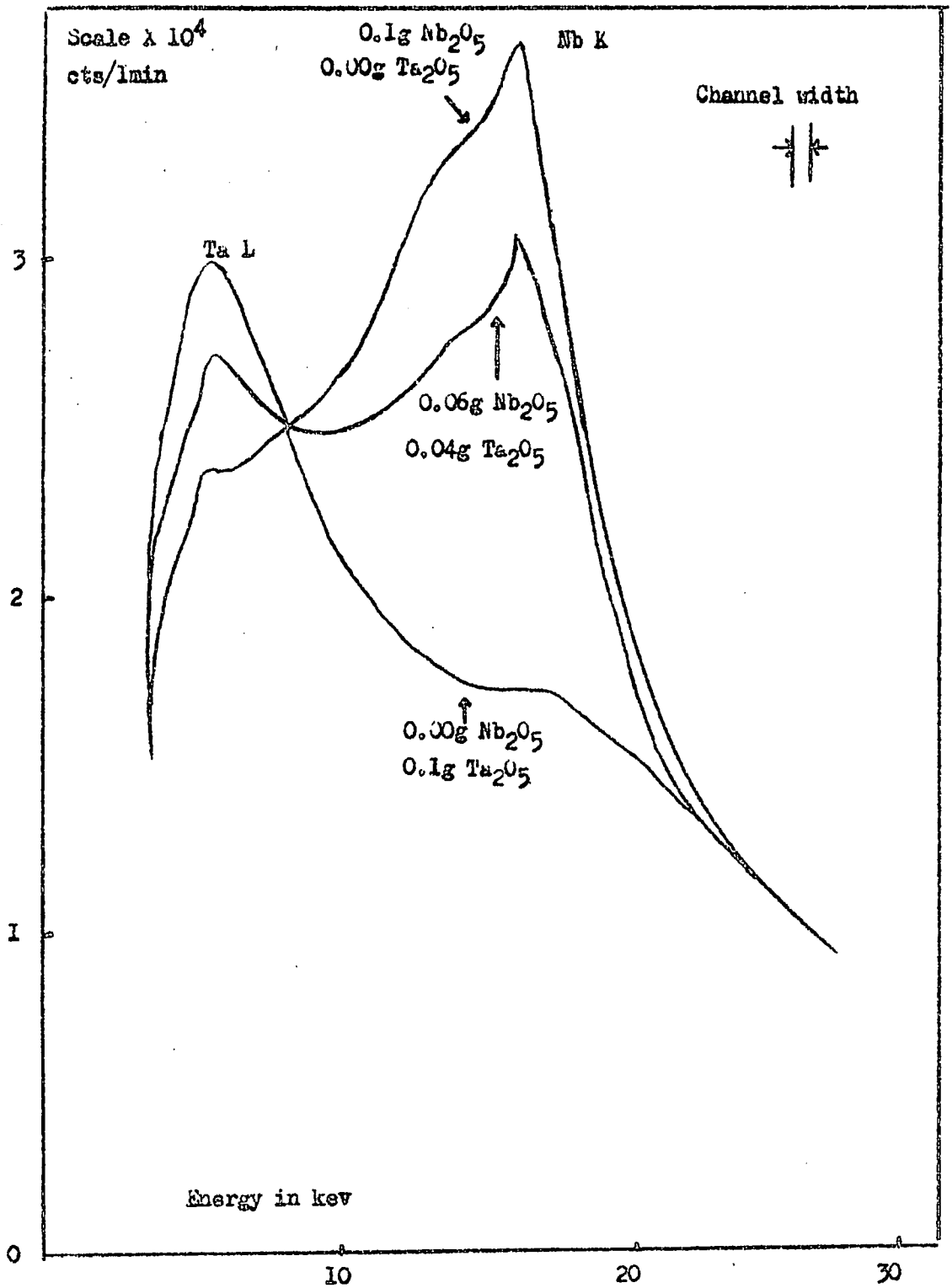

Fig. 5-5 0.1g of mixture of Ta and Nb oxides in 10g perspex

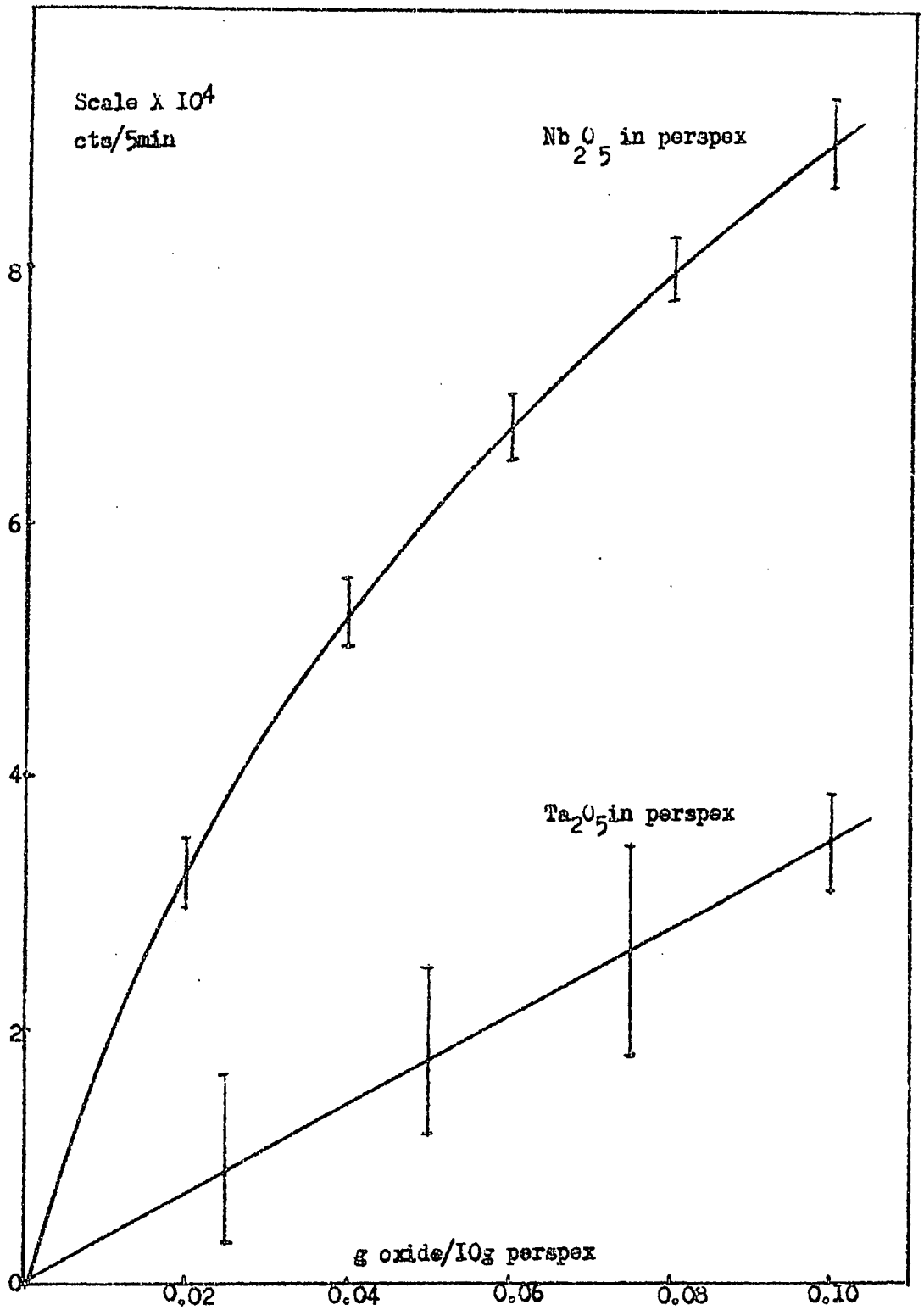

Fig. 5-6 Single oxide in perspex

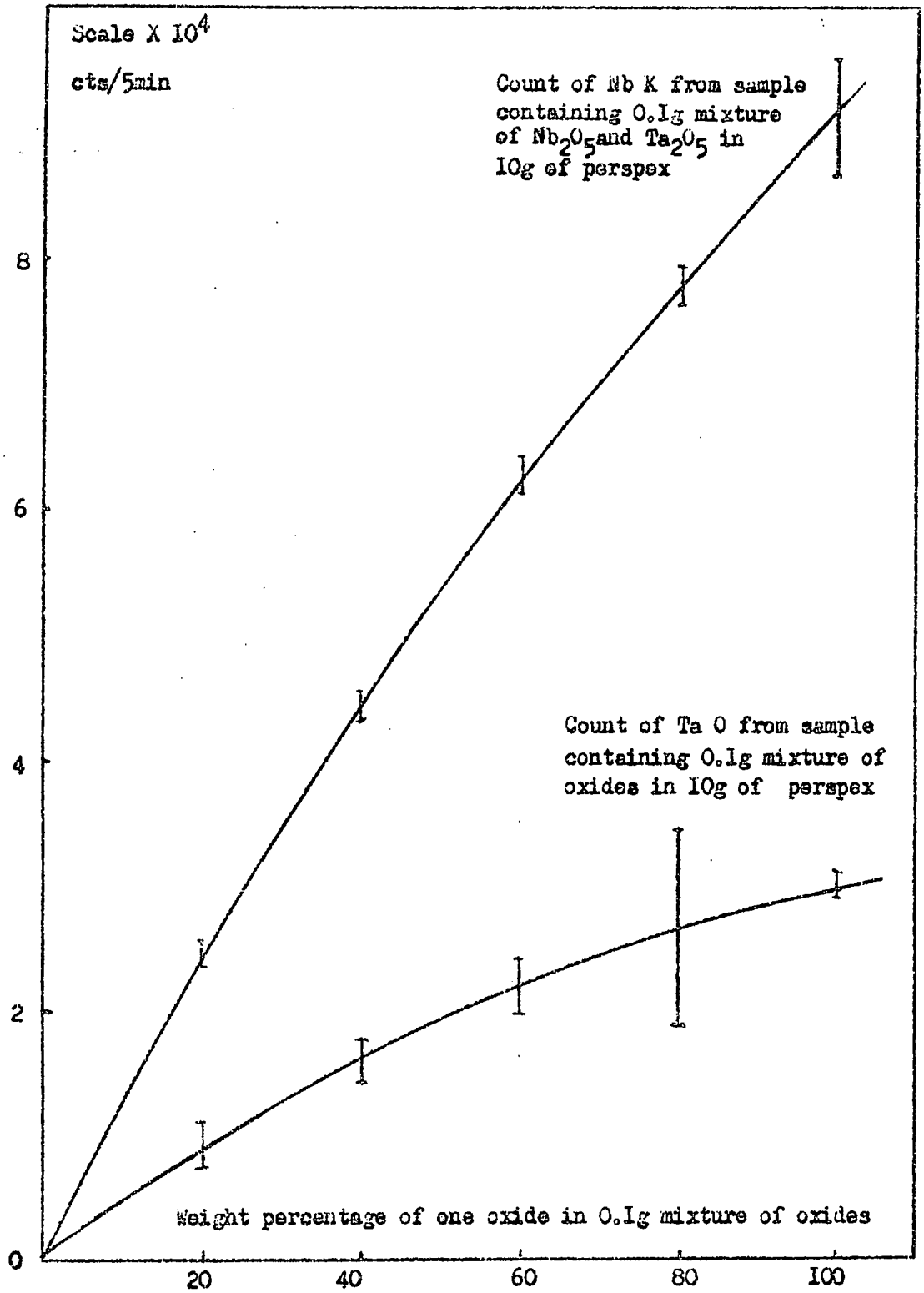

Fig.5-7 Mixture of oxides in perspex

the borax samples (page 41), the results being given in Table 5.7.

Table 5.7.

Sample	A	B	C	
Element	Nb	Ta	Nb	Ta
Detection limit	0.07	0.42	0.8	2.4

A:- Niobium oxide in perspex (10 gms)

B:- Tantalum oxide in perspex (10 gms)

C:- Mixture of tantalum and niobium oxides (0.1 gram of mixture in 10 gms of perspex).

CHAPTER 6

Summary of results

In Table 6.1 the collected results of the detection limits for the three sample systems studied are presented. The values are given in the case of the single element systems in terms of grams of element oxide in 1000 grams of solvent, and in the case of mixtures in terms of the weight percentage of the element oxide in the standard sample system (see before).

Table 6.1.

Single element systems			
	Dilute HF solution	Borax sample	Perspex sample.
Nb_2O_5	0.11	0.08	0.07
Ta_2O_5	0.20	0.31	0.42
Mixtures of elements			
Nb_2O_5	0.4.	0.67	0.8
Ta_2O_5	-	2.67	2.4

It is clear from these results that the detection limits for the three systems are very similar, the small variations being probably due to the method adopted for background correction. A choice between the three systems must depend upon grounds other than sensitivity.

Some brief comments on the sample systems are given below:-

A. Liquid solution

Where the material to be analysed is in a soluble form this method represents a rapid and simple form of preparation which results in a homogeneous system. A comparatively large volume of sample is required to approach the critical thickness value, but this is of some advantage in that the system is very tolerant to small displacements of the sample cell. The system has a much higher background level and scattering of radiation is significantly higher than for the other sample systems, and this results a broader fluorescent peak (see Figures 4-19). Because of the difficulty involved in background correction a value for the detection limit of tantalum oxide in the mixed oxide sample cannot be obtained.

B. Sodium borate sample

The solubility of metal oxides in sodium borate is generally low, but with the sample concentrations of interest this is not a great restriction. The time required for sample preparation is long, and varies widely (45 to 90 minutes), but it may be possible to reduce this by the use of specially designed burners for forming the melt (78). Being a solution the resulting sample is homogeneous, but variations in weight of the standard sample inevitably occur when pouring the viscous melt from the crucible to the sample mould. Such variations appear however to have little effect on the fluorescence intensity (c.f. sample reproducibility). The fluorescent peak obtained with these samples is sharp (see Figs. 5-1).

C. Mounting powder (perspex) samples

This method is not restricted by the solubility of the material to be analysed, but as the resulting sample is not a solution homegeneity is a problem. The results obtained strongly suggest that the method adopted for sample preparation is largely responsible for the errors observed. It is believed that this situation could be improved.

In the method of preparation previously described a mixture of the oxide and perspex mounting powder was heated to 170°C in a mounting press. At such a temperature the perspex would be liquid and gravitational settling of the much heavier oxide is inevitable. If however the mixture was heated to such a temperature that the perspex was only softened a coherent mass could be obtained without settling, and a homogeneous system obtained. Apart from reducing errors this would also bring about a considerable reduction in the time required for preparation.

The possibility of variation in the fluorescence intensity with particle size also exists in this method, but this could be overcome by careful milling of the material.

A fixed and reproducible size of sample is obtained in a matrix lighter than that of sidium borate (density of perspex is 2.1 gms/cc as against 3.1 gms/cc for borate), and sharp fluorescent peaks are obtained. Of the three sample systems studied the perspex method also requires the least quantity of material. The background is lower for the solid samples, and correction can be made more accurately. On these grounds the solid sample systems are to be preferred to the liquid solution.

CHAPTER 7

Spectra of Elements Excited by Co^{57}

Before entering on a discussion of the spectra of elements using the Co^{57} source, a consideration of some features of the detection process within the proportional counter will prove useful.

An X-ray photon entering the counter transfers its energy to an orbital electron of one of the atoms of the counter filling gas, the electron being ejected from that atom. The energy of this photoelectron, which is equal to that of the initial X-ray photon less the orbital electron binding energy, is then used up in ionisation of the counter filling gas. An orbital vacancy will be left in the residual atom from which the photon was ejected, and the filling of this vacancy will give rise to emission of a characteristic X-ray of that atom. Two processes can then occur:-

(a) The characteristic X-ray is absorbed within the counter giving rise to further ionisation which supplements the initial ionisation. The whole of the initial photon energy is thus available within the counter.

(b) The characteristic X-ray is not absorbed within the counter, and hence the energy available for ionisation is lower than the initial photon energy.

Thus in the spectrum of the initial X-ray photon two peaks might be expected to occur. When a scintillation counter is used to detect X-ray photons two peaks are indeed observed

in the spectrum, the high density of the detecting crystal ensuring a substantial contribution from process (a). The lower energy peak arising from process (b) is referred to as the "escape peak". The peaks are characterised by their constant energy separation, this separation being equal to that of the characteristic X-ray of the scintillation material. In the case of the proportional counter the relatively low density of the filling gas, and the transparency of atoms to their own characteristic radiations ensures little contribution from process (a) only one peak being observed, the "escape peak".

In the present work the filling gas of the proportional counter was the element Xenon. This has a further consequence in that fluorescent K X-rays of energy lower than the K absorption edge of Xenon will have insufficient energy to eject photoelectrons from the K shell of Xenon, and the principal photoelectron emission will be produced from the L shell. The fluorescent X-rays having energy greater than the Xenon absorption edge can eject K electrons from Xenon. This means that a higher proportion of the energy of the fluorescent X-ray photon is available for ionisation within the counter for elements of atomic number lower than cerium (Ce K = 34.7 kev) than is the case for heavier elements. The net result of this is that the fluorescent peaks of the heavier elements appear at lower apparent energies than would be expected on the basis of their characteristic X-ray energies. Thus the K fluorescent peak for tantalum (Z = 73) appears at roughly the same energy as that for silver (Z = 47) - see Figure 7-3.

Element Spectra

The secondary spectra of the elements in the form of pure metals or compounds in the solid state, obtained using Co^{57} as the primary X-ray source are similar to those using Pm^{147} bremsstrahlung (cf. Figures 3-6 7-1). There are slight differences being more obvious in the higher energy regions of the L spectra (cf. Figures 3-6a and 7-2). A number of

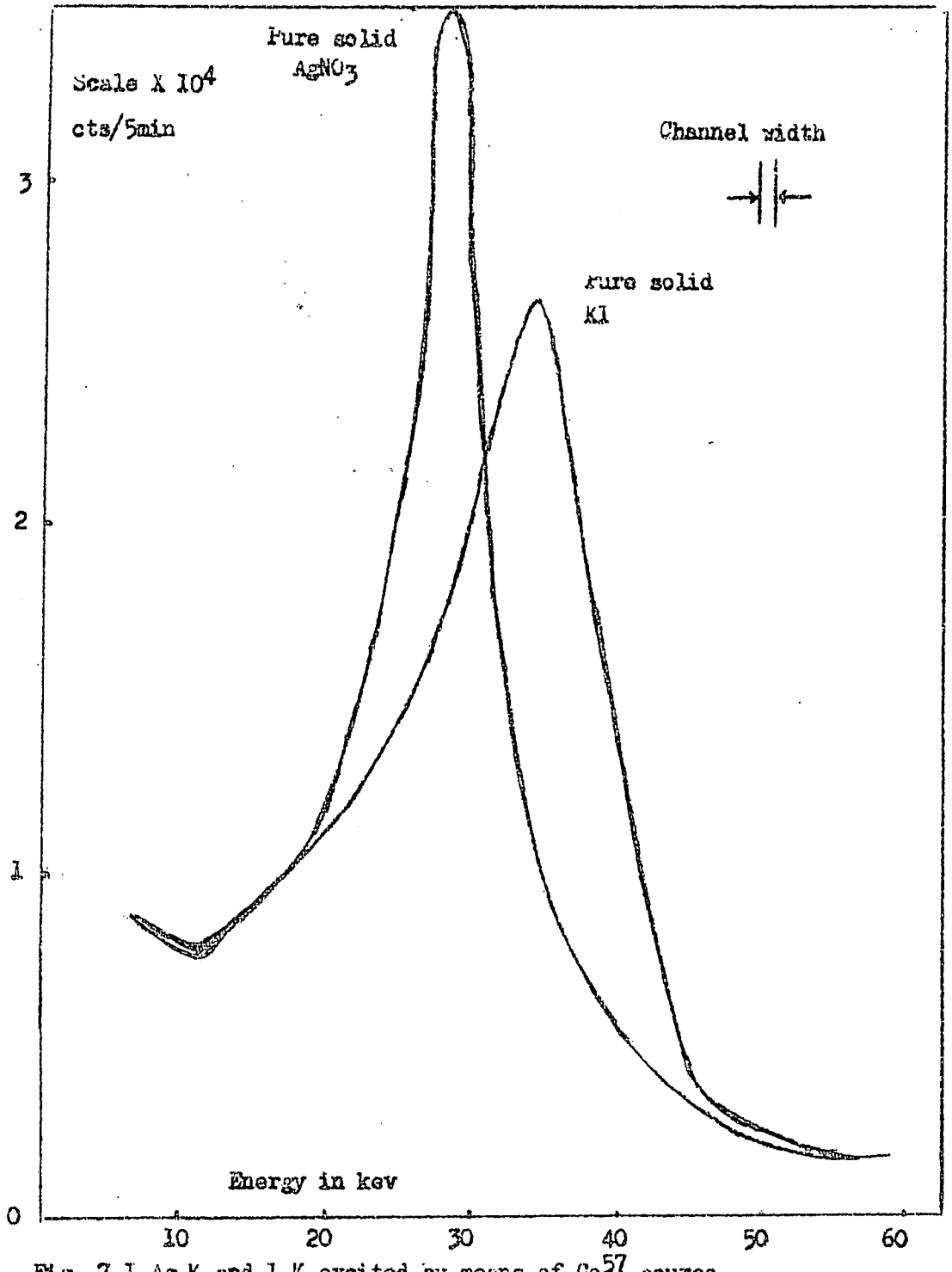

Fig. 7-1 Ag K and I K excited by means of Co^{57} source

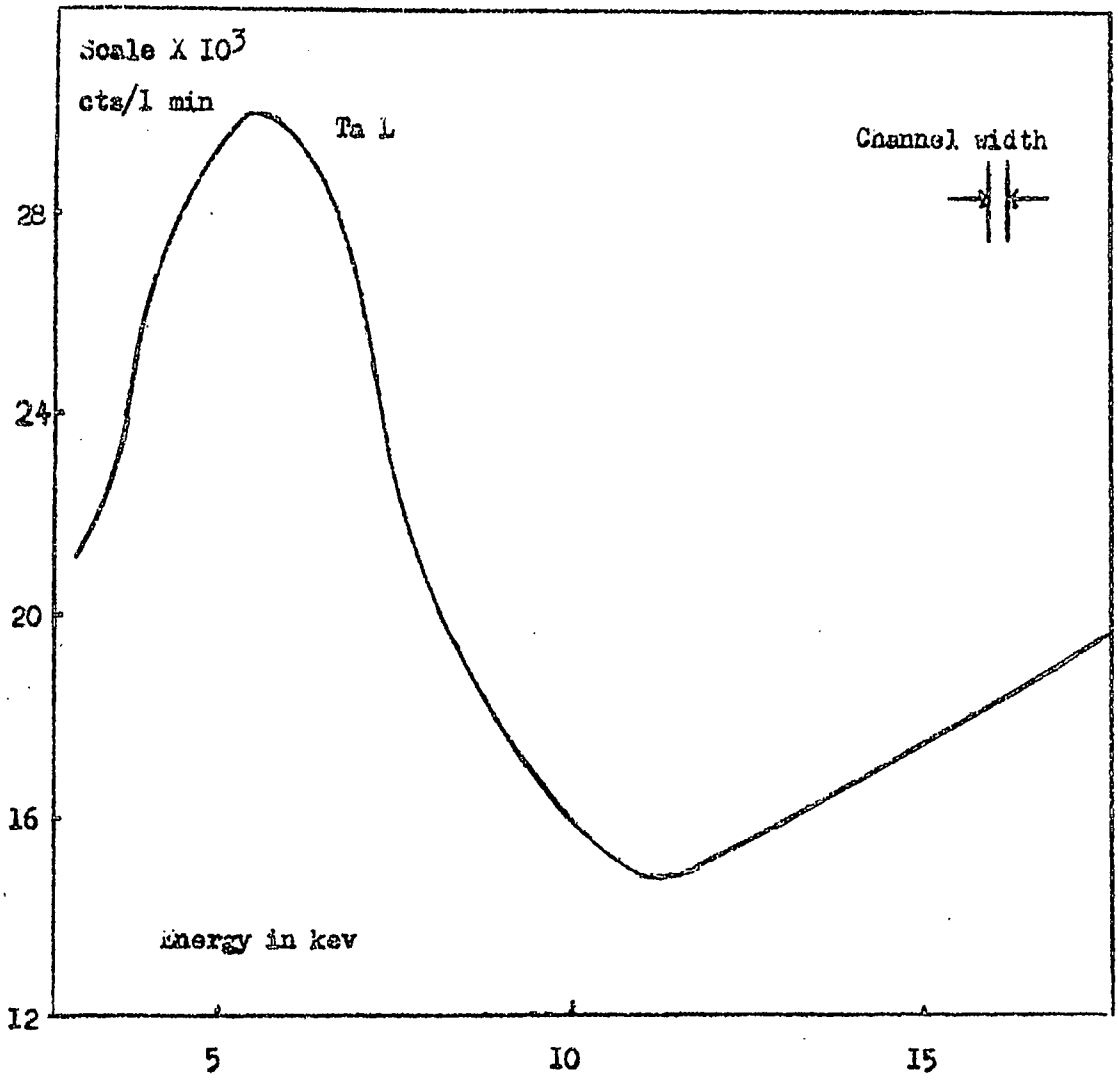

Fig. 7-2 Ta L from Ta foil by means of Co source

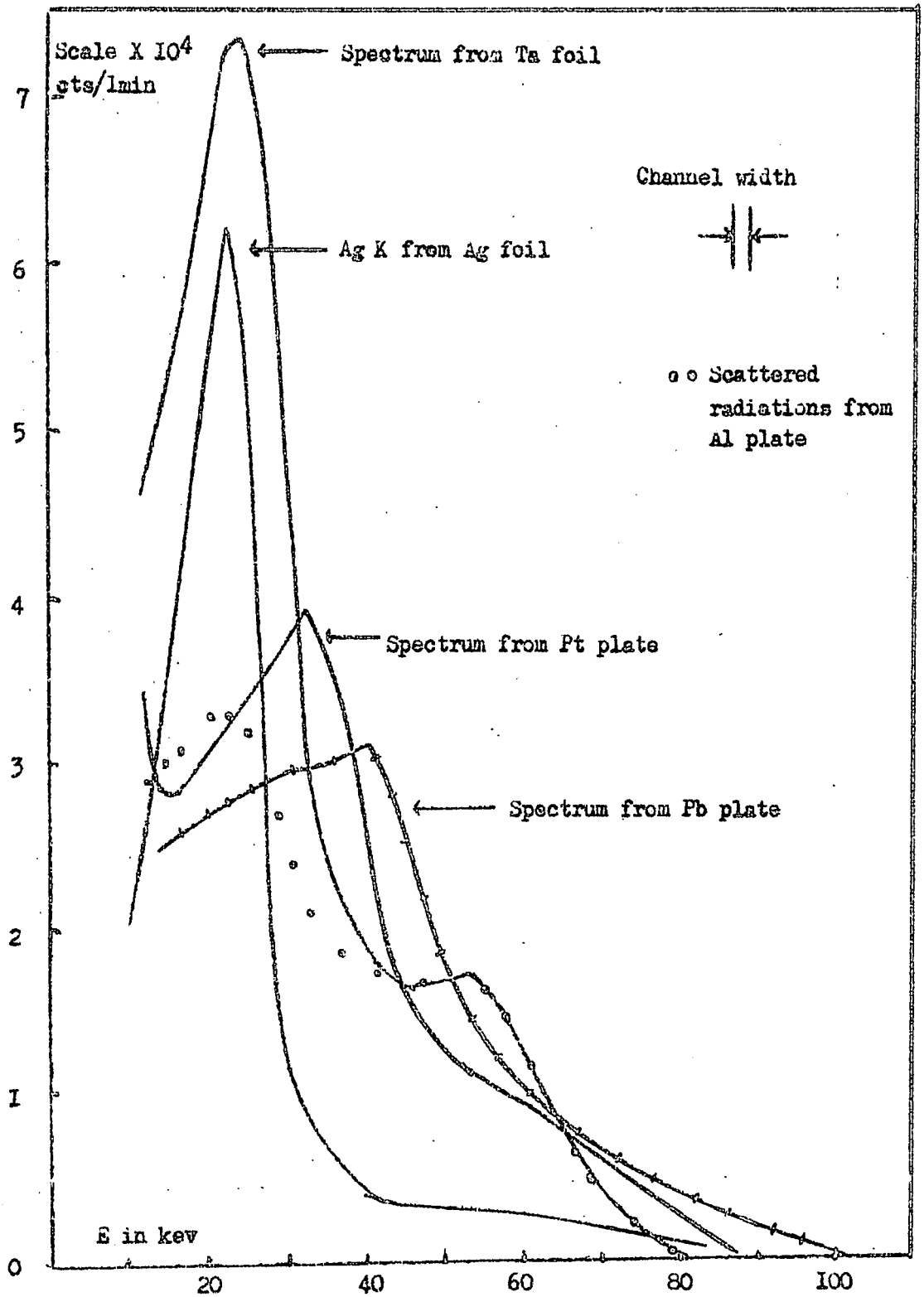

Fig. 7-3 Secondary radiations from various materials by means of Co^{57} source

representative spectra are illustrated in Figure 7-3. The energies of the peaks were assigned using the silver peak as reference, the energy of the latter being taken as that of Ag K (22.18 kev), and assuming linearity of the instrument response over this energy region. In Table 7.1 the observed energy is compared with that of the known K radiation of the element.

Table 7.1.

Element	Atomic number	K_{α} energy (kev)	Observed energy (kev)	Difference (kev)
Ag	47	22.18	22.18	0.
Sn	50	25.21	25.5	0.3
I	53	28.6	30.2	1.6
Ba	56	32.2	33.1	0.9
Ta	73	57.6	24.2	33.4
W	74	59.4	26.2	33.2
Pt	78	66.6	34.2	32.4
Pb	82	75	40.3	34.7

The energy difference in the last column of Table 7.1 is small for those elements whose characteristic K X-ray energy is below that of the absorption edge of Xenon (34.57 kev) and can be explained by the difficulty in deciding the peak energy accurately. The difference in the case of the heavier elements is sensibly constant, the variations from the mean value being probably caused by the peak energy assignment as before. However the mean difference is larger than the characteristic K energy of Xenon (29.8 kev), and must be due to a systematic error in the peak energy assignment.

Table 7.2

Material	gms/cm^2	Atoms/cm^2 (x6.02 x 10^{25})	Electrons/cm^2 (x6.02 x 10^{25})
Al	1.71	6.34	32.4
Cu	0.072	0.11	3.28
Ag	0.1505	0.14	6.56
Sn	0.033	0.07	3.7
Ta	0.166	0.092	6.7
W	0.121	0.066	4.8
Pt	0.69	0.35	27.5
Pb	0.0	0.06	316

In Table 7.2 some details are given of the metal samples used to obtain the spectra illustrated in Figure 7-3. These spectra were obtained at a high amplifier attenuation of 56 dB in order to include a wide range of elements on the same energy scale. The spectra of copper, tin, and tungsten are not illustrated in Figure 7-3 for the sake of clarity.

Copper: no peaks, but a broad spectrum of low intensity.

Tin: similar to the spectrum for silver but displaced to higher energy.

Tungsten: similar to tantalum spectrum but with the displacement to higher energy.

For the range of elements given the spectra do not have a uniform shape, and it is difficult with the data available to decide the cause of this. Aluminium for which no fluorescent peaks are expected shows two distinct peaks of relatively high intensity, one of which overlaps the tantalum spectrum. This overlap suggests the possibility that the aluminium spectrum is due to scattering of the primary X-rays from the source, which should be proportional to the number of electrons per unit area. However the area density of electrons for the silver sample is similar to that for tantalum (see Table 7.2), but silver shows no corresponding peak at the position where the aluminium and tantalum spectra overlap. Moreover platinum

and lead with higher area density of electrons show no prominent features in this region. It is clear that scattering alone cannot account for the variation in shape of the spectra.

The sample of aluminium used was a ¼ inch plate formed by a rolling process which gives rise to preferred orientation of the crystals. Since aluminium is well known to have a high reflecting power for X-rays the two peaks observed could well be due to Bragg reflections from the crystals. This might well have been checked using a sample of cast aluminium which would not show preferred orientation of the crystals, but such a sample was not available.

The spectrum of tantalum (and tungsten) shows a subsidiary peak on the high energy side of the main peak. The difference in energy between the two peaks, allowing for the inevitable errors in location of the peak positions, corresponds to the energy of the Xenon characteristic K X-ray (29.8 kev). Such a situation would arise when the tantalum (or tungsten) fluorescent K X-ray ejects an electron from the L shell of Xenon with the result that a higher proportion of the fluorescent X-ray energy is available for ionisation in the counter. No second peak would be expected for silver and tin since their fluorescent K X-rays have insufficient energy to remove electrons from the Xenon K shell. The second peak would however be expected in the platinum and lead spectra, but may not be detectable for these elements owing to the lower intensity of the peaks. This would appear to be the most satisfactory explanation of the shape of the observed spectra.

CHAPTER 8

Liquid solutions - Co^{57} source

Geometrical arrangement B (Figure 4-1) was adopted, the Co^{57} source being mounted on a 9.5 mm column of lead to reduce direct access to the counter of the 122 kev gamma ray. The sample to window distance was 1.5 cms. All other parameters were the same as described in Chapter 4, e.g. the volume of solution, pulse analyser channel width, counter voltage, and the time constants of the amplifier.

Spectra of elements in solution

For the elements examined the spectra were similar to those obtained with the Pm^{147} source except for the very much higher background level (see Figures 8-1, 8-2). On both sides of the characteristic peak the spectrum of the solution meets that of the blank with the exception of the solution of tantalum oxide in hydrofluoric acid. In this latter case the characteristic X-ray observed was Ta L, and the higher than background intensity on the high energy side of this peak can be considered as due to Compton scattering of the Ta K escape peak (see figure 8-2).

Calibrations

The construction of a calibration curve of fluorescence intensity against element concentration was made in the same way as for the Pm^{147} source (see Chapter 4). The calibration curves are given in Figures 8-3, 8-4, and 8-5. For tantalum

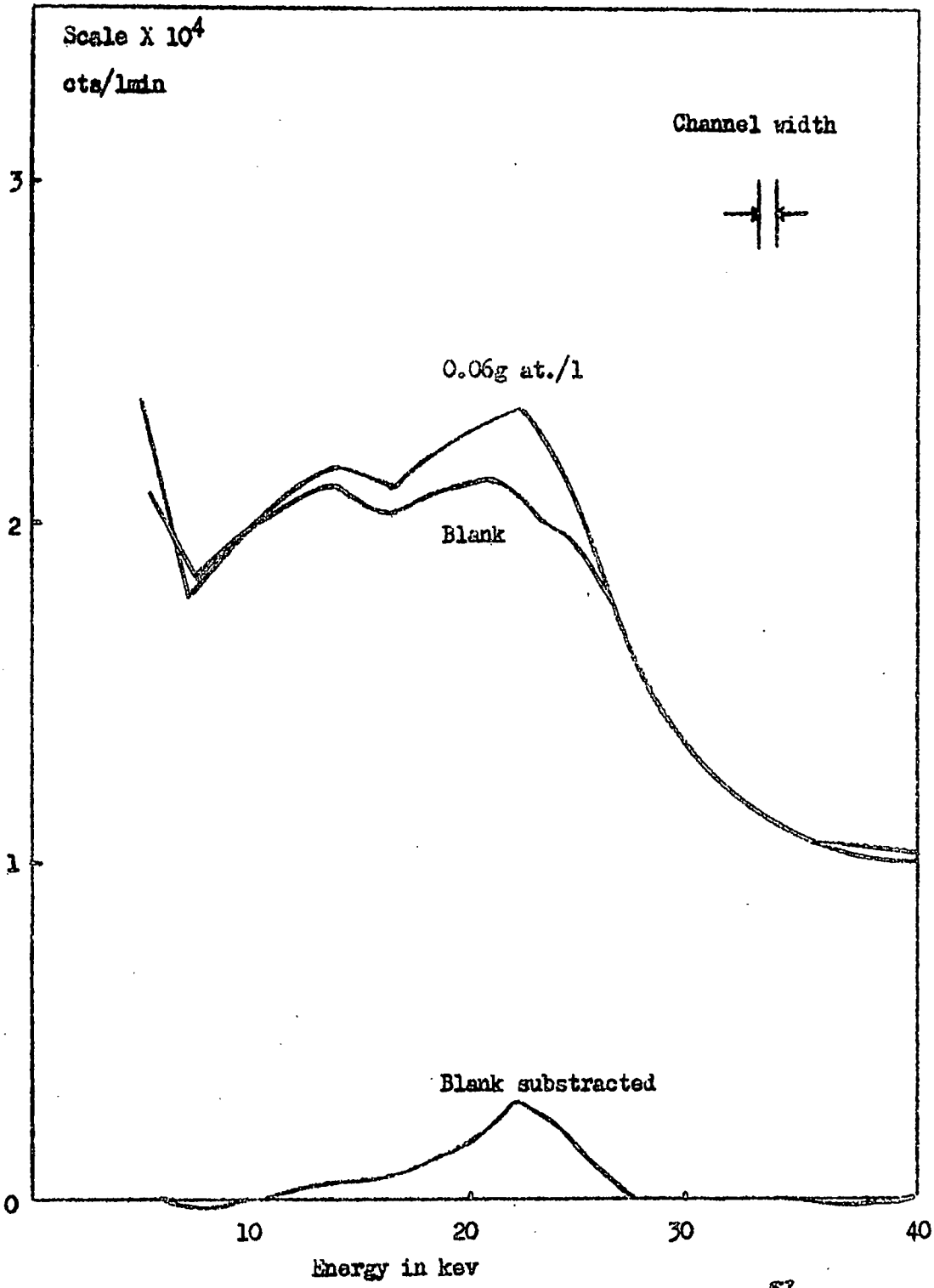

Fig. 8-1 AgK from $AgNO_3$ in dil. HNO_3 excited by means of Co^{57} source

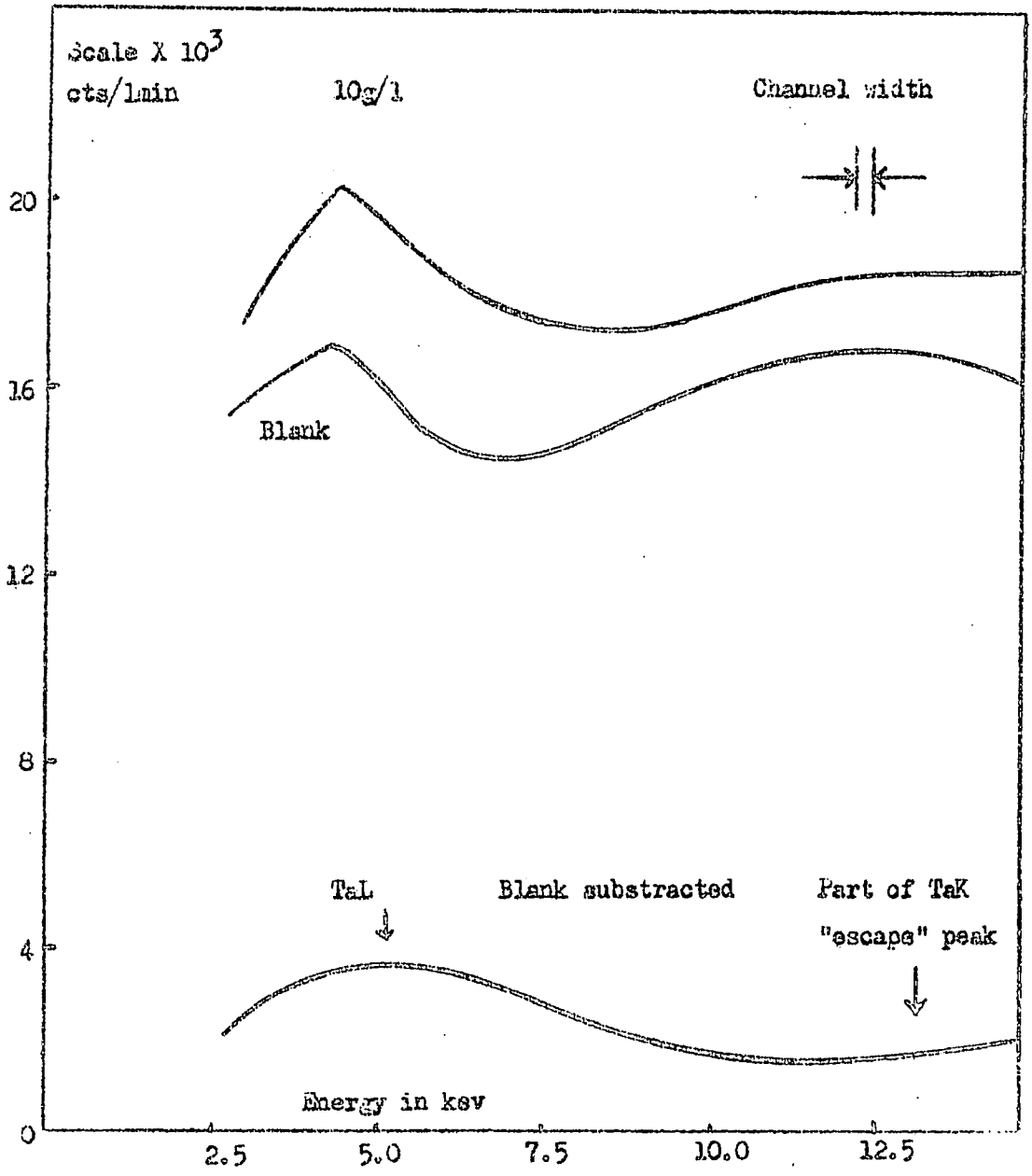

Fig. 8-2 10g tantalum oxide per litre Part of TaK "escape" peak is mixed up with TaL. Co^{57} Source used.

Arrangement B with Co^{57} as source (Fig. 8-3)

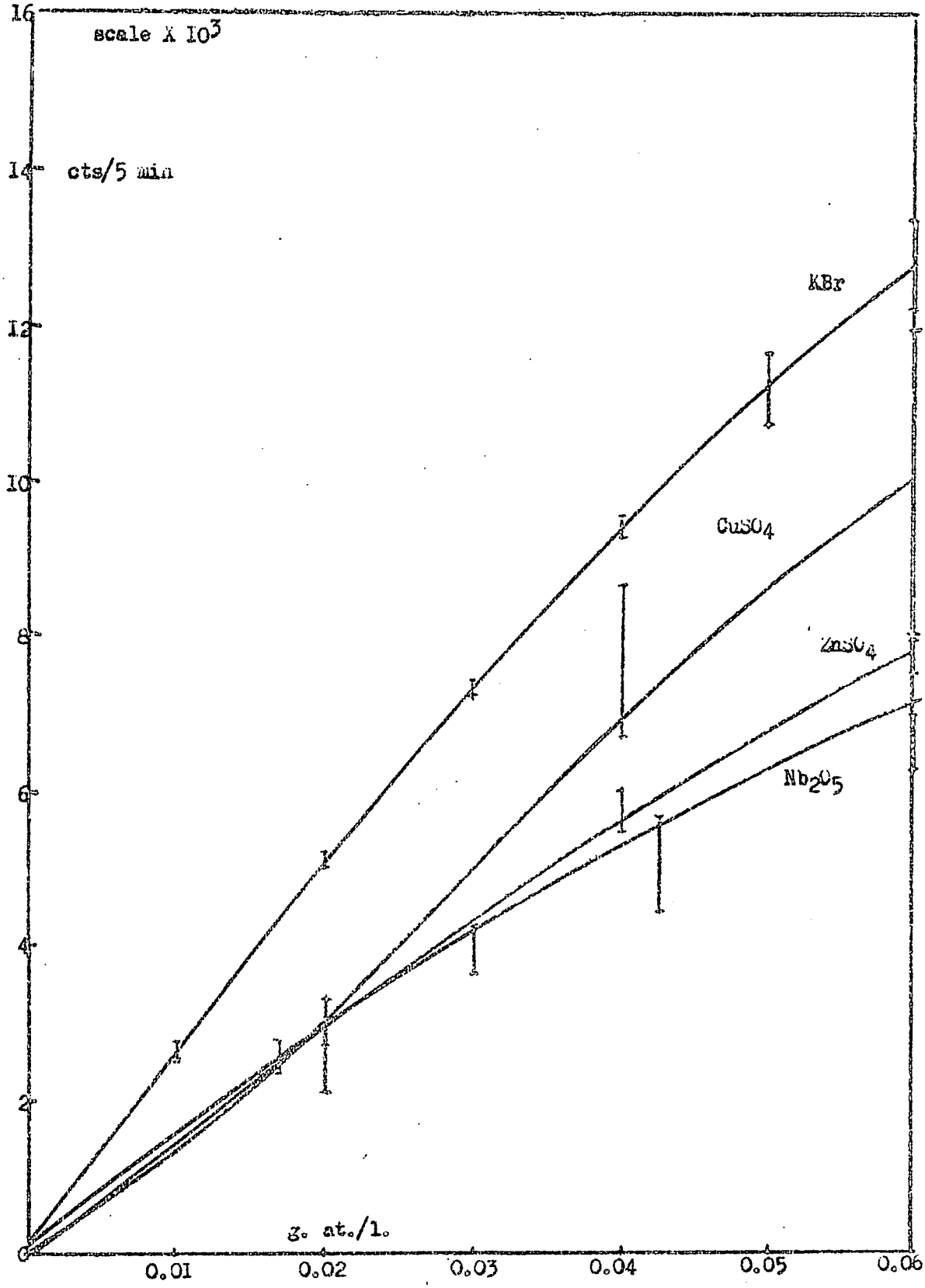

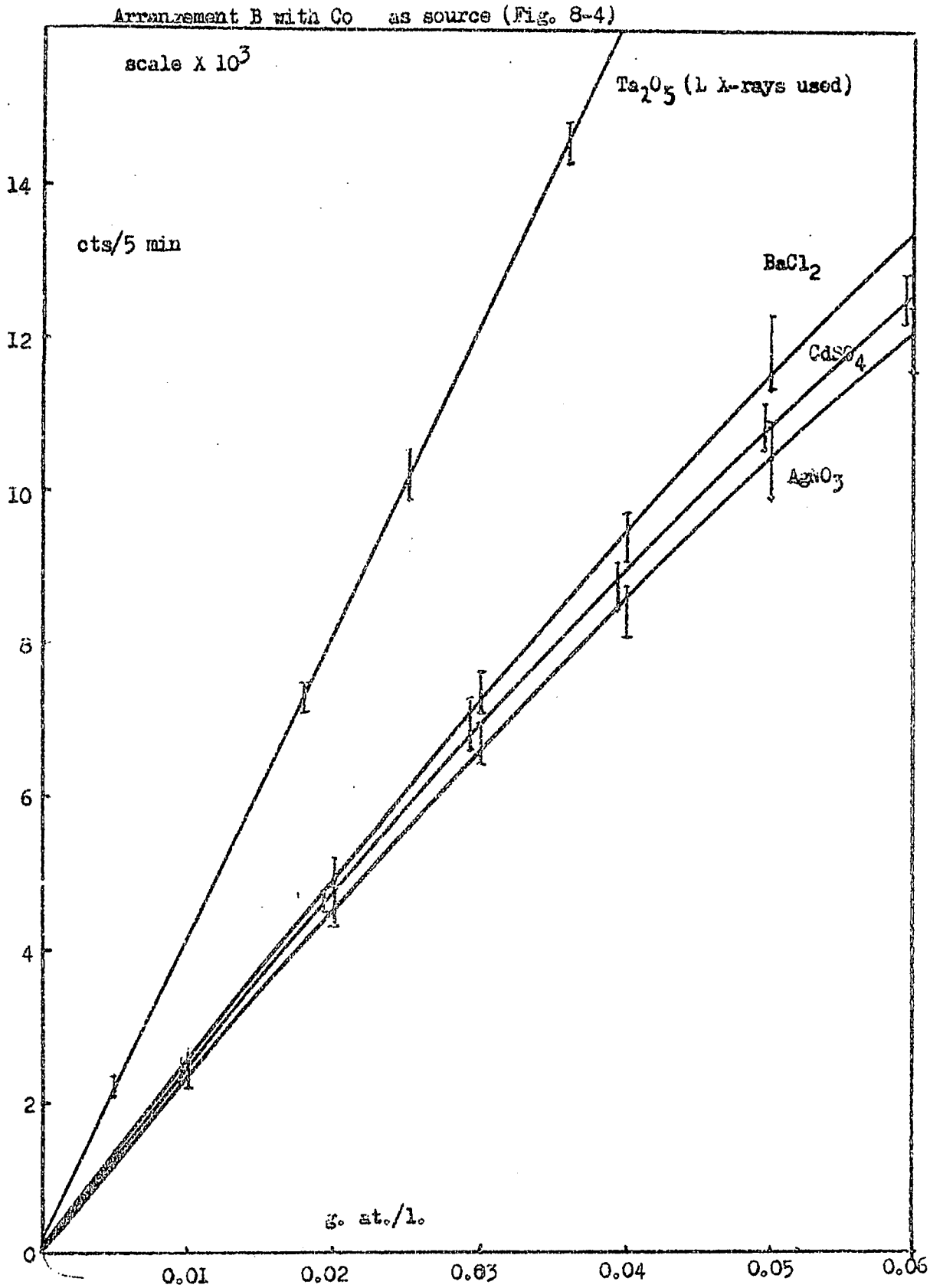
Arrangement B with Co as source (Fig. 8-4)
scale X 10^3
Ta_2O_5 (L x-rays used)
cts/5 min
$BaCl_2$
$CdSO_4$
$AgNO_3$
14
12
10
8
6
4
2
0
g. at./l.
0.01
0.02
0.03
0.04
0.05
0.06

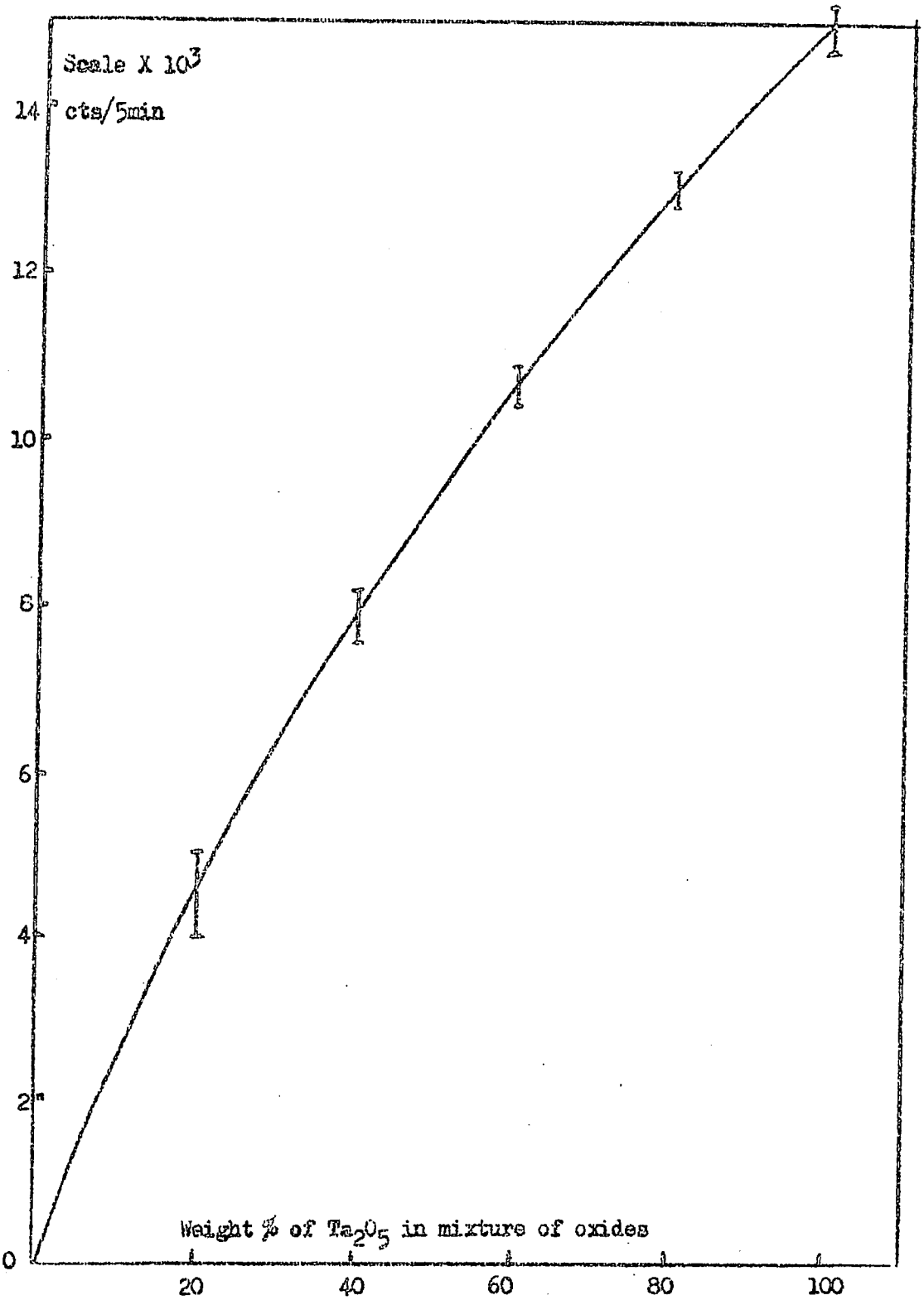

Fig. 8-5 Count of TaL against wt. % of tantalum oxide in mixture of niobium and tantalum oxides (Co^{57} source used)

oxide solutions the usual method of background correction (page 32) could hot be used owing to the interference of the Ta K escape peak in the background reference position, and the count rate at zero concentration was therefore adopted as the background correction for all concentration. The presence of the Ta K escape peak at the peak position for Nb K made impossible the construction of a calibration curve for niobium in tantalum - niobium mixtures. A calibration curve for tantalum in the mixtures was obtained.

Results

The detection limits (in gram atoms per litre of solution) for a number of elements are given in Table 8.1.

Table 8.1.

Element	Atomic number	Characteristic X-ray	Absorption Edge (kev)	Detection limit ($\times 10^{-3}$)
Cu	29	K	8.978	8.0
Zn	30	K	9.657	5.6
Br	35	K	13.471	3.4
Nb	41	K	18,981	6.24
Ag	47	K	25.5	4.0
Cd	48	K	26.704	3.5
Ba	56	K	37.399	4.0
Ta	73	L	11.681	2.7

The detection limit falls with increase in atomic number a minimum value being obtained at bromine. This is to be expected since the 14.4 kev gamma ray of Co^{57} is approaching the element absorption edge. Above bromine the K absorption edge will be higher in energy than 14.4 kev and the mass absorption coefficient will fall in value. Note the lower detection limit of tantalum compared to niobium, the Ta L absorption edge being lower than 14.4 kev and Nb K greater.

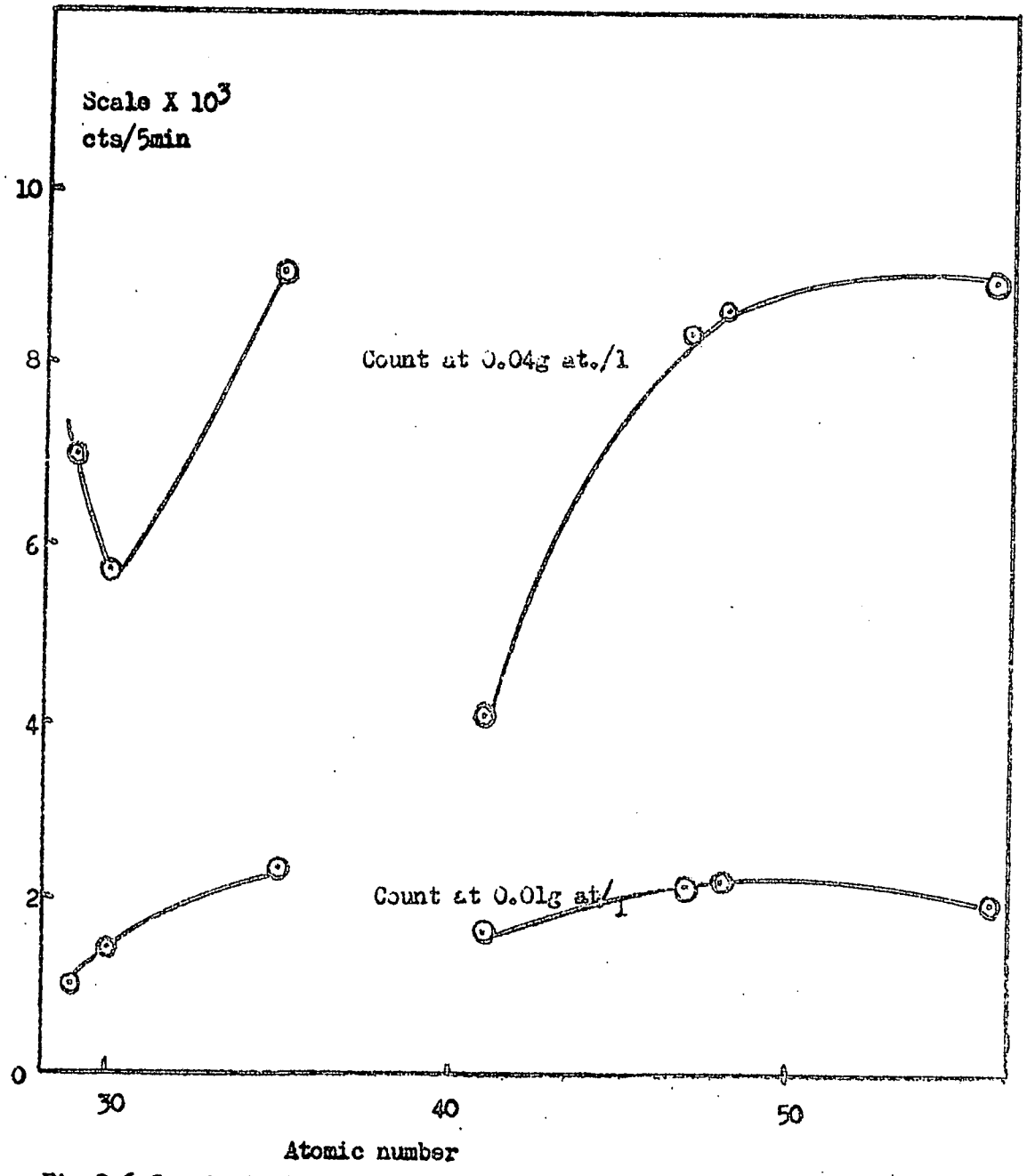

Fig.8-6 Count at given concentration against atomic number (Co^{57} source used)

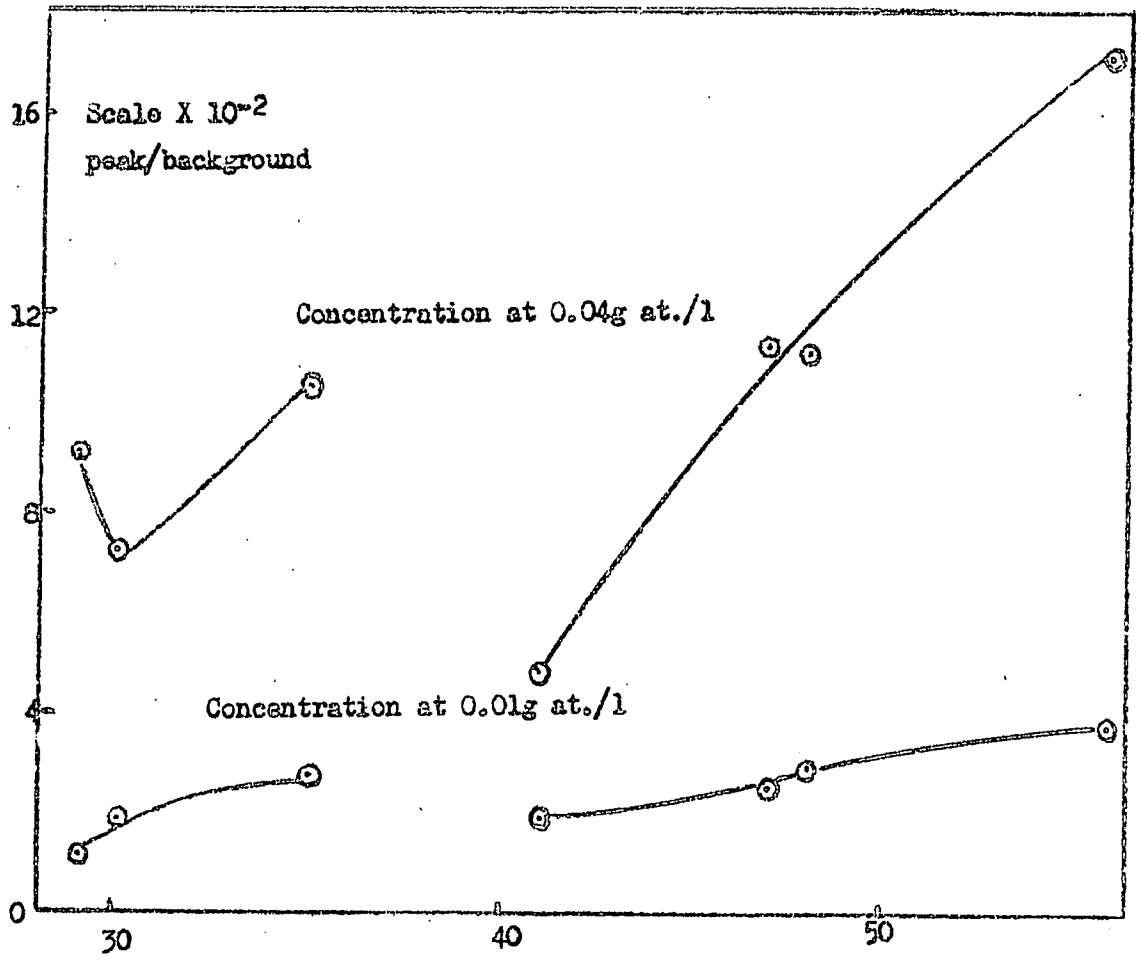

Fig.8-7 Peak/background against atomic number (Co^{57} source used)

This is the reverse of the situation observed with the Pm^{147} source.

Where the elements absorption edge is greater than 14.4 kev the principal excitation will arise from the 122 kev gamma ray. The photoelectric cross section of elements for a gamma ray energy of 122 kev will increase with the atomic number of the element (65), as also will the fluorescence yield. Thus a decrease of detection limit will be expected with increasing atomic number. The dependence will be more complicated however since the higher the energy of the fluorescent X-ray, the smaller will be the efficiency of the counter. This latter effect will arise since the mass absorption coefficient of Xenon will decrease the further one moves away from the Xe L absorption edge.

The detection limit for tantalum oxide in a mixture of tantalum and niobium oxides is 3.2 weight per cent in the mixture.

CHAPTER 9

Solid Samples - Co^{57} Source

The solid samples were prepared as described earlier. Geometrical arrangement B (page 30 a) was adopted for the source, sample, and counter, the Co^{57} source being mounted on a lead column 9.5 mms in height. The sample to window distance was set at 1.7 cms for the borate samples and at 1.2 cms for the samples bonded in perspex.

Spectra

The spectra observed for niobium oxide and tantalum oxide in the two sample systems are shown in figures 9-1, 9-2. The background intensity is high giving a low peak to background ratio value of which are given in Table 9.1.

Table 9.1.

wt of oxide in 100 gms of sample	Borax system		Perspex system	
	Nb_2O_5	Ta_2O_5	Nb_2O_5	Ta_2O_5
0.2	0.021	0.050	0.056	0.081
0.4	0.066	0.089	0.095	0.17
1.0	0.18	0.17	0.17	0.36

For samples containing tantalum oxide - niobium oxide mixture the background correction applied to the Nb K peak was again complicated by the presence of the Ta K escape peak (see Chapter 8).

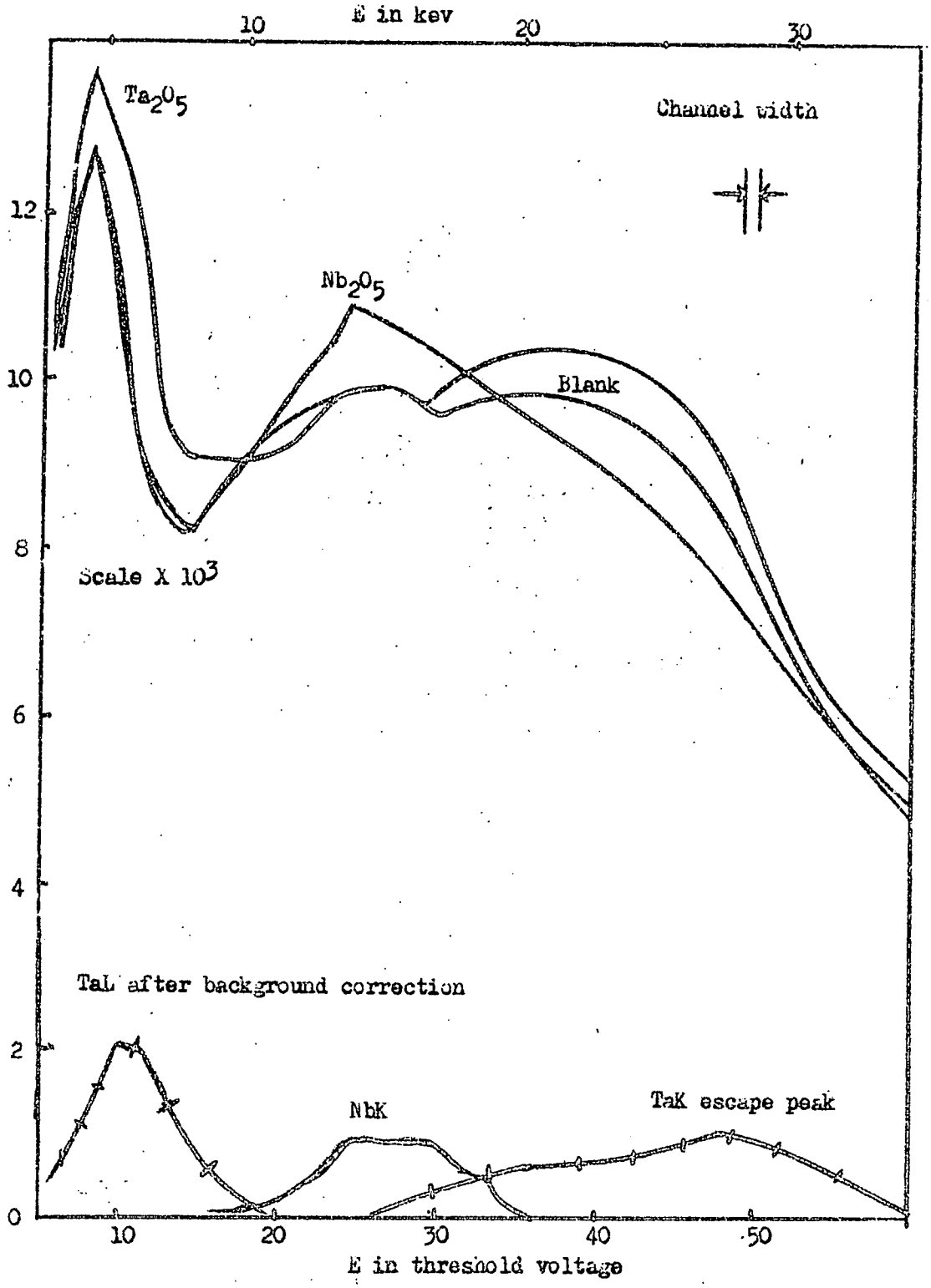

Fig. 9-1 Single oxide in borate(0.2g in 20g)
Co source used

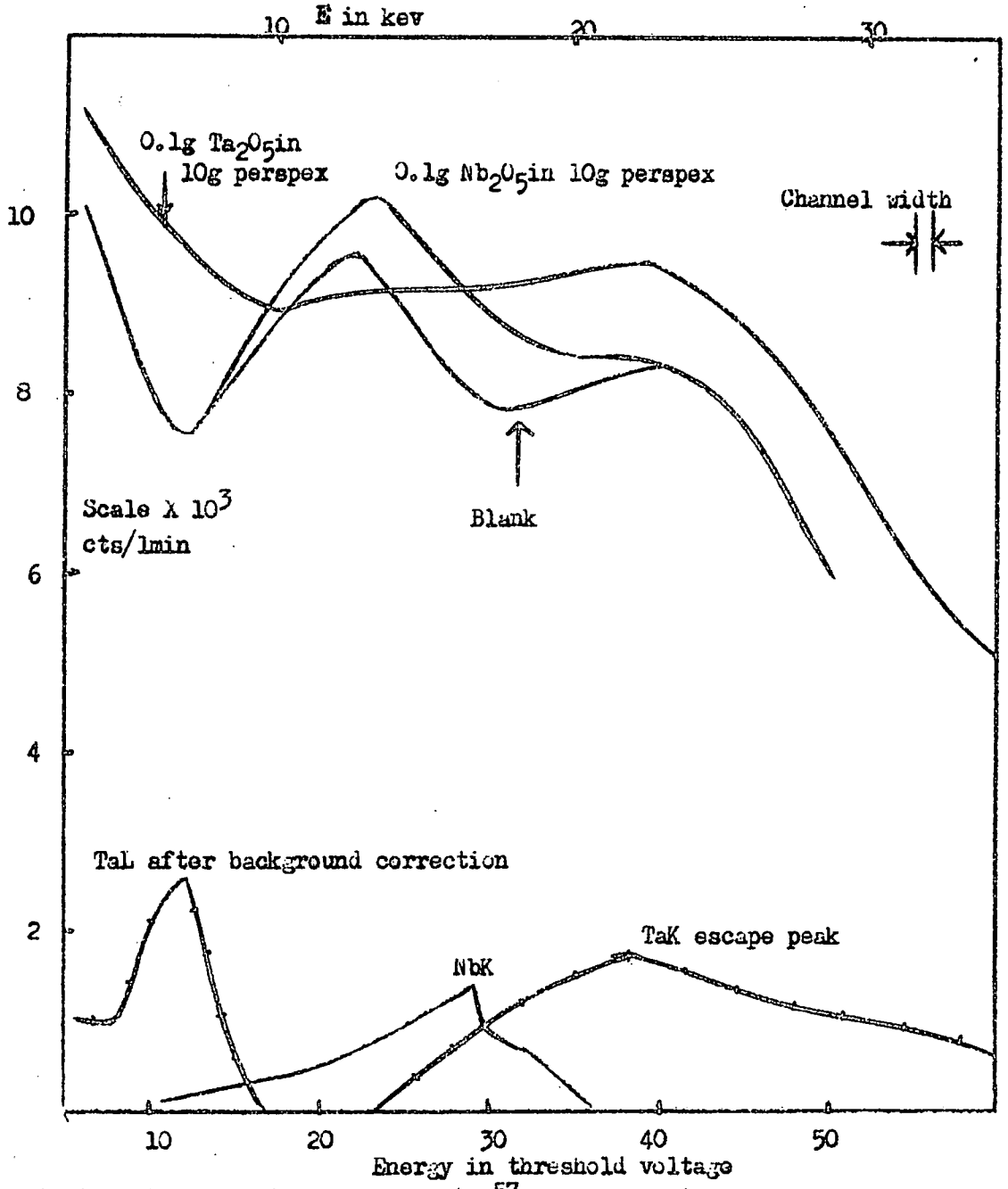

Fig.9-2 Single oxide in perspex (Co^{57} source used)

Calibration

The calibration curves for tantalum and niobium in the single and mixed oxide systems are shown in Figures 9-3, 9-4, 9-5 and 9-6. The results on the perspex samples again reveal the inadequacy of the method of preparation (see Chapter 5). The detection limits, expressed for the single oxide systems in grams of oxide per 1000 grams of matrix, and for the mixed oxides as weight % in 0.1 gms of mixture per 10 gms of perspex, or in 0.2 gms per 20 gms of borax, are given in Table 9.2.

Table 9.2.

	Single oxides	
	Borax	Perspex
Nb_2O_5	1.34	0.53
Ta_2O_5	4.75	0.84
	Mixed oxides	
	Borax	Perspex
Nb_2O_5	7.4	10
Ta_2O_5	4.8	5.3

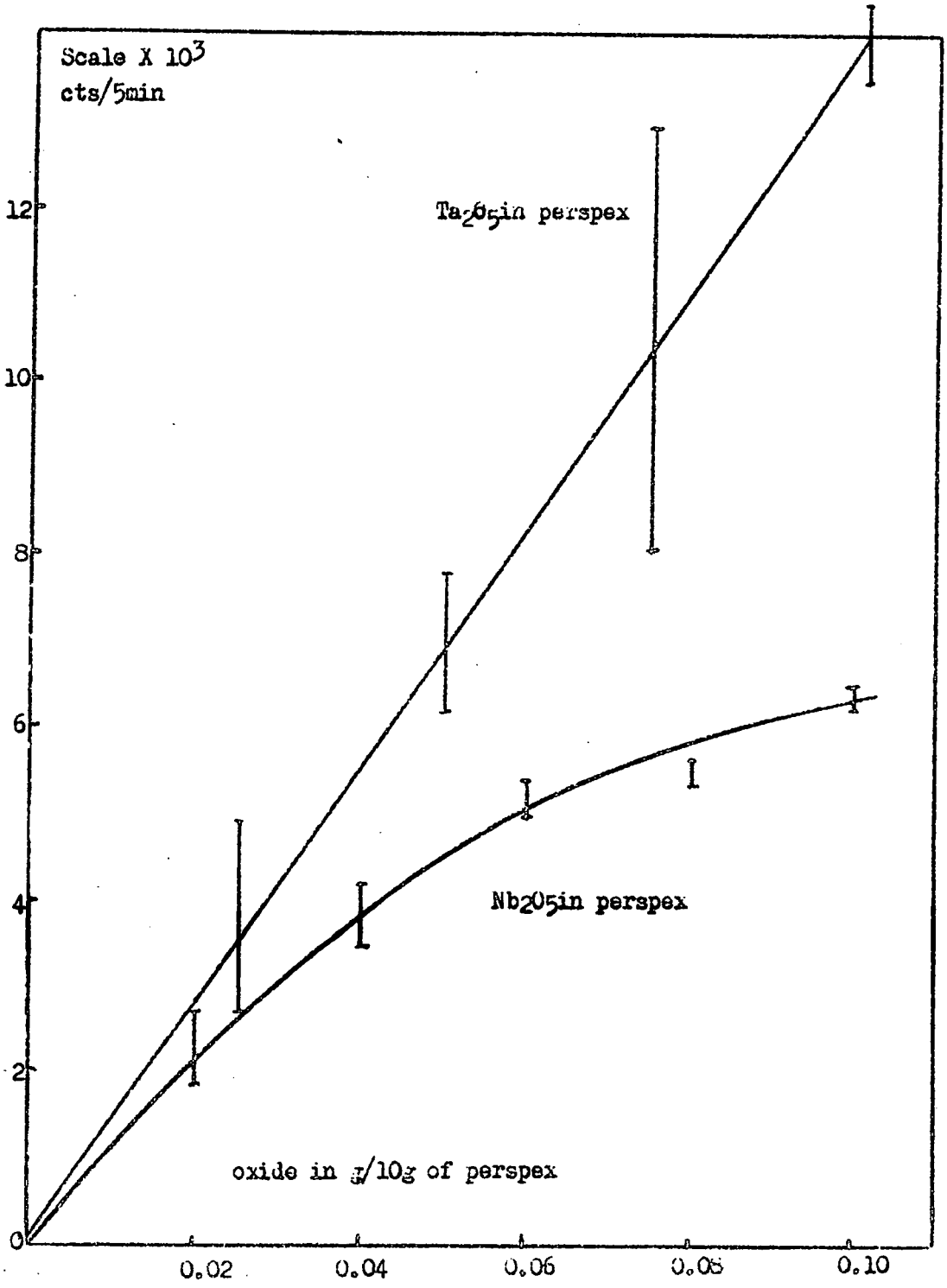

Fig.9-3 Count against concentration of single oxide in perspex (Co^{57} source used)

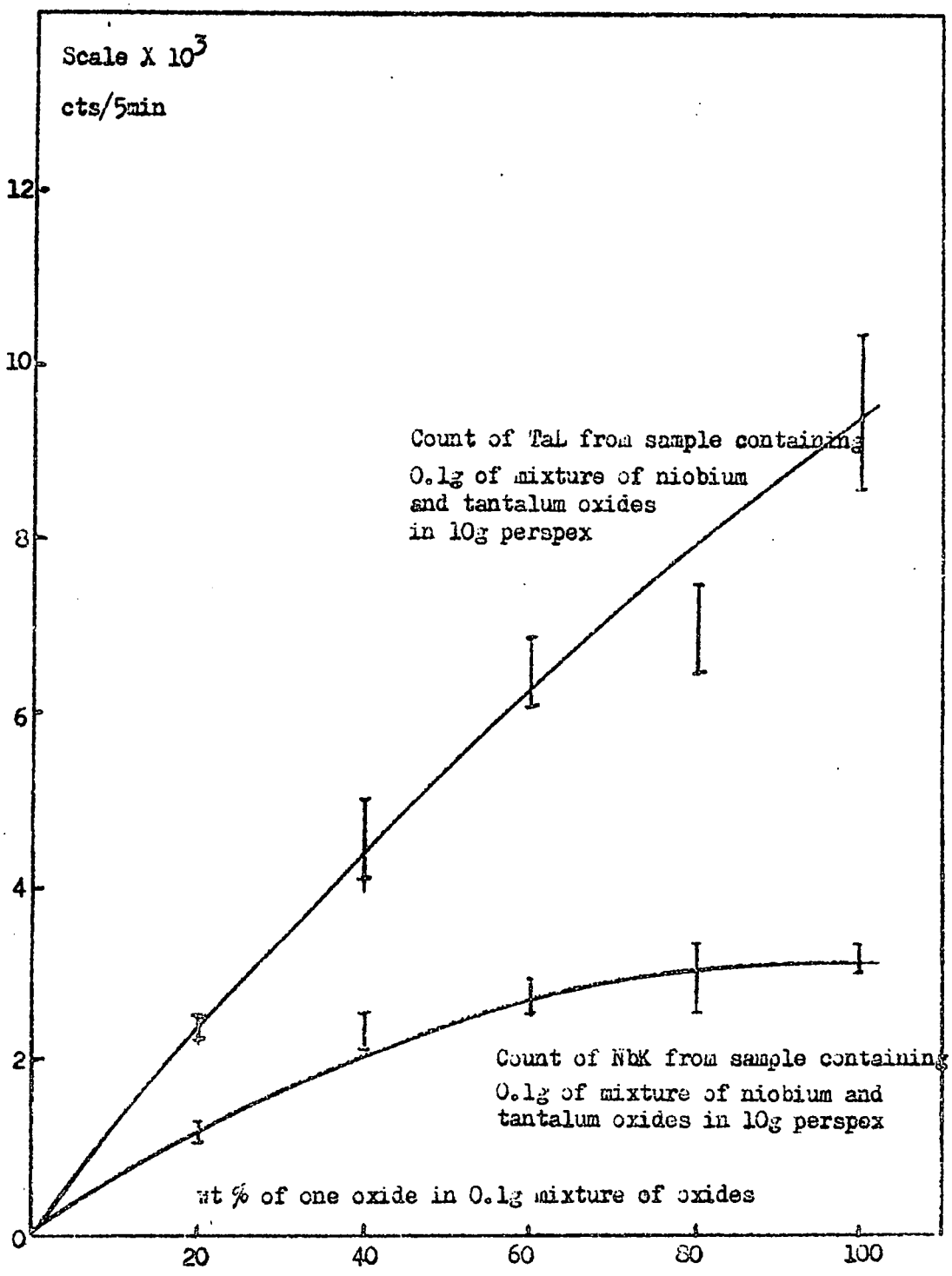

Fig.9-4 Count against wt % of oxide in mixture of oxides
(Co^{57} source used)

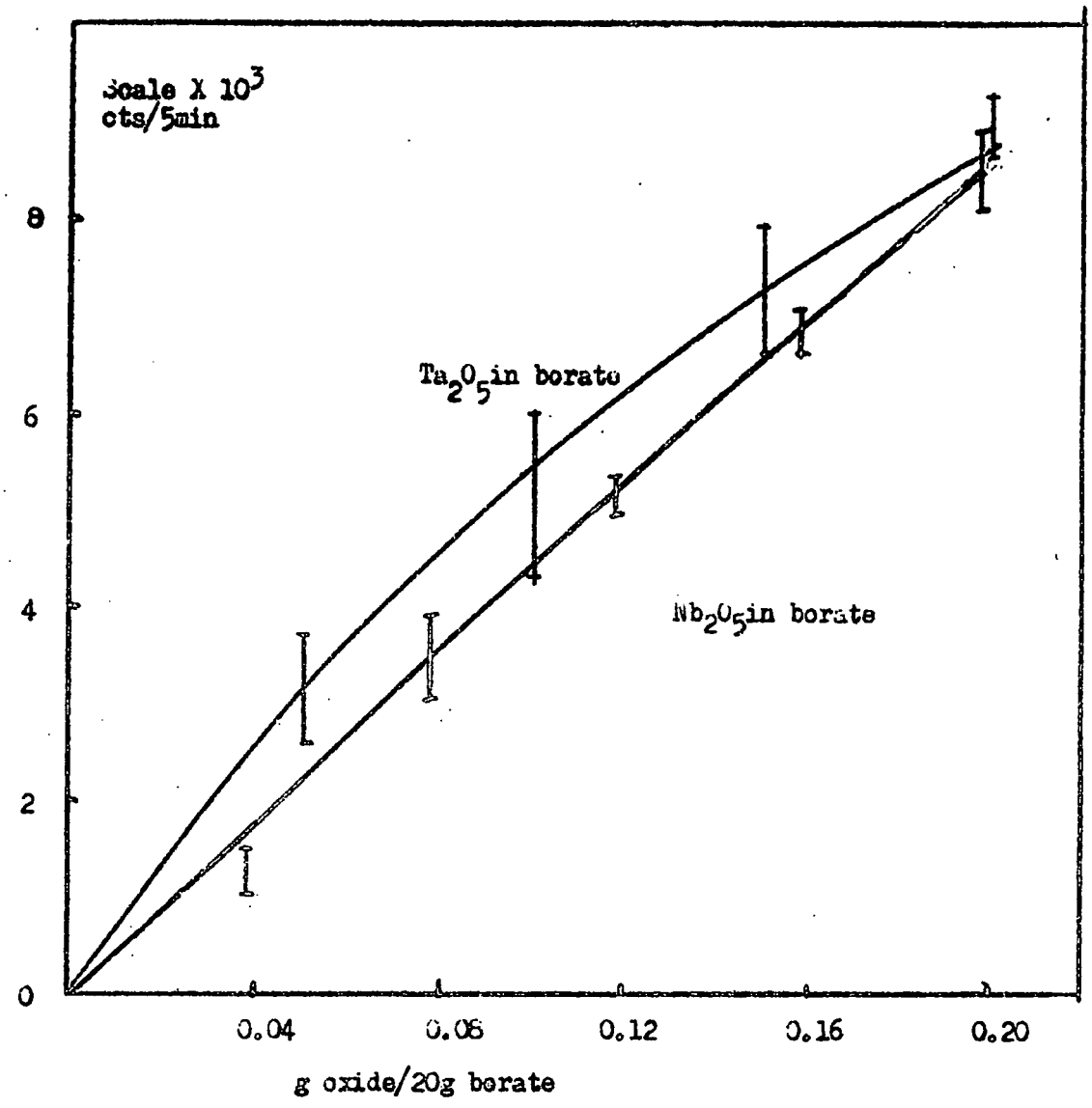

Fig.9-5 Single oxide in borate sample (Co^{57} source used)

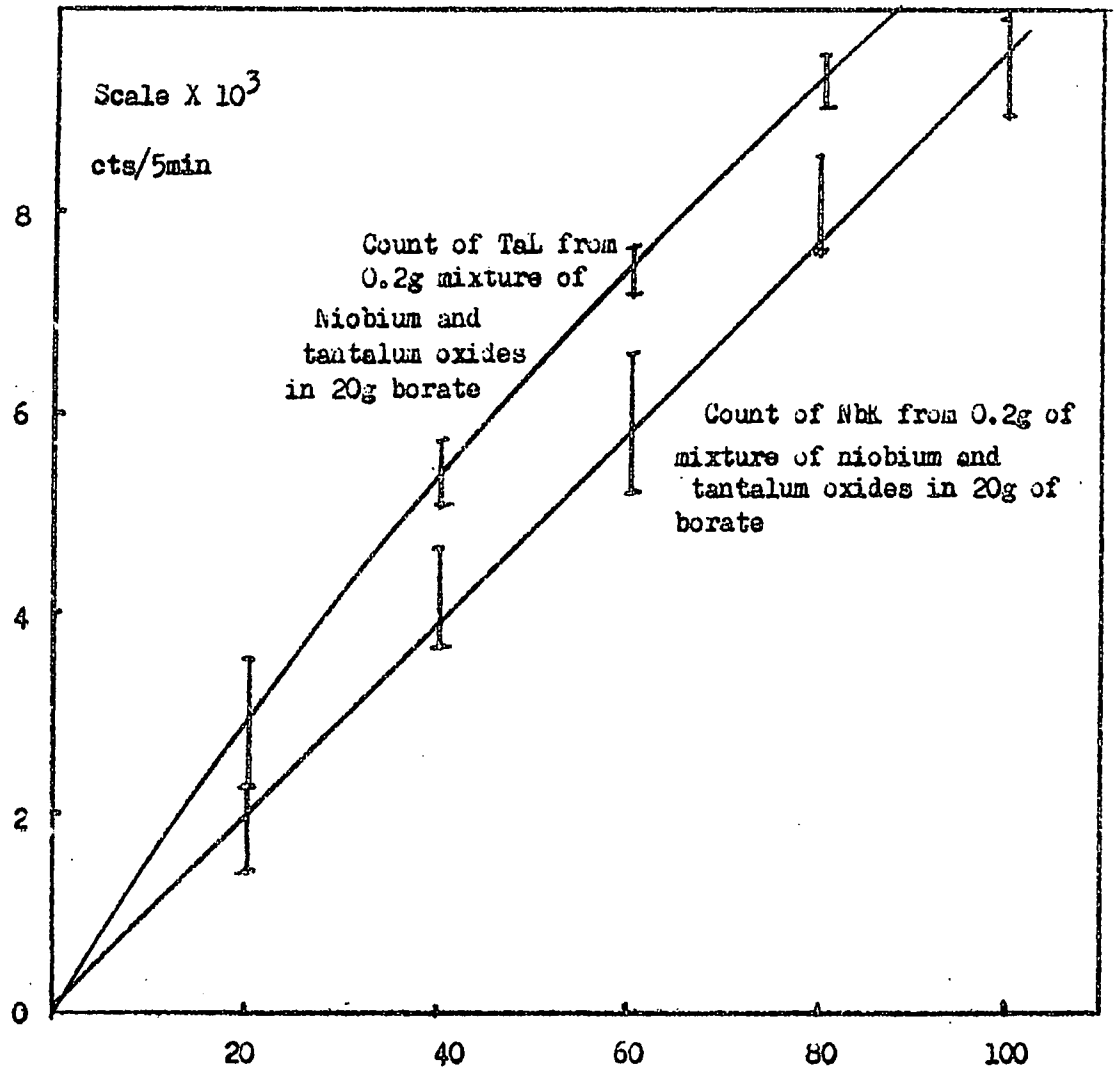

Fig. 9-6 Mixture of niobium and tantalum oxides in borate
(Co^{57} source used)

CHAPTER 10

Summary of results and conclusion.

Detection limits

In Table 10.1 the collected results of the detection limits for the single element systems containing niobium and tantalum oxides are presented. The values are expressed in terms of the grams of element oxide per 1000 grams of the sample matrix.

Table 10.1.

Source	Element detected	Matrix		
		dilute H.F.	Borax	Perspex
Pm^{147}	Nb	0.11	0.08	0.07
Co^{57}	Nb	0.83	1.34	0.53
Pm^{147}	Ta	0.20	0.31	0.42
Co^{57}	Ta	0.60	4.75	0.84

For the borax matrix and Co^{57} source a greater source to sample distance was used (see Chapters 8 and 9) and this accounts for the noticeably higher values obtained. Otherwise, for the same element and source, the detection limits are essentially the same for the three sample forms used. The results for the Pm^{147} source are somewhat lower than the corresponding results using Co^{57}, and this is remarkable when their relative source strengths are considered,

i.e. one curie of Pm^{147} in the brehmsstrahlung source against one millicurie of Co^{57}. A similar situation exists for other elements using these sources (cf. Figure 4-15 and Table 8.1).

The detection limits for the individual elements in mixtures of niobium and tantalum oxides are given in Table 10.2. The values are expressed as weight per cent of the element oxide in the standard sample forms. The weight concentrations of the mixture in the sample matrix are

Dilute H F: 10 gms of mixture/1000 gms of matrix
Borax : 10 gms of mixture/1000 gms of matrix
Perspex : 10 gms of mixture/1000 gms of matrix

Table 10.2.

Source	Element detected	Matrix		
		dilute HF	Borax	Perspex
Pm^{147}	Nb	0.4	0.67	0.8
Co^{57}	Nb	-	7.4	10.0
Pm^{147}	Ta	-	2.67	2.4
Co^{57}	Ta	3.2	4.8	5.3

Errors

The errors associated with the instrument stability and timing of the count are similar to those expected in nucleonic work. Statistical errors in the counting have standard deviations from the mean of not greater than one per cent since the total counts observed in a determination were generally in excess of 10,000. The largest sources of error are those arising from sample preparation, particularly in the case of samples bonded in perspex, and in the background correction. For the latter case the difficulties in establishing a definite criterion for background correction have been discussed, and in practice the correction method has to be considered for each individual case. This correction probably represents the

major source of error.

In general the errors observed are within the expected standard deviation, the only marked exception from this being that of the samples bonded in perspex. This exception could well be removed by improvements in the method of sample preparation.

Further work

It is considered that improvement in the samples bonded in perspex could be achieved, and suggestions to achieve this have already been outlined in Chapter 6. The sample form has a number of attractive features not least of these being its independence of solubility considerations.

The results obtained with Co^{57} suggest that radioactive sources giving low energy gamma rays or monochromatic X-rays would give useful results, particularly if they could be so chosen that the energy of the photons emitted was just above the absorption edge of the element to be determined. Sources at millicurie levels of activity could be used. A further advantage might be that a definite criterion for background correction could be applied.

In situations where a suitable source of low energy gamma rays or monochromatic X-rays was not available, another possibility is worthy of further study. This involves excitation of the fluorescent X-rays of an element by means of a radioactive source, the X-rays produced being used to excite the fluorescent radiation of the element to be determined. The first element could be so chosen as to give a fluorescent X-ray of energy just above the absorption edge of the second element.

APPENDIX

Derivation of equation (1-1) in Chapter 1

The derivation follows the method used by Hamos (79) and Birks (80).

After penetrating a distance x through the sample, the intensity of the primary X-ray will be reduced by absorption (See Figure).

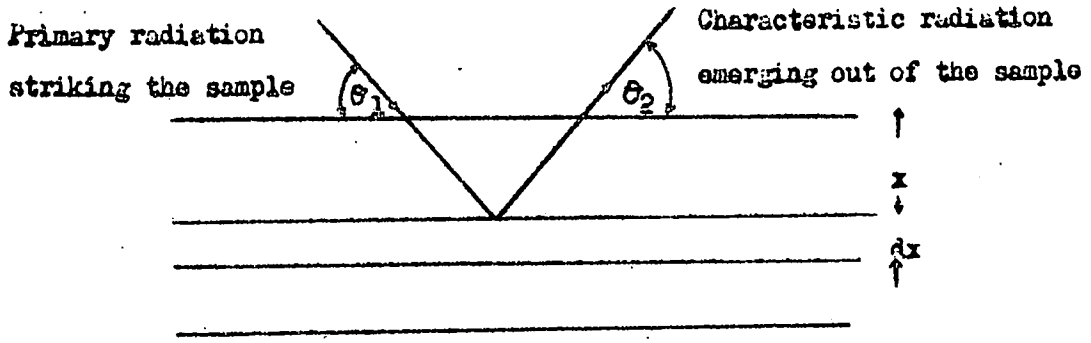

$$I_{pl} = I_{po} \exp. (-\mu_p \rho x \operatorname{cosec} \theta_1) \quad - - - - (1)$$

where θ_1 = angle at which the primary radiation strikes the sample.

θ_2 = angle at which the fluorescent line emerges.

I_{po} = intensity of the primary radiation before absorption

I_{pl} = intensity of the primary radiation after absorption

μ_p = mass absorption coefficient of the primary radiation.

ρ = density of the sample.

I_{p1} will excite the characteristic line of element i in the layer dx. The intensity will be

$$d\,I_{fo} = K\,C\,I_{p1}\,dx \qquad \text{- - - - - - - - - - (2)}$$

where K is a proportionality constant and C the concentration of the element i in the layer.

When this radiation emerges from the sample, it will have undergone absorption by the sample and the intensity will be

$$d\,I_{f1} = d\,I_{fo}\,\exp\,(-\mu_f \rho x \operatorname{cosec}\theta_2) \text{ - - -(3)}$$

substituting (1), (2) into (3)

$$d\,I_{f1} = K\,C\,I_{po}\,(\exp(-\mu_p \operatorname{cosec}\theta_1 - \mu_f \operatorname{cosec}\theta_2)\rho x)dx \text{ - -(4)}$$

Integrating equation (4) from zero to x

$$I_{f1} = \frac{K\,C\,I_{po}}{(\mu_p \operatorname{cosec}\theta_1 + \mu_f \operatorname{cosec}\theta_2)\rho}\left(1 - \exp(-\mu_p \operatorname{cosec}\theta_1 - \mu_f \operatorname{cosec}\theta_2)\rho x\right)$$

let x = infinity

$$I_{f1} = \frac{K\,C\,I_{po}}{(\mu_p \operatorname{cosec}\theta_1 + \mu_f \operatorname{cosec}\theta_2)\rho}$$

θ_1 and θ_2 are always constant and in most cases equal.

Therefore $$I_{f1} = \frac{K\,C\,I_{po}}{(\mu_p + \mu_f)\rho \operatorname{cosec}\theta}$$

The derivation of this equation is based on the assumption that the primary radiation is monochromatic.

Literature References Cited

(1) Sidgwick N.V.: Chemical Elements and their compounds Oxford University Press (1950), 1291.

(2) Sidgwick N.V.: Chemical Elements and their compounds Oxford University Press (1950), 1289.

(3) Birks L.S.: X-Ray Spectrochemical Analysis, Interscience Publishers (1959), 86.
Dyroff G.V.: Anal. Chem. 26, 1774-8(1954).

(4) Birks L.S. : X-Ray Spectrochemical Analysis, Interscience Publishers (1959), 98-123.

(5) Reiffel L. and Humphreys R.F.: The Proceedings of the International Conference on Peaceful uses of Atomic Energy, Vol. 15, 291 (1955, Geneva).

(6) Lévêque P., Martinelli P. and Chauvin R.: Proceedings of the International Conference on Peaceful uses of Atomic Energy, Vol. 15, 142 (1955).

(7) Daggs R.G.: Proceedings of International Conference on the Peaceful uses of Atomic Energy, Vol. 15, 174(1955).

(8) Zemany P.D. and al. : X-Ray Absorption and Emission in Analytical Chemistry, John Wiley & Sons. Inc. (1960). 3.

(9) Zemany P.D. and al. : X-Ray Absorption and Emission in Analytical Chemistry, John Wiley & Sons. Inc. (1960).111-124.

(10) Gulbransen L.B. : Anal. Chem. 27, 7, 1181-2 (1955).

(11) Hale C.C. and King W. H. Jr. : Anal. Chem., 33, 1, 74-7(1961).

(12) Gunn E.L. : Anal. Chem. 28,9,1433-6 (1956).
(13) Gulbransen L.B. : Anal. Chem., 28,10, 1632-4 (1956).
(14) Mitchell B.J. : Anal. Chem. 33,7,917-20 (1961).
(15) Birks L.S. and Harris D.L. : Anal. Chem., 34,8,943(1962).
(16) Adler I. and Axelrod J.M. : Spectrochimica Acta,Vol.7 91 - 9 (1955).
(17) Lewis G. J. Jr. and Goldberg E.D. : Anal. Chem., 28, 8, 1282 - 5 (1956).
(18) Kokotails G.T. and Damon G.F.: Anal. Chem. 25,8,1185 - 7 (1953).
(19) Axelrod J. M. and Adler I. : Anal. Chem., 29,9,1280 - 1 (1957).
(20) Campbell W.J. and Carl H.F.: Anal. Chem., 29,7,1009 - 16 (1957).
(21) Longobucco R. : Anal. Chem., 34, 10, 1263 - 7 (1962).
(22) Jones R. A. : Anal. Chem., 31,8, 1341 - 4 (1959).
(23) Dwiggins C.W. Jr. and Dunning H.N. : Anal. Chem., 31, 6, 1040 - 2 (1959).
(24) Dwiggins C.W. Jr. and Dunning H.N. : Anal. Chem., 32, 9, 1137 - 41 (1960).
(25) Heidel R. H. and Fassel V. A. : Anal. Chem. 30. 2, 176 - 8 (1958).
(26) Kehl W.L. and Russell R.G. : Anal. Chem. 28, 8, 1350 - 1 (1956).
(27) Fagel J. E., Jr., Liebhafsky H.A. and Zemany P.D. : Anal. Chem., 30, 12, 1918 -20 (1958).
(28) Pish G. and Huffman A. A. : Anal. Chem. 27, 12, 1875 - 8 (1955).
(29) Adler I. and Axelrod J. M. : Anal. Chem. 27, 6, 1002 - 3 (1955).
(30) Hakkila E.A. and Waterbury G.R. Talenta, Vol. 6, 46 - 51 (1960).
(31) Campbell W.J. and Carl H.F. : Anal. Chem., 26, 5, 800 - 5 (1954).

(32) Adler I. and Axelrod J.M. : Anal. Chem., 26,5,9 31 - 2 (1954).
(33) Luke C.L. : Anal. Chem., 35, 1, 56 - 58 (1963).
(34) Andermann G. and Kemp J.W. : Anal. Chem., 30, 8, 1306 - 9 (1958).
(35) Fagel J.E. Jr., Balis E.W. and Bronk L.B. : Anal. Chem., 29, 9, 1287 - 9 (1957).
(36) Meyer J.W. : Anal. Chem., 33, 6, 692 - 6 (1961).
(37) Tomkins M.L., Berun G. . and Fahlbusch W.A. : Anal.Chem., 34, 10, 1260 - 62 (1962).
(38) Mitchell B. J. : Anal. Chem., 30, 12, 1895 - 1900 (1958).
(39) Manevan D.R; and Lovell H.L. : Anal. Chem.-32,10, 1289 - 92 (1960).
Andermann G. : Anal. Chem. 33,12,1689 - 95 (1961).
Sarian S., Weart H.W. and Hall. O. : Anal. Chem., 35, 1, 115 (1963).
(40) Sherman J. : Spectrochimica Acta, 466-470 (1959).283-306(1955)
(41) Mitchell B.J. : Anal. Chem., 32, 12, 1652 - 6 (1960).
(42) Gunn E.L. : Anal. Chem., 33, 7, 921 - 7 (1961).
(43) Liebhafsky H.A. and Zemany P.D.: Anal Chem.,28,4,455 - 9 (1956).
(44) Sun Shiou - Chuan : Anal. Chem., 31, 8, 1322 - 4 (1959).
(45) Andermann G. : Anal. Chem.,33,12,1695 - 99 (1961).
(46) Rhodes J.R. : Private Communication.interscience Publisher (1959).
(47) Birks L.S.: X-Ray Spectrochemical Analysis interscience Publisher (1959), 52 - 3.
(48) Zemany P.D. and al., : X-Ray absorption and Emission in Anal. Chem. John Wiley & Sons Inc. (1960), 269 - 278.
(49) Zemany P.D. and al., : X-Ray Emission and absorption in Anal. Chem. John Wiley & Sons Inc. (1960), 233.
(50) Mellish C.E. : Research, Vol. 12, 212 - 217 (June,1959).
(51) Rhodes J.R. : AE RE, Radioisotopes review sheet, D7, "X-Ray fluorescence Spectrometry".

(52) Starfelt N., Cederlund J. and Liden K. : I.J. of Appl. Radiation and Isotopes, Vol. 2. 265 - 273.

(53) Kereiakes J.G., Kraft G.R., Weir D.E. and Krebs A.T.: Nucleonics, 16, 30 (January 1958).

(54) Martinelli P. and Seibel G. : Colloquium spectroscopium Internationale Lucerne 307-313 VIII (1959).

(55) Cameron J.F. and Rhodes J.R. : I.J. of Appl. Radiation and Isotopes, 7, 244-250 (1960).

(56) Leveque P. Martinelli P and May S.: I. J. of Appl. Radiation and isotopes, 4, 41-44 (1958).

(57) Rhodes J.R., Florkowski T. and Cameron J.F.: AERE - R 3925.

(58) Traon J.Y. and Seibel G. : I.J. of Appl. Radiation and Isotopes, 14, 365 - 79 (1963).

(59) Ziegler C.A. and Mecae J.C. : I.J. of Appl. Radiation and Isotopes, 12, 1 - 5 (1961).

(60) Seibel G. and Traon J.Y. : I.J. of Appl. Radiation and Isotopes, 14, 259 - 71 (1963).

(61) Mackay K.J.H. : J. Inorg. and Nuclear Chem. No.½, 171 (1961)

(62) Cameron J.F., Rhodes J.R. and Berry P.F. : AERE - R 3086.

(63) Seibel G. : I.J. of Appl. Radiation and Isotopes, 15, 25 - 41 (1964).

(64) Compton A.H. and Allison, S.K. : X-Ray in Theory and Experiment, D.Van Norstrand Company, Inc., 488 - 489-490, 491 - 492.

(65) Fermi E. : Nuclear Physics, University of Chicago press (1951) 39.

(66) Compton A.H. and Allison S.K. : X-Rays in Theory and Experiment, D. Van Norstrand Company, Inc., 482.

(67) Yuan and Wu : Methods of Experimental Physics, Academic Press (1961 and 1962) 79.

(68) Zemany P.D. and Al. : X-Ray absorption and Emission in Analytical Chemistry, John Wiley & Sons Inc. (1960), 61 - 62.

(69) Rhodes J.R., Florkowski T. and Cameron J.F. : AERE - R 3925 (1962).

(70) Rhodes J.R. : Radioisotopes review sheet, D7, X-Ray Fluorescence Spectrometry.
Also Cameron J.F., Rhodes J.R. and Berry P.F.: AERE, R - 3965 (1962).

(71) Straminger, Hollander and Seaborg : Rev. Mod. Phys.30, 727, (1958).

(72) Straminger, Hollander and Seaborg : Rev. Mod. Phys.30, 733 (1958).

(73) Parrish W. and Kohler T.R. : Rev. Sci. Instr., 27,795 (1956).

(74) Zemany P.D. and al. : X-Ray absorption and Emission in Analytical Chemistry John Wiley & Sons. Inc. (1960), 309.

(75) Martin G.R. : Nuclear Inst. and Method 13 (1961) 263.

(76) Radiochemical Centre (U.K.A.E.A.) : Radioactive Products, 116.

(77) Zemany P.D. and al. : X-Ray absorption and Emission in Analytical Chemistry, John Wiley & Sons, Inc., (1960), 308, 311, 316.

(78) Luke C.L. : Anal. Chem., 35, 1, 56-8 (1963).

(79) Von Hamas L. ; Arkiv f. Matematik och Fysik 31a,Article No. 25 (1945).

(80) Birks L.S. : X-Ray Spectrochemical Analysis. 58 - 59.